A Flowing Afterglow Study of $(OC)_2Fe^{\bullet-}$ and $(OC)_3Mn^-$ with Amines, Fluorocarbons and CH_3OCH_3

by

Daniel J. Reed

B.S., Arkansas College, 1986

A MASTER'S THESIS

submitted in partial fulfillment of the

requirements for the degree

MASTER OF SCIENCE

Department of Chemistry

KANSAS STATE UNIVERSITY

Manhattan, Kansas

1989

Approved by:

Major Professor

LD
2668
.T4
CHEM
1984
R44
c.2

A11208 315604

Table of Contents

List of Tables....................iv

List of Figures....................vi

Introduction....................1

I. The Chemistry of $(OC)_2Fe^{\bullet -}$, $(OC)_3Mn^-$ and Related Complexes.....2

A. Background....................2

1. Condensed-Phase Background Literature....................2

a. C-H Bond Activation....................2

b. Hydride Migrations and Eliminations....................11

1. β-Hydride Migration....................12

2. α-Hydride Migration....................17

c. Ligand Substitution Reactions....................25

d. N-H Bond Activation....................29

e. C-F Bond Activation....................35

2. Gas-Phase Background Literature....................37

a. C-H Bond Activation....................38

b. β- and α-Hydride Migration....................42

c. Ligand Substitution Reactions....................43

d. N-H Bond Activation....................46

e. C-F Bond Activation....................48

B. Objectives of this Investigation....................50

C. Experimental....................51

1. General Procedure for the Study of Ion/Molecule Reactions in the Flowing Afterglow....................51

2. The Flow Tube....................52

3. The Ion Production Region....................53

4. Differentially Pumped Analysis Section....................54

  a. Quadrupole Mass Filter and Electron Multiplier..........54

5. Kinetics..56

6. Materials...62

7. Generation of $(OC)_2Fe^{\bullet -}$ and $(OC)_3Mn^-$......................63

D. Results and Discussion....................................68

1. Reactions of $(OC)_{2,3,4}Fe^{\bullet -}$ and $(OC)_{3,4,5}Mn^-$..............68

  a. With Amines...68

  b. With $F_2C=CH_2$..87

  c. With o-Difluorobenzene..................................98

  d. With CH_3OCH_3.......................................102

E. Summary..115

F. References...118

Acknowledgement...136

List of Tables

Table I. Relative Rates for C-H Oxidative Addition per C-H Bond by Irradiation or $Cp^{*}LIr(H)(H)$ and $Cp^{*}LRh(H)(H)$ with the Hydrocarbon......................9

Table II. Relative Rate Constants for β-Hydride Migration Reactions of Various Platinum Metallocycles in CH_2Cl_2..15

Table III. Bond Dissociation Energies for L_nM-R Complexes........30

Table IV. Product Distributions of Atomic Transition Metal Cations with Alkanes.................................41

Table V. Lens Settings and Potentials for Optimized Signals in the Extrel C-50 Mass Spectrometer..................56

Table VI. Summary of Product and Kinetic Data of $(OC)_2Fe^{\bullet -}$ with Amines...69

Table VII. Summary of Product and Kinetic Data of $(OC)_3Mn^{-}$ with Amines...70

Table VIII. Summary of Product and Kinetic Data of $(OC)_3Fe^{\bullet -}$ with Various Neutral Substrates......................71

Table IX. Summary of Product and Kinetic Data of $(OC)_4Fe^{\bullet -}$ with Various Neutral Substrates......................72

Table X. Summary of Product and Kinetic Data of $(OC)_4Mn^{-}$ with Various Neutral Substrates......................73

Table XI. Summary of Product and Kinetic Data of $(OC)_5Mn^{-}$ with Various Neutral Substrates......................74

Table XII. Comparison of Rate Constants for the Reactions of $(OC)_2Fe^{\bullet -}$ and $(OC)_3Mn^{-}$ with Amines................77

Table XIII. Calculated Rate Constants from Individual Slopes from the Reactions of $(OC)_2Fe^{\bullet -}$ with $(CH_3)_2NH$ and $(CD_3)_2NH$......86

Table XIV. Summary of Product and Kinetic Data for the Reactions of $(OC)_2Fe^{\bullet -}$ and $(OC)_3Mn^-$ with Fluorocarbons......89

Table XV. Summary of Product Data for Secondary Ion/Molecule Reactions of Various Iron Complexes......90

Table XVI. Summary of Product Data for Secondary Ion/Molecule Reactions of Various Manganese Complexes......91

Table XVII. Summary of Product and Kinetic Data for the Reactions of $(OC)_2Fe^{\bullet -}$ and $(OC)_3Mn^-$ with CH_3OCH_3 and CD_3OCH_3......103

List of Figures

Figure 1. Schematic diagram of the flowing afterglow............51

Figure 2. Conversion dynode for negative ion detection..........55

Figure 3. Mass spectra of dissociative electron attachment of $Fe(CO)_5$..64

Figure 4. Mass spectra of dissociative electron attachment of $Mn_2(CO)_{10}$..65

Figure 5. Correlation of gas-phase proton affinity and N-H bond strengths with the normalized bimolecular rate constants for the reaction of $(OC)_2Fe^{\bullet -}$ with NH_3 and amines.......................................79

Figure 6. Semi-log plots for the reaction of $(OC)_2Fe^{\bullet -}$ and $(OC)_3Mn^-$ with $(CH_3)_2NH$..............................83

Figure 7. Semi-log plots for the reaction of $(OC)_2Fe^{\bullet -}$ with $(CH_3)_2NH$ and $(CD_3)_2NH$...............................86

Introduction.

The area of organometallic chemistry has shown considerable advancement in the past thirty years. The interest in this area of chemical research is documented in a number of publications and in the establishment of several new specialized journals, e.g., Journal of Organometallic Chemistry (Elsevier Publishing), Transition Metal Chemistry (Verlag Chemie), and Organometallics (American Chemical Society), originating in 1963, 1976, and 1981, respectively.

In the early 1970's, the first publications appeared concerning the ion/molecule reactions of transition metal complex positive[1] and negative[2] ions in the gas phase. In these studies, ion cyclotron resonance (ICR) spectrometry was used to monitor the reactions. There are currently a number of groups active in gas-phase research,[3] and the ion/molecule chemistry of anionic transition metal atoms[4,5] and complexes[3,5] is a major thrust.

A second gas-phase method, the flowing afterglow (FA) apparatus, has been employed in a number of similar investigations[3f,6] and was developed in the early 1960's by Ferguson, Fehsenfeld, and Schmeltekoff[7] at the U.S. Department of Commerce National Oceanic and Atmospheric Administration Laboratories in Boulder, Colorado. The advantage of the FA vs. the ICR experiments is that the ion/molecule reactions are carried out at a relatively high pressure of a buffer gas (> 0.2 torr) assuring that the ion is in its vibrational ground state prior to reaction with added neutral reagents. The ICR, however, is operated at low pressure ($< 10^{-5}$ torr), such that collisional stabilization of the ions is substantially diminished.

I. The Chemistry of $(CO)_2Fe^{\bullet -}$ and $(CO)_3Mn^-$, and Related Complexes.

I.A. Background.

I.A.1. Condensed Phase Background Literature.

The reactions which are considered in this section are C-H, N-H, and C-F bond activation, β- and α-hydride migrations, and ligand substitution reactions. C-H, N-H and C-F bond activation refer to the oxidative insertion reaction (eq 1) in which a metal complex inserts into a generic X-Y bond.[8] Likewise, β- and α-hydride migration refer to an intramolecular oxidative insertion of a X-H bond, where β- or α- refer to the position of X relative to the metal.[9] Equation 2 illustrates β-hydride migration.

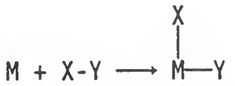

$$M + X\text{-}Y \longrightarrow \overset{X}{\overset{|}{M}}\!-\!Y \qquad (1)$$

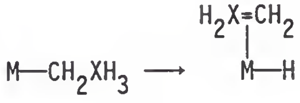

$$M\!-\!CH_2XH_3 \longrightarrow \overset{H_2X=CH_2}{\overset{|}{M}}\!-\!H \qquad (2)$$

I.A.1.a. C-H Bond Activation.

The basis of transition metal catalysis centers on the oxidative insertion reaction. C-H bond activation is a specific oxidative insertion reaction which has been the subject of many reviews.[10] The initial requirement for an oxidative insertion reaction is that the transition metal complex must have a vacant coordination site on the metal. This requirement was derived from Tolman's 18-electron rule which stated that (a) diamagnetic organometallic transition metal complexes existed in significant concentrations at moderate temperatures only if the metal valence shell contained 16- or 18-electrons, and (b) organometallic reactions proceeded by elementary steps involving species that possess 16- or 18-electrons.[11] The number of valence electrons (NVE) for a given complex was defined as the number of s, p, and d valence electrons from the metal as well as those donated to the metal by any ligands bonded in the complex. However, for every rule there were exceptions, most notably VCl_4 (NVE = 9), TaF_7^{2-} (NVE = 14), NiF_6^{4-} (NVE = 20), and $Ni(H_2O)_6^{2+}$ (NVE = 20).[11]

Insertion of a metal center into a C-H bond could occur by an intermolecular (eq 3) or an intramolecular oxidative addition mechanism (eq 4). The intramolecular C-H oxidative addition, also known as

$$\mathrm{M} + \mathrm{C\text{-}H} \longrightarrow \mathrm{H\text{-}M\text{-}C} \tag{3}$$

$$\overbrace{\mathrm{M}\quad\mathrm{C}}\mathrm{\text{-}H} \longrightarrow \mathrm{H\text{-}}\overbrace{\mathrm{M{-}\!{-}C}} \tag{4}$$

cyclometalation[12] (eq 4) or orthometalation when an o-aromatic C-H bond is involved, are common. The first isolated cyclometalation product was reported by Kleiman in 1963 which involved the aryl C-H bonds of azobenzene.[13] Since that time, cyclometalation has been an important process in the activation of C-H bonds in alkanes.[9,10b,14] More recently, Hawthorne and co-workers[15] utilized thermal and photochemical decomposition of metallocycles to generate coordinatively unsaturated iridium complexes which oxidatively inserted into the C-H bonds of coordinated alkyl and aryl groups. The cyclometalation reaction was found to be accelerated by severe steric strain in the starting transition metal complex due to the stable metallocycle that was formed.[16]

Intermolecular C-H oxidative insertion was a less common occurrence than intramolecular C-H insertion.[10b,17] This was presumably due to the entropic advantage to be gained in the intramolecular reaction and to the thermodynamic stability of the cycloadduct. The earliest examples of intermolecular C-H insertion involved compounds which were believed to first form a π-complex with the metal prior to C-H oxidative insertion reaction (eq 5).[18] These

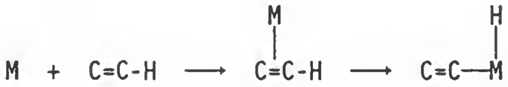

$$M + C{=}C\text{-}H \longrightarrow \overset{\overset{M}{|}}{C}{=}C\text{-}H \longrightarrow C{=}C\text{—}\overset{\overset{H}{|}}{M} \qquad (5)$$

examples of intermolecular C-H oxidative insertion involve insertion into aryl C-H bonds via prior π-complexation due to the direct observation of an η^2-arene complex by ^{1}H NMR.[19] However, Stoutland and Bergman suggested that in the reaction of $(\eta^5\text{-}C_5Me_5)(PMe_3)IrH_2$ (1) with ethylene, oxidative addition occurs "with concurrent, but not prior formation of the π-complex" due to the observation of invariant ratios of both the π-complex and the C-H insertion complex.[20] This was later confirmed by an isotopic labeling study which proved that the π-complex was not an intermediate in the formation of the iridium vinyl hydride complex due to the different isotope effects observed for formation of the π-complex (0.82) and the vinyl hydride complex (1.18).[21] In the reaction of arenes with D_2 catalyzed by transition metal complexes, Parshall suggested that H/D exchange occurred by a coordinatively unsaturated η^2-C_6H_6 metal complex.[10o] This process was later confirmed by Jones and Fehrer from data for the decomposition of $(C_5Me_5)Rh(PMe_2CH_2Ph)(Ph)(H)$.[19b]

Oxidative insertion into C-H bonds of saturated hydrocarbons had eluded researchers until 1982 when the first examples of intermolecular C-H oxidative addition reactions with alkanes was reported by Bergman and Janowicz (eq 6).[22] This was quickly followed by a similar report

$$\underset{\mathbf{1}}{(\eta^5\text{-}C_5Me_5)(PMe_3)IrH_2} \xrightarrow[h\nu]{RH} (\eta^5\text{-}C_5H_5)(PMe_3)Ir(H)(R) \qquad (6)$$

$R = C_6H_5$, $\underline{c}$-C_6H_{11}, $CH_2C(CH_3)_3$

by Hoyano and Graham.[23] This was a significant discovery since saturated hydrocarbons are abundant industrial materials, but are generally unreactive in the absence of a catalyst. This is because the alkane C-H bond is strong (D° = 104 kcal/mole in CH_4)[24] relative to the product M-H bond (D° = 29.6 kcal/mole in Fe-H)[25] and M-C bonds (D° = 68 kcals/mol in Fe-CH_3).[26] Before 1982, the only suggestion of C-H bond activation with saturated hydrocarbons was with coordinatively unsaturated species generated from Ir and Re complexes.[27] However, both of these systems involved multiple hydrogen atom loss from the hydrocarbon and required the addition of an alkene as a hydrogen acceptor where hydrogenation of the alkene was suggested to occur by activation of the alkane C-H bonds. In addition, the metal complexes reacted preferentially with RH versus the methylene chloride solvent.

Janowicz and Bergman irradiated **1** with RH molecules as solvent which gave the corresponding C-H bond oxidative insertion product **4** in eq 7.[28] This was the first instance of intermolecular oxidative insertion of a completely unactivated hydrocarbon. When 1 was irradiated in the presence of a 1:1 mixture of neopentane and cyclohexane, 53% of the product was insertion the C-H bond of neopentane. This indicated that insertion slightly favored primary over secondary C-H bonds and that a radical mechanism was not involved. The proposed mechanism is given in equation 7.[28]

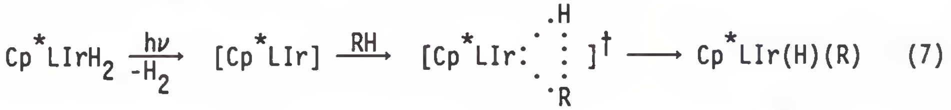

$$\mathrm{Cp^*LIrH_2} \xrightarrow[-H_2]{h\nu} [\mathrm{Cp^*LIr}] \xrightarrow{RH} [\mathrm{Cp^*LIr}\!:\overset{\cdot H}{\underset{\cdot R}{\vdots}}\,]^{\dagger} \longrightarrow \mathrm{Cp^*LIr(H)(R)} \qquad (7)$$

1 **2** **3** **4**

$Cp^* = \eta^5\text{-}C_5Me_5$, $L = PMe_3$

Briefly, irradiation of 1 was proposed to lead to an excited electronic state which rapidly eliminates H_2 forming the coordinatively unsaturated complex 2 as a transient intermediate. The reactive 16-electron complex **2** underwent oxidative insertion into the C-H bond of the solvent RH molecule via a three-centered transition state **3** which yields the product **4**. A radical mechanism, as shown in Scheme I, was ruled out. Mechanism A was tested by irradiation of 1 in the presence

Scheme I

$$\text{(A)}\quad \mathrm{Cp^*LIrH_2} \xrightarrow{h\nu} \mathrm{CpLIrH\cdot} + \mathrm{H\cdot}$$

$$\mathrm{H\cdot} + \mathrm{RH} \longrightarrow \mathrm{H_2} + \mathrm{R\cdot}$$

$$\mathrm{Cp^*LIrH\cdot} + \mathrm{R\cdot} \longrightarrow \mathrm{Cp^*LIr(H)(R)}$$

$$\text{(B)}\quad \mathrm{Cp^*LIrH_2} \xrightarrow{h\nu} \mathrm{Cp^*LIr} + \mathrm{H_2}$$

$$\mathrm{Cp^*LIr} + \mathrm{RH} \longrightarrow \mathrm{Cp^*LIrH\cdot} + \mathrm{R\cdot}$$

$$\mathrm{Cp^*LIrH\cdot} + \mathrm{R\cdot} \longrightarrow \mathrm{Cp^*IrL(H)(R)}$$

of C_6D_6. The only product of the reaction was $Cp^*LIr(D)(C_6D_5)$ and H_2. If the radical mechanism A was operating, there resulting products should have been $Cp^*LIr(H)(C_6D_5)$ and HD. Mechanism B was tested by a competition experiment in which **1** was irradiated in the presence of p-xylene. If mechanism B were operating, the 16-electron intermediate should attack the benzylic C-H bonds preferentially over the aromatic C-H bonds based on the different bond dissociation energies ($D°(C_6H_5CH_2\text{-}H)$ = 88.0±1 kcal/mol, $D°(C_6H_5\text{-}H)$ = 110.9±2 kcal/mol).[29] However, attack occurred 3.7 times faster at the aromatic ring than at the methyl groups.[28] However, the assumption that C-H bond activation would depend primarily on the C-H bond that was broken is only partly true. C-H bond activation also depends on the strength of the M-C and M-H bonds that are being formed. In this case, it was recently shown that the results of preferential attack on the aromatic C-H bonds was due to the very strong Ir-Ph bond (D° = 80.6 kcal/mol)[30] that was formed relative to the $Ir\text{-}CH_3$ bond (D° = 32.4 kcal/mol) in $(PMe_3)_2(Cl)(CO)Ir(CH_3)_2$.[30]

Further evidence to rule out mechanism B was shown in the reaction of **1** with cyclopropane. Cyclopropane has relatively weak C-C bonds (the typical D°(C-C) for alkanes is 80 kcal/mol and insertion into the cyclcopropane ring would also relieve ring strain),[29] and relatively strong C-H bonds (D° = 106 kcal/mol)[29] due to the large amount of s-character in the C-H bonds.[31] Due to the large C-H bond strengths alkyl radicals abstract hydrogen from cyclopropane very slowly. Based on the weak C-C bond strength, one might expect the iridium complex **2** to insert preferentially into the C-C bond over the C-H bond. However, the resulting product from irradiation of **1** in cyclopropane at -35° C was the hydrido cyclopropyl complex.[28] It had been shown that the hydrido cyclopropyl rhodium complex $(Cp^*(PMe_3)Rh(2,2$-dimethylcyclopropyl)(H)) rearraged to the C-C bond activation product $(Cp^*(PMe_3)\overline{RhCH_2CMe_2CH_2})$ at higher temperatures (-15° C).[32]

Confident of the three-centered oxidative insertion mechanism, Janowicz and Bergman set out to determine relative rates of C-H insertion with a variety of hydrocarbons in the presence of $Cp^*LIr(H)(H)$ and $Cp^*LRh(H)(H)$.[28,33] These data, summarized in Table I, illustrated the selectivity differences between the Rh and Ir complexes as determined by ^1H and ^{13}C NMR. The rhodium complex appeared to oxidatively insert specifically into primary C-H bonds in the presence of secondary C-H bonds while the iridium complex showed a preference for primary C-H bonds, but would insert into secondary C-H bonds. The results of these studies indicated that the reactive intermediate preferred to attack the bonds having the larger bond dissociation energies, i.e., acyclic primary, aromatic and cyclopropane C-H bonds over those with lower bond dissociation energies, i.e., secondary, tertiary, and benzylic C-H bonds. In a similar study, Bergman and co-workers irradiated $(\eta^5-C_5Me_5)Re(PMe_3)_3$, which was thought to produce the coordinatively unsaturated complex $(\eta^5-C_5Me_5)Re(PMe_3)_2$.[33b] This intermediate was found to oxidatively insert into cyclopropyl, aromatic, vinyl, methyl, and primary C-H bonds, but not into secondary or tertiary.

To investigate why metals appeared to add faster to the strongest

Table I. Relative Rates for C-H Oxidative Insertion per C-H Bond by Irradiation of $Cp^{*}LIr(H)(H)^{a}$ and $Cp^{*}LRh(H)(H)$ with the Hydrocarbon.[a,b]

Hydrocarbon	k_{rel}(Rh)	k_{rel}(Ir)
$\underline{c}$-C_6H_{12}	1.0	1.0
$\underline{c}$-C_5H_{10}	1.8	1.1
$\underline{c}$-C_3H_6	10.4	2.1
$\underline{c}$-C_7H_{14}	0.14	----
$\underline{c}$-C_8H_{16}	0.06	0.09
$\underline{c}$-$C_{10}H_{20}$	----	0.23
$HC(CH_3)_3$	3.6	----
C_6H_6	19.5	3.9
$C(CH_3)_4$	----	1.14
$CH_3CH_2CH_3$	2.5	1.5
$CH_3(CH_2)_4CH_3$	5.9	2.7(1.0)[c]
CH_2=CH_2	2.4	----
CH_3CH_3	2.0	----

[a] $Cp^{*} = (\eta^5\text{-}C_5Me_5)$, L = (PMe_3). [b] Ref. 33a. [c] Secondary C-H bond.

bonds in the alkane, Periana and Bergman investigated the C-H oxidative insertion mechanism with the reactive metal species $(\eta^5\text{-}C_5Me_5)Rh(PMe_3)$.[33c] This coordinatively unsaturated fragment was generated either by irradiation of $(\eta^5\text{-}C_5Me_5)Rh(PMe_3)(H)(H)$ or thermal decomposition of $(\eta^5\text{-}C_5Me_5)Rh(PMe_3)(H)(neopentyl)$. The authors observed that this reactive metal species exclusively formed the oxidative insertion products from primary C-H bonds, but that the relative rate constants correlated to the number of secondary C-H bonds in the alkane. Using specifically deuterium labelled alkanes, the authors concluded that oxidative insertion occurred in all the C-H bonds of the alkane, which then underwent fast intramolecular rearrangements to yield the primary C-H bond insertion products even at -100 °C.[33c]

Using competition experiments, Jones and Feher observed that aliphatic and aromatic C-H oxidative insertion favored the intermolecular process when the hydrocarbon was the solvent.[34] However, they also found a high thermodynamic preference for intramolecular C-H bond activation in alkyl and aryl ligands. This presents the intuition that unimolecular reactions to form five or six membered rings are favored over bimolecular reactions in thermodynamic terms but not in kinetic terms. For C-H insertion reactions, the implication is that for the many metal containing molecules known to activate C-H bonds intramolecularly, the products of intermolecular C-H insertion may have been overlooked due to a lack of thermal stability of the hydridoalkyl metal complex.[34]

Crabtree recently summarized the requirements for a transition metal complex to bring about intermolecular alkane C-H oxidative addition.[10b] (a) The transition metal complex must be coordinatively unsaturated or have the potential to become so through thermal, chemical, or photochemical means. (b) The metals of choice are the second row and, especially, the third row transition metals due to their strong M-C and M-H bonds. (c) The coordinatively unsaturated ML_n molecule should be sterically uncongested. (d) The ligands around the metal should not be able to undergo cyclometalation as this could shut down the intermolecular oxidative addition reaction channel. (e) The metal should have a filled orbital able to interact with the C-H σ^* orbital. (f) Coordination of the alkane is necessary and can be facilitated by using the alkane in as high a concentration as possible, preferably as neat solvent.

I.A.1.b. Hydride Migrations and Eliminations.

In surveying the literature, there seemed to be a conflict in terminology as to what the term α- or β-elimination actually means. In most cases, β-elimination refers to the process of a β-hydrogen migrating from a ligand to the metal center, M, with concurrent formation of an alkene ligand (eq 8). However, other authors use the term β-elimination to refer to a β-hydride migration and loss of the hydrogen donating ligand from the metal center (eq 9). In contrast, α-elimination almost always denotes migration of an alpha hydrogen to the metal center with formation of the resulting carbene (eq 10). Therefore, in the present context, α- or β-migration will refer only to

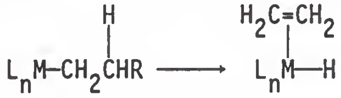

$$L_nM\text{—}CH_2\overset{\displaystyle H}{\overset{|}{C}}HR \longrightarrow L_n\overset{\displaystyle H_2C{=}CH_2}{\overset{|}{M}}\text{—}H \qquad (8)$$

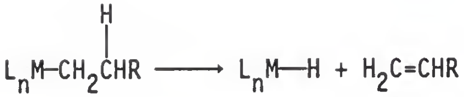

$$L_nM{-}CH_2CH(H)R \longrightarrow L_nM{-}H + H_2C{=}CHR \qquad (9)$$

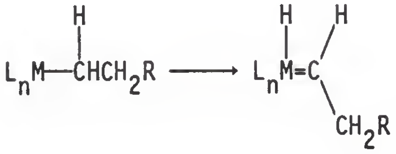

(10)

migration of hydrogen to a metal center with retention of all metal ligands, while α- or β-elimination will refer to migration to the metal with concurrent loss of the ligand from the metal center. Hydride migrations fall into two categories, namely, α-hydride migration (eq 10) and β-hydride migration (eq 8). Of these two reaction types, the β-hydride migration is the most widely known and studied.[35]

I.A.1.b.1. β-Hydride Migration.

Considerable information was gained concerning the β-hydride migration reaction from studies with the transition metal complex $Pt(PPh_3)_2(\underline{n}\text{-}C_4H_9)_2$ (5) by Whitesides and co-workers.[36] Thermal decomposition of **5** gave 1-butene and n-butane as reaction products. The thermal decomposition of **5** was proposed to give intermediate **6** which underwent the β-hydride migration as shown in eq 11.

Since addition of PPh_3 was found to decrease the rate, it was concluded that decomposition of **5** was a first-order unimolecular process. This decrease in rate was presumably due to inhibited dissociation of PPh_3 from **5**, which implied that a vacant coordination site was needed to facilitate the decomposition reaction. Deuterium in

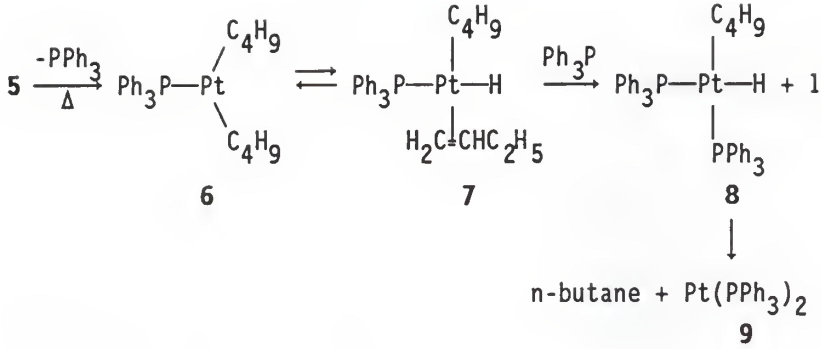

(11)

the bis-(α,α-d_2-butyl) derivative was scrambled (presumably through a sec-butyl intermediate) in the 1-butene product. The scrambling suggested that β-H migration from the n-butyl group to the metal and the microscopic reverse are faster than the loss of 1-butene or reductive elimination of n-butane. To confirm the proposed equilibrium between **6** and **7**, a known concentration of $CH_2{=}CHCH_2CH_3$ was added to the reaction mixture containing the deuterated derivative. After the reaction was complete, the authors observed the same initial concentration of protio 1-butene that was originally added. This result suggested that the scrambling was occurring via an equilibrium between intermediates **6** and **7**, and not by 1-butene reassociating with intermediate **8**. Although intermediate **9** was not isolated, addition of CH_3I to the reaction mixture yielded $(PPh_3)_2Pt(CH_3)(I)$.[36a] The reversibility of the β-hydride migration was convincingly confirmed in the study shown in eq 12, where the intermediates **10** and **11** were

$$Ni(\eta^3\text{-allyl})(Et)PPh_3 \rightleftharpoons \underset{\mathbf{10}}{Ni(\eta^3\text{-allyl})(H)(C_2H_4)PPh_3} \rightleftharpoons$$

$$C_2H_4 + \underset{\mathbf{11}}{Ni(\eta^3\text{-allyl})(H)PPh_3} \longrightarrow Ni + C_3H_6 + PPh_3 \qquad (12)$$

isolated and characterized.[37]

Whitesides and co-workers showed that the β-hydride migration was facilitated by a 0° dihedral angle in the M-C-C-H complex.[36c] The relative rates of β-hydride migration decreased as the dihedral angle in the metal moiety increased by using platinum metallocycles which could not achieve the optimal geometry; the results are given in Table II. Two features of the complexes given in Table II are important. First, the platinocycles **14-16** are markedly more stable thermally than are the acyclic platinum alkyls **12** and **13** or the larger and conformationally more mobile platinocycle **17**. Second, the products of decomposition of **14-16** suggest that the mechanism by which decomposition occurs is similar to the decomposition mechanism in **13**. That is, **13** decomposes by initial metal β-hydride migration followed by reductive elimination of alkene from an intermediate hydridoplatinum(II) alkyl.[36a] Given these facts, the relative rate data suggested that a M-C-C-H dihedral angle that cannot approach zero inhibited the metal hydride formation which reduced that reaction rate.[36c]

There are certain constraints concerning the β-hydride migration transition state which must be considered in order to understand the relative rates of reaction and ultimate products. It was determined that migration of a β-hydrogen was a more labile process than migration of β-alkyl group.[38] However, Bercaw and co-workers reported the β-alkyl elimination in the reaction of scandocene hydride derivatives with various pentadienes to yield primarily 1,4-pentadienes.[39] It was also generally accepted that formation of the 1-alkene was favored over

Table II.[a] Relative Rate Constants ($k \times 10^4$ sec^{-1}) for β-Hydride Migration Reactions of Various Platinum Metallocycles in CH_2Cl_2.

	Rate at		Decomposition Products (%)			
Compound[b]	60°	120°	n-Alkane	1-Alkene	2-Alkene	Diene[c]
L_2PtEt_2 **(12)**	4.5	---	50	50	0	f
$L_2Pt(n\text{-}Bu)_2$ **(13)**	3.8	9000[d]	50	49	1	f
$L_2\overline{Pt(CH_2)_4}$ **(14)**	---	0.53	0	78	20	2
$\mathrm{Diphos}\overline{Pt(CH_2)_4}$[e] **(15)**	---	0.17	0	93	7	0
$L_2\overline{Pt(CH_2)_5}$ **(16)**	---	0.40	0	75	17	8
$L_2\overline{Pt(CH_2)_6}$ **(17)**	1.7	---	0	83	17	0

[a] Ref. 36c. [b] L = PPh_3. [c] Predominantly α,ω. [d] This value was obtained by extrapolation of kinetic data obtained at 50, 60, and 70° C. [e] Diphos = bis-1,2-(diphenylphosphino)ethane. [f] Formation of the diene was not possible.

formation of the 2-alkene.[36c] In the general equation 8, β-migration is not restricted to hydrogen with examples also reported for alkyls[39,40] and halogens.[41] β-Migration was also invoked for the decomposition of metal alkoxides to yield metal hydrides,[42] and was proposed in the homogeneous oxidation of amines by Mo complexes.[43] In the thermal decomposition of certain chromium alkyls, conformational preferences favored elimination of the trans-2-alkene rather than the cis-isomer.[44] In a series of vinyl iridium complexes, $Ir(CR^1{=}CR^2R^3)(CO)(PPh_3)_2$ (R^1, R^2, R^3 = H or Me) migration of the cis-β-vinyl-H (**18**) was preferred over the β-allyl-H (**19**) with no formation of product from migration of the trans-β-vinyl-H (**20**) or the γ-allyl-H (**21**)[45]. The predominant migration via **18** was attributed to the stability of the resulting products, hydrido-acetylene vs. hydrido-allene complexes.

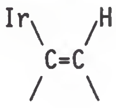

18

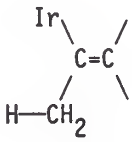

19

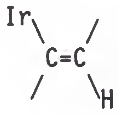

20

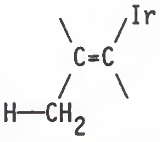

21

Deuterium labelling established that it was the β-hydrogen that was transferred to the metal.[36] Examples are provided with the copper complex in eq 13,[46] and in a number of alkychromium complexes.[44] The

$$[CuCH_2CD_2C_2H_5(PBu_3)] \longrightarrow CuD(PBu_3) + CH_2{=}CDCH_2CH_3 \qquad (13)$$

deuterium kinetic isotope effect for the β-hydrogen migration, k_H/k_D = 2.28 ± 0.2, was determined for the decomposition of the alkyliridium complexes $Ir(CH_2CHRC_6H_{13})(PPh_3)_2$ (R = H or D).[47] β-Hydrogen migration was rate determining where both Ir-H and Ir-C bond formation was important.

The above discussion has concentrated mainly on alkyl ligands. However, β-migration has also been proposed for the decomposition of metal aryls.[48] This was evident in the formation of a coordinated benzyne[49] (eq 14) which was later confirmed by deuterium labeling experiments.[50]

$$TiPh_2(\eta^5\text{-}C_5H_5)_2 \longrightarrow PhH + [Ti(C_6H_4)(\eta^5\text{-}C_5H_5)_2] \qquad (14)$$

However, Erker and co-workers have also demonstrated the intermediacy of a benzyne complex and suggest that the benzyne complex was formed from a concerted elimination of benzene from a diphenyl complex and not by a β-hydride migration/reductive elimination sequence.[51]

I.A.1.b.2. α-Hydride Migration.

α-Hydride migration is the name given to the reactions which form metal alkylidene hydride complexes from metal alkyl complexes. This process was first demonstrated by Cooper and Green with tungsten methyl complexes (eq 15),[52] and was more fully characterized by Schrock using tantalum neopentyl derivatives (eq 16).[53]

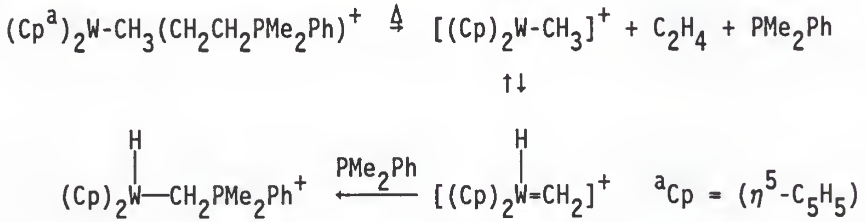

$$(Cp^a)_2W\text{-}CH_3(CH_2CH_2PMe_2Ph)^+ \xrightarrow{\Delta} [(Cp)_2W\text{-}CH_3]^+ + C_2H_4 + PMe_2Ph$$

$$\uparrow\downarrow$$

$$(Cp)_2\overset{H}{\overset{|}{W}}\text{—}CH_2PMe_2Ph^+ \xleftarrow{PMe_2Ph} [(Cp)_2\overset{H}{\overset{|}{W}}{=}CH_2]^+ \qquad {}^aCp = (\eta^5\text{-}C_5H_5) \qquad (15)$$

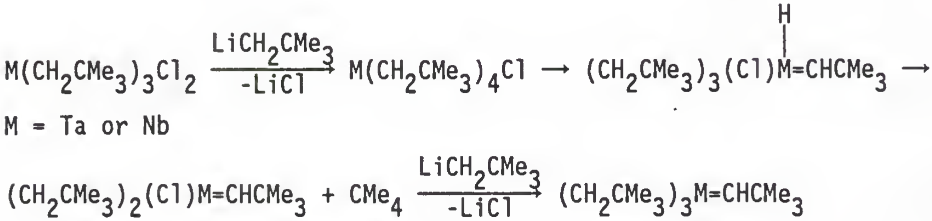

$$M(CH_2CMe_3)_3Cl_2 \xrightarrow[-LiCl]{LiCH_2CMe_3} M(CH_2CMe_3)_4Cl \rightarrow (CH_2CMe_3)_3(Cl)\overset{H}{\overset{|}{M}}{=}CHCMe_3 \rightarrow$$

M = Ta or Nb

$$(CH_2CMe_3)_2(Cl)M{=}CHCMe_3 + CMe_4 \xrightarrow[-LiCl]{LiCH_2CMe_3} (CH_2CMe_3)_3M{=}CHCMe_3 \qquad (16)$$

It appears that α-hydride migration is more labile than β-hydride migration in sterically congested complexes,[54] and in complexes in which the alkyl ligands possess no β-hydrogens.[53a] The α-hydride migration reaction is also thought to be reversible. Shilov and co-workers proposed α-elimination to explain multiple H/D exchange in their studies of platinum alkyls.[55] A clear cut example is given in eq 17,[56] where the isolated alkyl hydride complex was shown to

$$(Me_3P)_3(I)_2Ta{=}CHCMe_3(H) \rightleftharpoons (Me_3P)_3(I)_2Ta{-}CH_2CMe_3 \qquad (17)$$

interconvert with the α-hydrogen on the neopentyl ligand by a technique referred to as Magnetization Transfer Proton NMR.[57] Alkylidene complexes have also been shown to interconvert to alkylidyne hydride complexes through α-hydride migration on the NMR time scale.[58]

Alpha- and β-hydride migrations can be competetive. Schrock and co-workers isolated a 1:1 mixture of the α- and β-hydride migration products from the reaction shown in eq 18 at -30° C.[59] Shapley and

$$2Ta(Np)_2(Et)(Cl)_2 \xrightarrow{PMe_3} Ta({=}CHCMe_3)(Et)(Cl)_2(PMe_3)_2 + Ta(C_2H_4)(Np)(Cl)_2(PMe_3)_2 + 2CMe_4 \qquad (18)$$

$(Np) = CH_2CMe_3$

co-workers observed both α- and β-migration processes in the osmium complex $HOs_3(CO)_{10}(C_2H_5)$ **22** to yield the alkylidene complex **23** from α-migration and the dihydride complex (**24**) from β-migration followed by reductive elimination of C_2H_4 (eq 19).[60]

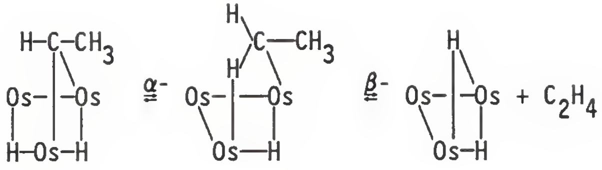

23 **22** **24**

(19)

In the latter study, a single ^{1}H NMR peak was observed for the methylene protons on C_α in **22**, but its high field position (δ = 4.71) suggested that the two protons were equilibrating between two different positions. One position was a normal C-H bond while the other was an "agostic"[61] three center-two electron C··H··Os bond. When the temperature of a solution of **22** was raised above -20° C, the ^{1}H NMR signals due to **22** decreased while four new signals appeared. These signals were due to the ethylidene complex **23** formed from α-migration of a C_α-H bond. Upon raising the temperature to 19° C, a β-migration process was observed with the formation of **24** and ethylene. At this temperature, the rate of α-migration was ≈100 times greater than that of β-migration. Treatment of **24** with excess ethylene (5 atm) resulted in 10% of **22** + **23** (≈ 3 hr). This indicated that the overall β-migration process was reversible.

More recently, Crabtree and co-workers observed competitive α- and β-hydrogen migration processes in an iridium hydride complex.[62] The H/D exchange reaction of $Ir(D)_2(\eta^2\text{-}O_2CCF_3)(PAr_3)_2$ (**25**) (Ar = p-C_6H_4F) with t-$BuCH{=}CH_2$ (**26**) at 25° C in benzene gave exchange products where deuterium was incorporated into each of the vinylic positions at equal rates (eq 20). The deuterated product was found to be 85% tert-Bu-ethylene-d_2 by GC-MS analysis. Similar rates and reactivities were

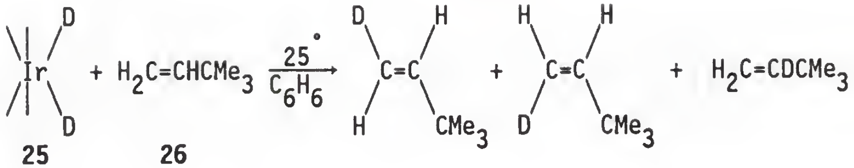

25 **26** (20)

25 = $Ir(D)_2(\eta^2\text{-}O_2CCF_3)(P(\underline{p}\text{-}C_6H_4F)_3)_2$

found for **26** = styrene, stilbene, α-methylstyrene, and ethyl vinyl ether.

An alkene insertion/β-migration mechanism was first considered to explain these results. This mechanism is shown in Scheme II with **25**

Scheme II.

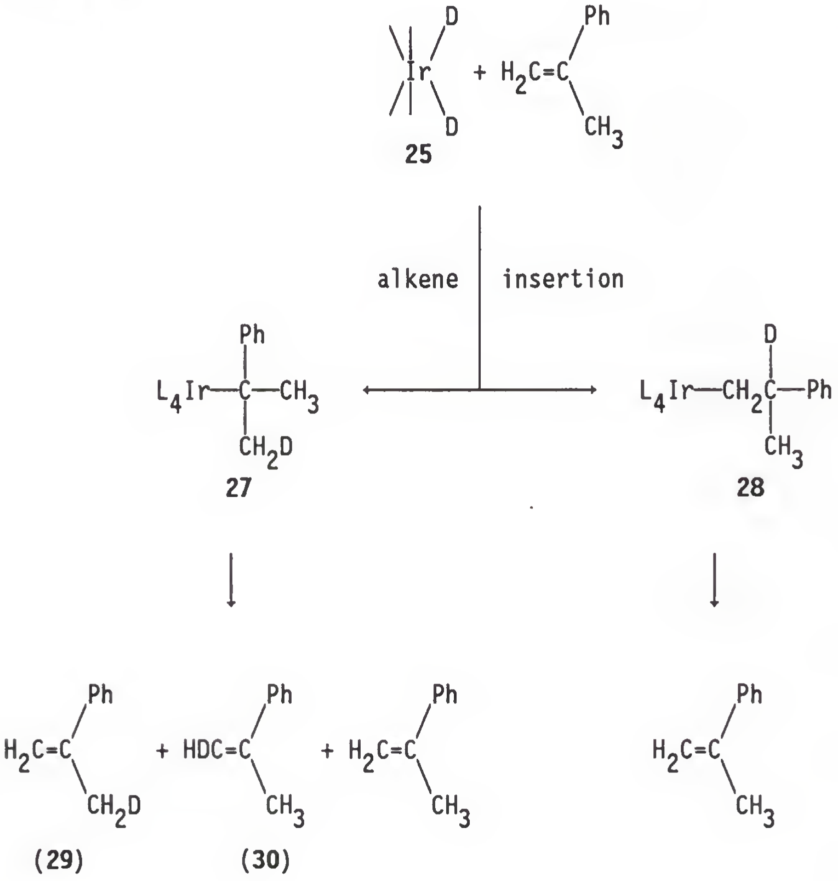

and α-methylstyrene. α-Methylstyrene could insert into the Ir-D bond toyield either **27** or **28**. From **27**, β-hydride migration followed by reductive elimination could occur at either of the methyl groups to yield **29** and **30**, respectively, with a statistical probability favoring formation of **29**. Insertion to give **28**, however, could only proceed to yield the starting material since **28** has no β-hydrogens present. The results of this experiment gave compound **30** as the primary product, with less than 2% reaction yielding **29**. Based on these results, a mechanism involving both α-hydrogen migration and β-hydride migration followed by reductive elimination was proposed to account for the equal incorporation of deuterium into each of the vinylic hydrogen positions of tert-butyl-ethylene at equal rates. This mechanism is given in Scheme III.

This mechanism proceeds by alkene insertion to give the 1° alkyl **31**. Intermediate **31** could undergo β-hydride migration and reductive elimination to yield **32**, which would account for the deuterium in the internal vinylic position. However, to incorporate deuterium in the terminal vinylic position, α-hydrogen migration of **31** to yield **33** was proposed. Intermediate **33** was in fast equilibrium with **34**, which could undergo β-D or β-H migration followed by reductive elimination to yield **35** or **36**, respectively. It is important to note that since 85% of the olefin product is D_2, the resulting D—Ir—H complex will repeat the mechanistic cycle with **35** and **32** to give an olefin-d_2 and an H—Ir—H complex. The driving force for this was the equilibrium isotope effects which will favor incorporation of deuterium in the C_α position due to the difference in zero point energy of the reactants (M-H:M-D =

Scheme III.

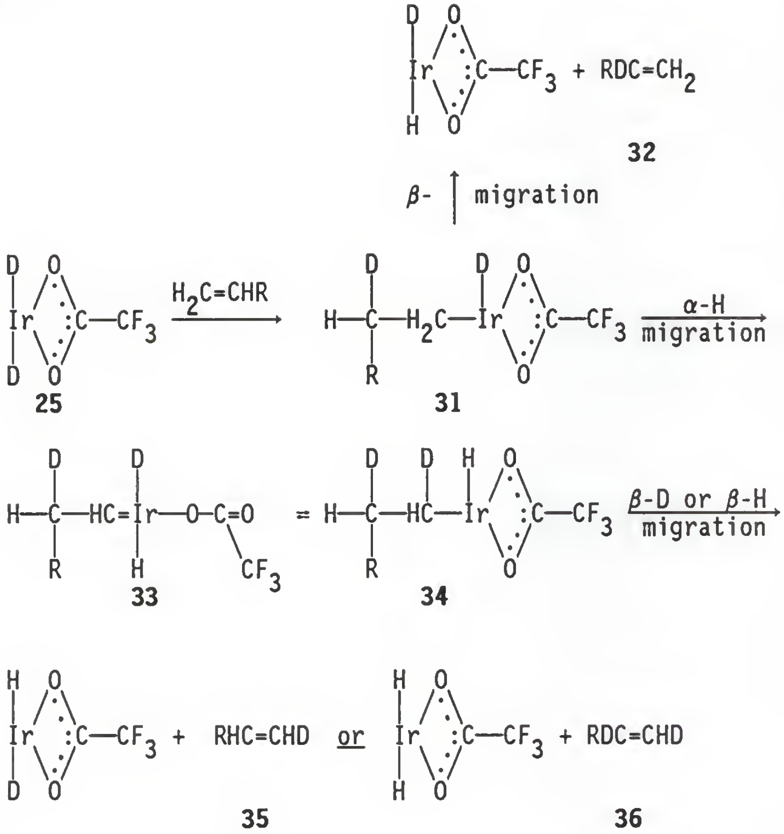

R = CMe_3

small $\Delta E_{\circ}$) vs. that in the products (C-H:C-D = large $\Delta E_{\circ}$). At each step in the mechanism, trifluoroacetate anion can associate or dissociate to preserve an 18-electron configuration about Ir. The incorporation of deuterium into each vinyl position at equal rates was a consequence from a balance between the equilibrium isotope effects of α-migration, which should favor **34** over **31**, and the β-migration kinetic deuterium isotope effect, which should favor H-migration.[19] Thus, the normal isotope effect to favor β-hydride migration over β-deuterium migration was negated by the inverse equilibrium isotope effect for α-hydride migration. These results suggested that α-hydride migration competes with β-hydride migration.

Bercaw and co-workers studied a competitive α- and β-hydride migration mechanism in the decomposition of $(C_5Me_5)_2Ta{=}C{=}CH_2(H)$.[63] They found that the α-migration product was favored over the β-migration product by a factor of 10^8 ($k_\alpha/k_\beta = 10^8$). However, this system was biased against β-migration due to unfavorable strain in the transition state such that $k_\alpha/k_\beta = 10^7$.[63] The reverse process of α-hydrogen migratory insertion in $(C_5Me_5)_2Ta{=}CH_2(H)$ was found to be 10^3 times faster than β-hydrogen migratory insertion in $(C_5Me_5)_2Ta(H_2C{=}CH_2)(H)$.[63]

Chisholm and co-workers studied competetive α- and β-hydrogen migration in tungsten clusters $W_2(CH_2R)_2(MeCCMe_2)(O\text{-}\underline{i}\text{-propyl})_4$ (R = Me, Et, or i-propyl).[64] The mechanism was thought to proceed by an initial β-H migration from the (CH_2R) group to form a common alkene intermediate, since formation of the products did not depend on the number of β-hydrogens in the metal-alkyl ligand. Competetive α- or β-hydrogen migration in the intermediate alkene complex led to formation of the two respective products. The rate and course (formation of α- or β-hydrogen migration products) of the reaction appeared to correlate with the relative stability of the alkene intermediate; the more sterically hindered alkenes dissociated faster to produce more of the β-migration product. When the intermediate was a less sterically hindered alkene, formation of the α-migration product became the dominant pathway.

Puddephat and co-workers studied the decomposition reaction of $(\mathrm{Cl})_2\mathrm{P}\overbrace{\mathrm{t\text{-}CH_2CHMeC}}\mathrm{Me_2}$ in $\mathrm{CHCl_3}$ initiated by pyridine association.[65] This decomposition mechanism had been previously thought to proceed by β-hydrogen migration.[66] However, Puddephat and co-workers repeated the experiment using $(\mathrm{Cl})_2\mathrm{P}\overbrace{\mathrm{t\text{-}CD_2CHMeC}}\mathrm{Me_2}$ in order to elucidate whether the mechanism proceeded by α-migration (eq 21) or β-migration (eq 22).

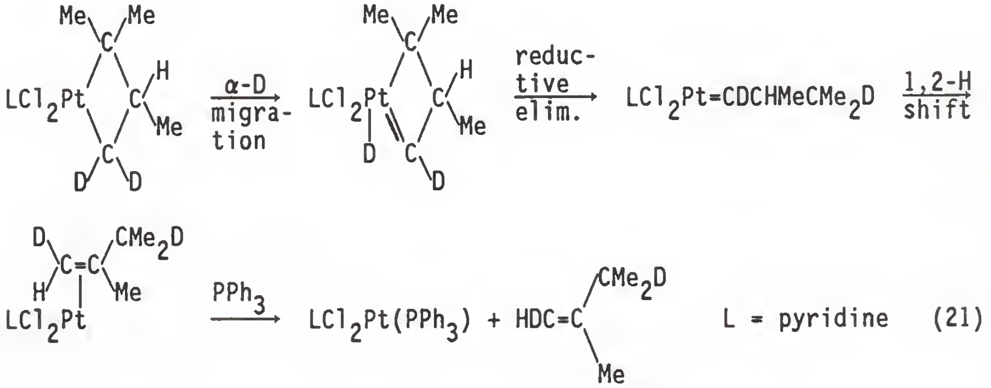

L = pyridine (21)

37

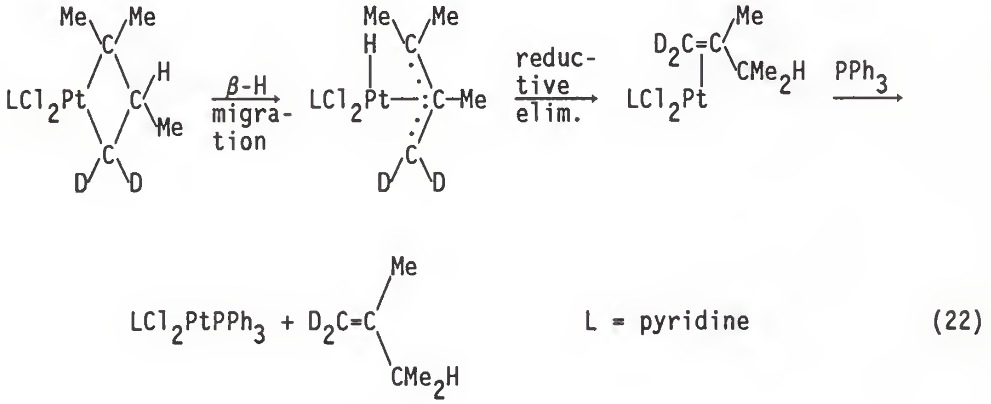

L = pyridine (22)

38

Note that the two deuterated alkenes **37** and **38** generated by the two separate mechanisms are different. Puddephat and co-workers observed only formation of the α-migration product **37** and no β-migration product. In the ^{1}H NMR spectrum of **37**, the $\mathbf{Me}_2$CD resonance appeared as a 1:1:1 triplet with $^3J(HD) = 1$ Hz. The =CHD resonance at δ 4.7 ppm integrated for 1 proton. In the ^{2}H NMR spectrum, equal intensity peaks were observed for the =CHD and the Me_2CD resonances at δ 4.7 and δ 2.2 ppm, respectively. The data were consistent with structure **37**, but not with the olefin **38** generated from the β-migration mechanism. Structure **38** should give a doublet for the $\mathbf{Me}_2$CH and a strong signal for the Me_2CH proton. The authors concluded that the platina(IV)cyclobutanes undergo α- rather than β-hydride migration.[65a]

α-Migration was also favored in the decomposition of certain silicon complexes (eq 23).[67] α-Migration was postulated to explain

$$Cl_3SiCF_2CFCl_2 \xrightarrow{\Delta} Cl_3SiF + \underset{\substack{\text{(product of}\\ \beta\text{-migration)}}}{F_2C{=}CCl_2\ (7\%)} + \underset{\substack{\text{(product of}\\ \alpha\text{-migration)}}}{FClC{=}CFCl\ (80\%)} \qquad (23)$$

the unimolecular isomerization reactions of carbenes in tungsten complexes[68] and iron complexes,[69] and was also established for the main group metals Li, Sn, Zn, and Hg (eq 24).[70]

$$LMCRR'R'' \longrightarrow LMR + CR'R'' \qquad (24)$$

$M = Li^+$, Sn, Zn, Hg: R = Halogen or OR: L = H

I.A.1.c. Ligand Substitution Reactions.

Ligand substitution reactions (eq 25) are among the most extensively studied class of reactions in organometallic chemistry.

$$M(CO)_x + yL \longrightarrow M(CO)L_y + (x-y)CO \qquad (25)$$

Other ligands besides CO may be bound to the metal; however, in the present study, all negative ion complexes were metal carbonyl complexes. The ligand L may be a π-type ligand (olefin, aromatic, diene, etc.), or a σ-type ligand (thioether, phosphine, amine, etc.). Several extensive reviews give a comprehensive understanding of the ligand substitution reaction.[71] Ligand substitution reactions follow two basic reaction mechanisms, (i) the dissociative mechanism (eq 26) and (ii) the associative mechanism (eq 27).[72]

$$M(CO)_x \underset{k_{-1}}{\overset{k_1}{\rightleftharpoons}} M(CO)_{x-1} + CO \xrightarrow[L]{k_2} M(CO)_{x-1}L \qquad (26)$$

$$M(CO)_x + L \xrightarrow{k_{diff}} M(CO)_xL \underset{k_{-2}}{\overset{k_2}{\rightleftharpoons}} M(CO)_xL \xrightarrow[-CO]{k_3} M(CO)_{x-1}L + CO \quad (27)$$

The dissociative mechanism proceeds by initial dissociation of a ligand from the starting metal complex as the rate limiting step with the rate = $k_1[M(CO)_x]$. This dissociation step generates the coordinatively unsaturated metal complex $M(CO)_{x-1}$ which rapidly coordinates the ligand, L. The associative mechanism proceeds by association of the ligand L to the metal complex, such that the rate = $k_{diff}k_2[M(CO)_x][L]$. In accordance with the 18-electron rule, the associative mechanism does not take place with 18-electron complexes unless the ligand adds to one of the ligands on the metal or a ligand changes its hapticity. Otherwise, attack of L on the metal would yield a 20-electron intermediate which is not known to occurr.[71c]

The metal carbonyls $Ni(CO)_4$, $Cr(CO)_6$, $Mo(CO)_6$, and $W(CO)_6$ react with ^{13}CO,[73] amines,[74] and phosphines[75] to give ligand exchange by the dissociative mechanism. This is the expected pathway since reaction via the associative mechanism would yield 20-electron species. However, $V(CO)_6^-$,[76] $Mn(CO)_6^+$,[77] $Re(CO)_6^+$,[77] and $Fe(CO)_5$[78] do not undergo ligand substitution reactions with either labeled CO or phosphines.

Considerable effort was expended in determining the labelizing effects of L on the CO ligands in $M(CO)_XL$ complexes,[71c] especially for $Mn(CO)_5L$ ($L = CO^+$, H, Cl, Br, I).[79] It was found that CO dissociation in $Mn(CO)_5Br$ was considerably more labile than with $Mn(CO)_6^+$ or $Mn(CO)_5H$. In addition, the CO groups that were cis to Br were found to be more labile than the trans-CO groups due to the π-donor ability of the lone pair on Br with an appropriate empty metal orbital.[79a-c] The ease of dissociation of CO ligands in $Mn(CO)_5L$ and $Re(CO)_5L$ decreased as $L = I < Br < Cl$.[79d-i] The reason for this is because iodine is the least electronegative and the most polarizable halide and donates the largest amount of electron density to the metal. This fact increases the Mn-CO backbonding character and greater Mn-CO bond strengths result. This explanation is consistent with the fact that both $Mn(CO)_5L$ and $Re(CO)_5L$ (L = I, Br, Cl) undergo CO exchange whereas $Mn(CO)_6^+$ does not.[79e-i] The CO ligands in $Mn(CO)_5L$ were found to be more labile than these in $Re(CO)_5L$ for a given L.[79j]

Metal carbonyl olefin complexes reacted by the dissociative mechanism to give products of ligand substitution.[80] The lability of the olefins decreased in the series C_2H_4 > dimethyl maleate > dimethyl fumarate >> maleic anhydride. This order was in accord with the increased back bonding from the metal to the olefins based on the electron withdrawing groups on the olefins. The ease of dissociation of a CO ligand in these complexes was Mo >> Cr > W.[80]

Ligand substitution reactions that proceeded by the associative mechanism do so with complexes which possess ligands that have variable coordination numbers. For example, in order to accommodate an incoming ligand, the bound allyl ligand can change from a η^3-C_3H_5 (π) to a η^1-C_3H_5 (σ) in order to accommodate the incoming two electron donor ligand.[81] This change in hapticity is well established for the allyl ligand and is an important factor in the catalytic activity of complexes with allyl ligands.[71c,81d-h] Examples of ligand substitution reactions by the associative mechanism are given in eqs 28 and 29. The

$$\begin{array}{ll}(\eta^3\text{-C}_3\text{H}_4\text{R})\text{Fe(CO)}_2\text{NO} + \text{L} \longrightarrow & (\eta^1\text{-C}_3\text{H}_4\text{R})\text{Fe(CO)}_2\text{(NO)L} \\ & \qquad\qquad\qquad\downarrow \\ & (\eta^3\text{-C}_3\text{H}_4\text{R})\text{Fe(CO)(NO)L} + \text{CO}^{81a\text{-}b} \end{array} \qquad (28)$$

R = 1-CH_3, 2-CH_3, 1-Cl, 2-Cl, 1-CN, 2-Br, 1-C_6H_5

L = PPH_3, PPh_2Et, P(n-Bu)$_3$, $P(OEt)_3$, $P(OCH_3)_3$

$$\begin{array}{ll}(\eta^3\text{-C}_3\text{H}_5)\text{Co(CO)}_3 + \text{L} \longrightarrow & (\eta^1\text{-C}_3\text{H}_5)\text{Co(CO)}_3\text{L} \\ & \qquad\qquad\downarrow \\ \text{L} = \text{PPh}_3,\ \text{P(OR)}_3 & (\eta^3\text{-C}_3\text{H}_5)\text{Co(CO)}_2\text{L} + \text{CO}^{81d\text{-}h} \end{array} \qquad (29)$$

allyl hapticity change in eq 28 was determined by infrared spectroscopy.[81a-b] However, the η^3-allyl ligand does not always change its hapticity as seen in the fact that the rate of decarbonylation of $(\eta^1\text{-}C_3H_5)Mn(CO)_5$ was ≈100 times slower than CO substitution in $(\eta^3\text{-}C_3H_5)Mn(CO)_4$ with PPh_3.[81c] This implied that $(\eta^1\text{-}C_3H_5)Mn(CO)_5$ was not an intermediate in the CO substitution reaction and a dissociative mechanism was postulated.

Other ligands which are well known to have variable hapticity are NO ($\eta^3 \rightleftharpoons \eta^1$) and cyclopentadienyl ($\eta^5 \rightleftharpoons \eta^3$).[71a-c] Indenyl complexes of rhenium, $(\eta^5\text{-}C_9H_7)Re(CO)_3$,[82] and manganese, $(\eta^5\text{-}C_9H_7)Mn(CO)_3$,[83] have been shown to undergo $\eta^5 \rightarrow \eta^1$ slippage as well as $\eta^5 \rightarrow \eta^3$.[84] Arenes are also thought to change hapticity by an $\eta^6 \rightarrow \eta^4 \rightarrow \eta^2$ "unzipping" mechanism.[85]

Condensed-phase ligand substitution reactions can occur with a variety of ligands. Since the substitution reactions are ultimately governed by thermodynamics, it would be advantageous to predict which reactions would be thermodynamically favored. For this reason, some representative bond dissociation energies are given in Table III.

I.A.1.d. N-H Bond Activation.

The ammoxidation of propylene is a major industrial process by which eight billion pounds of acrylonitrile were produced in 1985.[86] In this process, a mixture of propylene, ammonia, and air is passed over a heterogeneous mixture of bismuth molybdate catalyst (eq 30).[87] The mechanistically related reaction in eq 31, using the same catalyst, produces acrolein in higher yields at lower temperatures.[87d-e]

Table III. Bond Dissociation Energies for $L_nM\text{-}R$ complexes.

L_nM	R	$D°(L_nM\text{-}R)$[a]	L_nM	R	$D°(L_nM\text{-}R)$[b]
$Mn(CO)_4$	CO	23.6	$Cr(CO)_5$	CO	35.3[c]
$Re(CO)_4$	CO	43.5	$Fe(CO)_4$	CO	41.0[c]
$Mn(CO)_5$	$Mn(CO)_5$	16.0	$Re(CO)_5$	$Re(CO)_5$	30.6[a]
$Cr(C_6H_6)$	$\eta^4\text{-}C_6H_6$	38.9	CpMn	$\eta^6\text{-}C_6H_6$	121.9
$Mn(CO)_5$	Br	61.7	Co^+	$\eta^2\text{-}H_2C{=}CHCH_3$	37 ± 2[d]
$Mn(CO)_5$	Cl	72.7	Co^+	$\eta^4\text{-}C_4H_6$	52.0[e]
$Cr(CO)_3$	$\eta^6\text{-}C_6H_6$	42.5	Co^+	$\eta^2\text{-}C_2H_4$	37 ± 2[f]
$Mo(CO)_3$	$\underline{c}\text{-}C_7H_8$	60.0	Co^+	$\eta^3\text{-}C_3H_5$	72.0[e]
$W(CO)_3$	$\underline{c}\text{-}C_7H_8$	74.3	Fe^+	$H_2C{=}CHCH_3$	37 ± 6[g]
$Cr(CO)_3$	$\underline{c}\text{-}C_7H_8$	35.9	Fe^+	$\eta^4\text{-}H_2C{=}CHCH{=}CH_2$	48 ± 5[h]
MnCp	$\eta^5\text{-}C_5H_5$	64.2	$(OC)_5Cr^+$	CO	37 ± 5[i]
$Fe(CO)_4$	$\eta^2\text{-}C_2H_4$	23.6	Co^+	$\eta^6\text{-}C_6H_6$	68 ± 5[h]
$Fe(CO)_3$	$\eta^4\text{-}C_4H_6$	48.5	Fe^+	$\eta^6\text{-}C_6H_6$	55 ± 5[h]

[a] These are average values in kcal/mol.[88] [b] These are individual bond energies in kcal/mol. [c] Ref.[89]. [d] Ref. [90]. [e] Ref. [91]. [f] Ref.[92]. [g] Ref. [93]. [h] Ref. [94]. [i] Ref. [95].

$$H_2C{=}CHCH_3 + NH_3 + 3/2\ O_2 \xrightarrow[400\ °C]{Bi_2O_3/MoO_3} H_2C{=}CHCN + 3\ H_2O \qquad (30)$$

$$H_2C{=}CHCH_3 + O_2 \xrightarrow[300\ °C]{Bi_2O_3/MoO_3} H_2C{=}CHCHO + H_2O \qquad (31)$$

The active site in the ammoxidation of propylene (eq 30) consists of two Mo-dioxo groups, which serve to activate ammonia N-H bonds sequentially to form a Mo-imido complex, HN=Mo=NH. The mechanism proceeds by abstraction of an allylic hydrogen from propylene by a Bi=O unit to form a Bi-π-allyl complex, which adds to the imido to form a σ-N complex, $HN=Mo-NH-CH_2CHCH_2$. A second imido group then abstracts the α-H from the σ-N complex in a rate limiting step and ultimately, acrylonitrile is formed by a third α-H abstraction by a Mo-oxo group.[87] The higher temperatures needed for the ammoxidation (eq 25) compared to the oxidation (eq 26) can be explained by the higher activation energy needed for the second H abstraction in the σ-N complex, $HN=Mo-NH-CH_2CHCH_2$ versus the σ-O complex $O=Mo-O-CH_2CHCH_2$.[87d-e]

Other than the interest in the ammoxidation of propylene, reports of N-H oxidative addition with transition metal complexes were rare until Sappa and Milone reported their findings from the reaction of aniline with $Ru_3(CO)_{12}$ in 1973.[96] These authors found that after two hours in benzene, the product was $(H)Ru_2(CO)_{10}HNPh$ in 35% yield. Although a crystal structure could not be obtained, the authors proposed two structures, both of which included a bridging nitrogen to the Ru atoms. The difference in the proposed structures was whether hydrogen was bridging between two Ru atoms or merely σ-bound. This result suggested that direct N-H oxidative insertion of a metal complex into an amine N-H bond might be possible. This possibility was later confirmed by the reaction illustrated in equation 32,[97] and by similar reactions with $Ru_3(CO)_{12}$.[98]

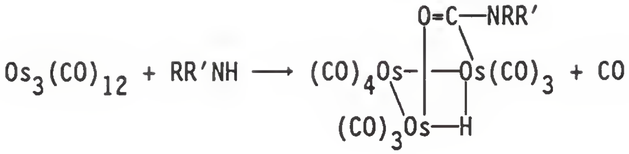

(32)

(a) R = Me, R′ = H; (b) R = R′ = Me; (c) R = n-propyl, R′ = H; (d) R = n-Bu, R′ = H; (e) R = Et, R′ = H

Amines are dehydrogenated by Ti clusters; the mechanism may involve N-H insertion. Armor reported the dehydrogenation of ammonia and simple amines by reaction with $CpTiC_5H_4TiCp_2$ (eq 33).[99] The

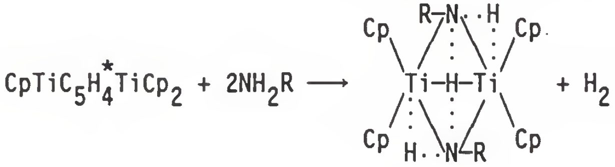

(33)

39

R = H, Et, t-Bu; $C_5H_4^* = \mu\text{-}(\eta^1{:}\eta^5\text{-cyclopentadienyl})$; Cp = $\eta^5\text{-}C_5H_5$

structure of **26** was determined by X-ray diffraction. However, the assignments of the hydrogens positions were not conclusive. Other techniques, e.g. infrared, ultraviolet-visivle, near-IR, raman spectroscopy, H/D exchange, hydride scavengers, stoichiometry, etc., led to the assigned structure.[99a]

Zirconocene and hafnocene dihydride complexes have also been observed to oxidatively insert into the N-H bonds of ammonia (eq 34).[100]

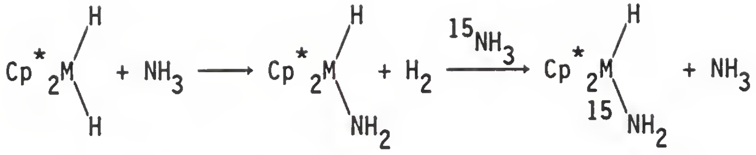

$$Cp^*{}_2M(H)_2 + NH_3 \longrightarrow Cp^*{}_2M(H)(NH_2) + H_2 \xrightarrow{{}^{15}NH_3} Cp^*{}_2M(H)({}^{15}NH_2) + NH_3 \qquad (34)$$

$Cp^* = \eta^5\text{-}C_5Me_5$; M = Zr, Hf

The first definitive example of N-H oxidative insertion by an iridium complex was demonstrated by Roundhill and co-workers in the reaction of $(Ph_3P)_2IrCl$ (in situ) with o-(diphenylphosphino)-N-benzoylaniline **40** at 25 °C in toluene (eq 35).[101] The ratio of **41**:**42**

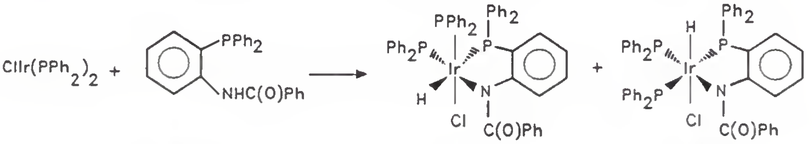

(35)

40 **41** **42**

was determined to be 1:2.4 as revealed by ^1H NMR. Compound **41** has hydride trans to one phosphorus and cis to two phosphorus atoms. Compound **42** has hydride trans to chloride and three magnetically inequivalent phosphines cis to hydride. Both compounds were oxygen sensitive, soluble in polar solvents, and were not separable by chromatography. Treatment of $(Ph_3P)_2IrCl$ with **40**, in which a deuterium atom was on nitrogen, gave the deuteride substituted compounds **41** and **42**, respectively.[101]

Ammonia was shown to oxidatively add to the iridium complex $(PEt_3)_2Ir(C_2H_4)_2Cl$ (eq 36).[102] In equation 36, the authors proposed oxidative insertion of the 14-electron species $(PEt_3)_2IrCl$ into the N-H bonds of ammonia. However, no mechanistic probing was performed other than the observation that the rate of ethylene production was much greater than the rate of ammonia consumption. Structure confirmation

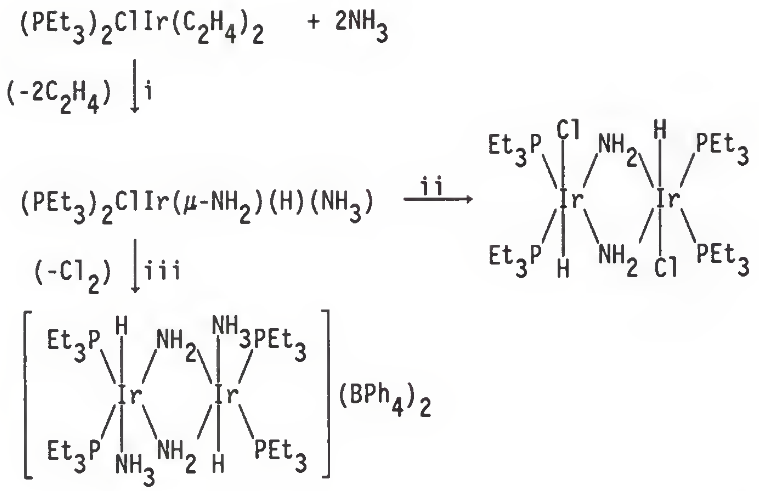

(36)

(i) 25 °C, 24 h, THF: (ii) 110 °C, 1 h, pyridine: (iii) $NaBPh_4$/acetone

of products was determined by ^{31}P NMR and ^1H NMR, IR, and X-ray diffraction.[102]

The most recent report of N-H activation involved the successful generation of an imidozirconocene complex by Bergman and co-workers (eq 37).[103] Mechanistic probes revealed that compound **44** could be trapped

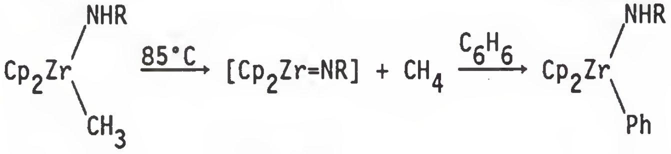

$$Cp_2Zr(NHR)(CH_3) \xrightarrow{85\,^\circ C} [Cp_2Zr{=}NR] + CH_4 \xrightarrow{C_6H_6} Cp_2Zr(NHR)(Ph) \qquad (37)$$

43 **44** **45**

Cp = η^5-C_5H_5 : R = t-Bu : Ph = C_6H_5

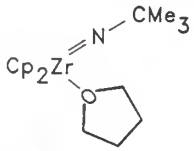

46

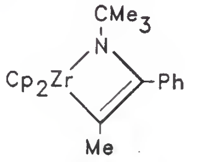

47

R′ = Me : R″ = Phenyl

by THF to give **46** or by 1-phenyl-1-propyne to give **47**. It was also shown that **45** reacted with 1-pheny-1-propyne to give the metallocycle **33**. In addition, thermolysis of **43** in the presence of excess Me_3CNH_2 yielded $Cp_2Zr(NHCMe_3)_2$ (**48**). These observations indicated that the mechanism proceeds by either α-hydride migration and reductive elimination of benzene from **45** or methane from **43** to yield the monomeric complex **44**. These results also suggested that the conversion of the amido complex **43** to the bis-amido complex **48** did not take place by transfer of a proton from the incoming amine to the departing methyl group, but instead proceeded by α-hydride migration followed by reductive elimination of CH_4 to give **44** followed by N-H activation.[103]

I.A.1.e. C-F Bond Activation.

Although transition metal complexes have wide utility in hydrocarbon transformations, the analogous chemistry of metal bonded fluorocarbons is largely unexplored. The greater abundance of systems capable of activating C-H bonds relative to C-F bonds is not surprising given the considerable strength of the C-F bond (125 kcal/mol in Ph-F vs. 110 kcal/mole in Ph-H)[104] even though the M-F bonds (relative to the M-H bonds) that are formed are very strong (Mn-F = 109.4 kcal/mol in MnF_2; Fe-F = 109.0 kcal/mol in Fe_2F_4).[105] Very few examples of oxidative insertion by a transition metal center into a C-F bond are known despite the continuing interest in fluoroinorganic chemisty.[106] Literature precedent for C-F bond cleavage includes the low yield, thermally unstable synthesis of trans-$Ni(PEt_3)_2(C_6F_5)F$ from $[Ni(PEt_3)_2(C_2H_4)]$ (in situ) and C_6F_6.[107] Bruce and co-workers observed orthometalation of $C_6H_5N{=}NC_6F_5$ by $Mn_2(CO)_{10}$ to give $[C_6H_5\overline{N{=}NC_6F_4Mn}(CO)_4]$.[108] A similar orthometalation reaction was also observed in the reaction of $MeRu(PPh_3)_2(\eta^5\text{-}C_5H_5)$ with perfluoroazobenzene to give $\overline{RuC_6F_4N{=}N}C_6H_5(Ph_2PC_6H_4\text{-}\eta^5\text{-}C_5H_4)$ in low yield.[109] Photochemical activation of an aromatic C-F bond has been reported in a 1,4-bis(pentafluorophenyl)tetrazine ligand coordinated to cobalt.[110] However, the fate of the fluorine atoms, and hence the mechanism, was not determined in the above cases.

One definitive example of intramolecular oxidative insertion into an aryl C-F bond in a tungsten complex has been reported (eq 38).[111]

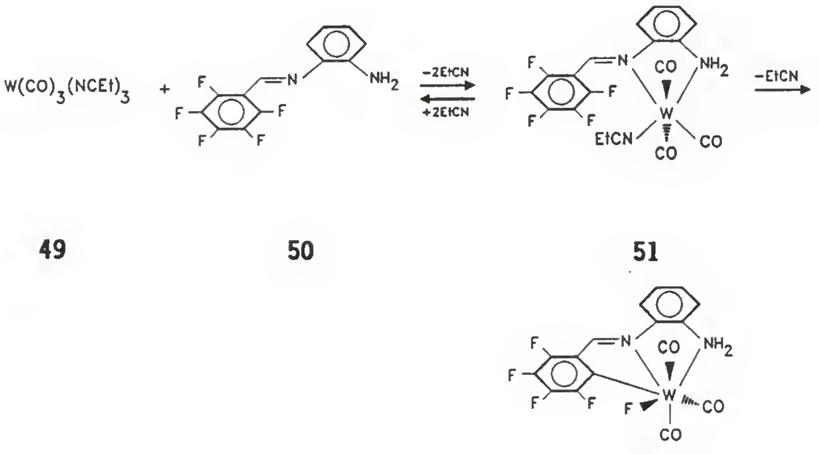

49 **50** **51**

(38)

52

Pentafluorobenzaldehyde reacted with 1.0 equivalent of 1,2-diaminobenzene in ethanol to give the yellow, crystalline Schiff base **50** in 92% yield. Reaction of **50** with **49**[112] at room temperature in THF provided the complex **52** in 69% yield.[111] The structure of **52** was assigned by IR, ^1H and ^{19}F NMR, and by single-crystal X-ray diffraction. The intermediate **51** could be isolated as a dark purple solid in 82% yield by conducting the reaction in methylene chloride and direct precipitation with hexanes. The mechanism of this reaction was not postulated, but must involve oxidative insertion of W into the C-F bond. Factors that may explain the facile C-F insertion include the chelating nature of the ligand which reduces the entropic barrier to reaction. Also, the conjugated, planar metallocycle was quite stable[113] and thermodynamic considerations suggested that the M-F bond was quite strong despite the low oxidation state of the metal.[114]

I.A.2. Gas-Phase Background Literature.

Gas-phase ion/molecule reactions yield information about an ions intrinsic reactivity compared to condensed-phase results. This intrinsic reactivity is derived from the absence of solvent or counter ion effects which is inherent in the condensed-phase. These effects, in some cases, can greatly alter the rate and/or product forming channels in a particular reaction. However, most of the underlying principles and mechanisms established in the condensed-phase are directly related to the understanding of the gas-phase results. In many cases, the condensed phase results are the basis for the gas-phase experiments.[115] Both areas of positive[116] and negative[5] transition metal ion chemistry have been recently reviewed.

The techniques currently employed to study gas-phase ion/molecule reactions of organometallic complexes include (i) ion-beam apparatus,[117] (ii) ion cyclotron resonance[118] (ICR) and fourier transform mass spectrometry[119] (FTMS), both of which use a trapped ion cell in a magnetic field, and (iii) flowing afterflow apparatus (FA),[7,120] and (iv) high pressure mass spectrometry (HPMS).[121] Most of the early work in gas-phase ion/molecule reactions was performed using ICR or FTMS methods.[122] In the ICR/FTMS experiment, the double resonance technique[123] allows the exclusive observation of one or more ions in the trapped ion cell while the other ions are ejected. This technique allows for clean ion/molecule reactions to be observed with a variety of neutral gaseous reagents.

There has been substantial effort in gas-phase ion/molecule transition metal chemistry toward the determination of ligand bond dissociation energies of the ion complexes (Table III) and other thermochemical data. Before the existence of the gas-phase methods, the best values available were derived from bomb calorimetry, which gave the average bond strengths of all neutral ligand-metal bonds in a particular complex.[88,124] Today, these values are mainly derived from the ion-beam technique which measures the threshold kinetic energy of a monoenergetic beam of ions that is required to break a metal-ligand bond.[125] Gas-phase ion/molecule techniques have also been used to determine gas-phase basicities,[122b,126] acidities,[127] electron affinities,[121,128] and ionization potentials[129] of various neutral transiton metal complexes.

I.A.2.a. C-H Bond Activation.

C-H bond activation by transition metal positive and negative ions has been well studied in the gas-phase.[5,116,130] Positive atomic transition metal ions are known to react with alkanes by both C-H and C-C bond activation.[90,131,132,133] Freiser observed that Fe$^+$ would oxidatively add to both the C-H and C-C bonds of butane (eq 39).[131a] The proposed mechanism is given in Scheme IV.[131a]

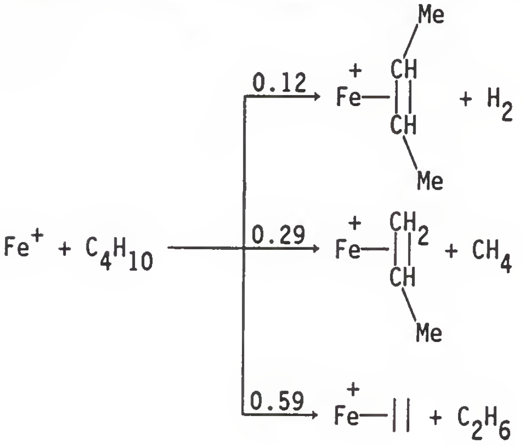

(39)

Scheme IV.

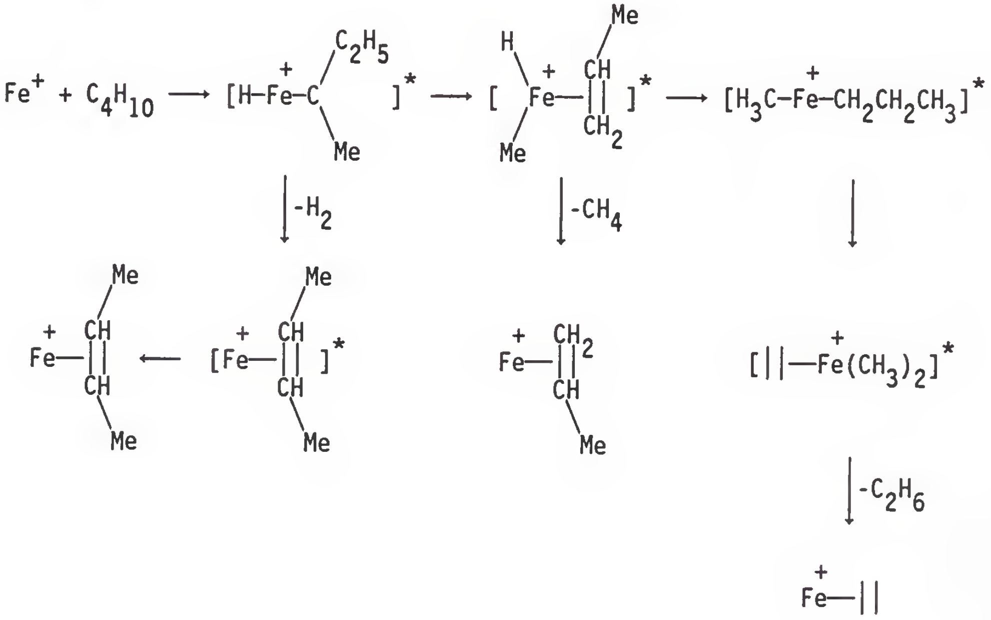

Some typical examples of products obtained from the reaction of atomic metal cations with alkanes are given in Table IV. Although C-C oxidative insertion is common in atomic positive ion chemistry, this process has yet to be observed in either condensed-phase or gas-phase negative ion chemistry.[5] The absence of C-C insertion in condensed-phase can be explained by formation of the relatively weak M-C bonds which constitute an overall endothermic process.[5,10b] However, D°(Fe^+-CH_3) = 69 ± 5 kcal/mol,[134] while D°(Fe^+-H) = 58 ± 5 kcal/mol in the gas-phase.[132d] The increased stabilization of the M^+-C bond relative to the solution phase M-C bond allows C-C oxidative insertion to be observed in the gas phase. To date, there have been no reports of exothermic oxidative insertion by a positive transition metal complex ion into the C-H bonds of methane. Beauchamp and co-workers observed the oxidative insertion and reductive elimination of H_2 via α-hydride migration in the reaction of methane with Co^+, but calculate the reaction to be 1.1 eV endothermic.[129a]

Gas-phase negative ion chemistry has also contributed to the examples of C-H insertion. McDonald and Jones found that the 14-electron complex, $Mn(CO)_3^-$, oxidatively inserted into the C-H bonds of ethane, propane, and isobutane, while the 15-electron $Mn(CO)_4^-$ and 17-electron $Mn(CO)_5^-$ did not react ($k < 10^{-13}$ cm^{-3} $molecule^{-1}$ s^{-1}) with alkanes.[130,135] Significantly, these authors found that the relative rates of oxidative insertion into primary (1°), secondary (2°), and tertiary (3°) C-H bonds were 3° > 2° > 1°.[130,135] $Mn(CO)_3^-$ reacted with the linear alkanes C_nH_{2n+2} (n = 2, 3, 4, 5, 6, 7) to give the (adduct-H_2) negative ion via oxidative insertion into a C-H bond

Table IV. Product Distributions of Atomic Transition Metal Cations with Alkanes.

		Neutral Product Lost					
Ion	alkane	H_2	$2H_2$	CH_4	(CH_4+H_2)	C_2H_4	C_2H_6
Sc^{+a}	_n_-butane	0.37	0.22	0.01	0.02	0.36	0.02
Ti^{+b}	ethane	1.00	---	---	---	---	---
Ti^{+b}	propane	1.00	---	---	---	---	---
Ti^{+b}	_n_-butane	---	1.00	---	---	---	---
Fe^{+b}	ethane	No Reaction					
Fe^{+b}	propane	0.30	0.70	---	---	---	---
Fe^{+b}	_n_-butane	0.12	0.29	0.59	---	---	---
Co^{+c}	propane	0.59	---	0.41	---	---	---
Co^{+c}	_n_-butane	0.29	---	0.12	---	---	0.59
Ni^{+c}	propane	0.20	---	0.80	---	---	---
Ni^{+c}	_n_-butane	0.24	---	0.17	---	---	0.59
Rh^{+d}	ethane	1.00	---	---	---	---	---
Rh^{+d}	propane	0.94	0.06	---	---	---	---
Rh^{+d}	_n_-butane	---	1.00	---	---	---	---
V^{+e}	_n_-butane	0.13	0.87	---	---	---	---
Mn^{+f}	This ion does not react with alkanes						
Cr^{+f}	This ion does not react with alkanes						

[a] Ref. 132e. [b] Ref. 131a. [c] Ref. 132c. [d] Ref. 131b. [e] Ref. 131e. [f] Ref. 132a.

followed by reductive elimination of H_2.[130]

The 13-electron complex $Fe(CO)_2^{\bullet -}$ also reacted with linear alkanes C_nH_{2n+2} (n= 2, 3, 4, 5) to give the (adduct-H_2) negative ion.[136] As was the case with $(OC)_{4,5}Mn^-$, the less coordinatively unsaturated ions, $(OC)_{3,4}Fe^{\bullet -}$ did not react ($k < 10^{-13}$ cm^3 $molecule^{-1}$ s^{-1}) with alkanes.[136] To date, the only negative ion observed to react with methane was $Fe(CO)_2^{\bullet -}$ to yield the total adduct negative ion.[137] However, the product generated from the reaction of $Fe(CO)_2^{\bullet -}$ with CH_4 was too small to perform any stucture determining experiments upon. The reaction of neopentane with $Fe(CO)_2^{\bullet -}$ also gave the total adduct negative ion, but in higher yield.[137] This total adduct negative ion was observed to undergo a single H/D exchange in a reaction with D_2. This and other results established the presence of one unique hydrogen so that the structure of the total adduct negative ion was that of oxidative insertion of Fe into a C-H bond. By analogy, the reaction of $Fe(CO)_2^{\bullet -}$ with methane was believed to give $(OC)_2Fe(H)(CH_3)^{\bullet -}$.

I.A.2.b. β- and α-Hydride Migration.

β-Hydride migrations are common in gas-phase ion chemistry. Both positive and negative ions formed by C-H oxidative insertion reaction will usually reductively eliminate H_2 if a β-hydrogen is present in the complex.[130,131,132,133,135,137] Conversely, reports of α-hydride migration are almost non-existent in the gas-phase literature. As previously mentioned, Beauchamp and Armentrout observed the (adduct-H_2) positive ion in reactions of Co^+, Ni^+, and Fe^+ with methane. However, the product distributions of the (adduct-H_2) ion were small relative to the major product forming channel and the overall reaction was calculated to be endothermic.[129a,132c] Freiser and co-workers found that atomic transition metal cations react with ammonia to give the (adduct-H_2) positive ion.[138] The mechanism for this transformation must involve oxidative insertion into an N-H bond followed by α-migration and reductive elimination of H_2. There have been no reports of α-hydrogen migration in gas-phase negative ion chemistry.

I.A.2.c. Ligand Substitution Reactions.

In contrast to the condensed phase, gas-phase ligand substitution reactions usually proceed by an associative mechanism (eq 27) for complexes that possess ligands that can change hapticity to accomodate the incoming donor ligand. For complexes with ligands that cannot change hapticity, ie., $(OC)_4Fe^{\bullet -}$, substitution can occur through collision with a neutral substrate L to form a complex bound by ion-dolple attractive forces $(L/(OC)_3Fe/CO)^{\bullet -}$ which can then undergo ligand substitution. The unimolecular dissociative mechanism known in the condensed phase cannot occur in the gas phase as once a metal ion complex is formed and thermally equilibrated, there is no energy available to effect ligand dissociation other than by collision with a neutral substrate. In addition, displacement of ligand L from the metal complex ML_n^- by L' requires that $D°(L'–ML_{n-1}^-) > D°(L–ML_{n-1}^-)$ since only exothermic or thermoneutral reactions can be observed in the gas phase when the entropy change is small.[139]

One of the first ligand substitution reactions to appear in transition metal gas-phase negative ion chemistry was reported by Beauchamp and Corderman (eq 40-42).[140] However, these authors observed

$$CpCo(CO)_2^{\bullet -} + NO \longrightarrow CpCo(NO)^{\bullet -} + 2CO \quad (40)$$

$$CpCo(CO)^{\bullet -} + NO \longrightarrow CpCo(NO)^{\bullet -} + CO \quad (41)$$

$$CpCo(CO)^{\bullet -} + PF_3 \longrightarrow CpCo(PF_3)^{\bullet -} + CO \quad (42)$$

$Cp = \eta^5\text{-}C_5H_5$

that both of the parent ions $CpCo(CO)_{1,2}^{\bullet -}$ failed to react with C_2F_4, NH_3, NMe_3, PMe_3, HCN, and ethylene oxide. These results were interpreted in terms of the π-acceptor abilities of the various ligands. PF_3 and NO were considered to be stronger π-acceptors than CO, while the unreactive ligands above were weaker π-acceptors than CO.[140] The implication was that the relative metal-ligand bond strengths were largely determined by the ability of L to backbond with the metal and that the σ-donor ability of L was less important. This was in marked contrast to the conclusions previously determined about the metal-ligand bond strengths in $CpNi^+$, where $D°(CpNi{-}L^+)$ was shown to be mainly dependent on the σ-donor ability of L.[141]

Recently, McDonald and Schell reported numerous ligand substitution reactions with the 17-electron complexes $(OC)_4Fe^{\bullet -}$,[142] $(OC)_5Cr^{\bullet -}$,[142] $(OC)_4MnH^-$,[142] $(OC)Fe(NO)_2^{\bullet -}$,[143] $(OC)_2Co(NO)^{\bullet -}$,[143] $(\eta^3\text{-}C_3H_5)Co(CO)_2^{\bullet -}$,[143] $(\eta^1\text{-}C_3H_5)Co(CO)_3^{\bullet -}$,[143] and $(\eta^3\text{-}Cp)Co(CO)_2^{\bullet -}$.[143] The reactions of the metal ion complexes that possess $\eta^3\text{-}C_3H_5$, NO, and Cp ($\eta^5\text{-}C_5H_5$) ligands were proposed to proceed by an associative mechanism where the bound ligands change their hapticities to accomodate the new incoming ligand ie., $\eta^3\text{-}C_3H_5 \rightarrow \eta^1\text{-}C_3H_5$, $\eta^3\text{-}NO \rightarrow \eta^1\text{-}NO$, and $\eta^3\text{-}Cp \rightarrow \eta^1\text{-}Cp$, resulting in 17-electron adduct intermediates. This supposition was consistent with the observation of reactant addition products and observable P_{He} effects.[143] For the complexes containing only ligands with constant hapticity, the mechanism for substitution was proposed to occur either via a Lewis acid-base intermediate as in the case of reaction with SO_2, by reaction with an incoming 1-electron donor ligand as in the case with NO or O_2, or by formation of a close orbiting collision complex bound by ion-dipole attractive forces as in the reaction of $(OC)_4Fe^{\bullet -}$ with and PF_3.[142] It is interesting to note, that in the reaction of $(OC)_4MnH^-$ with O_2, a primary product is the formate anion HCO_2^-. The proposed mechanism is shown in Scheme V. This was the first reported example of a migratory insertion reported in gas-phase negative ion chemistry.[142]

Scheme V.

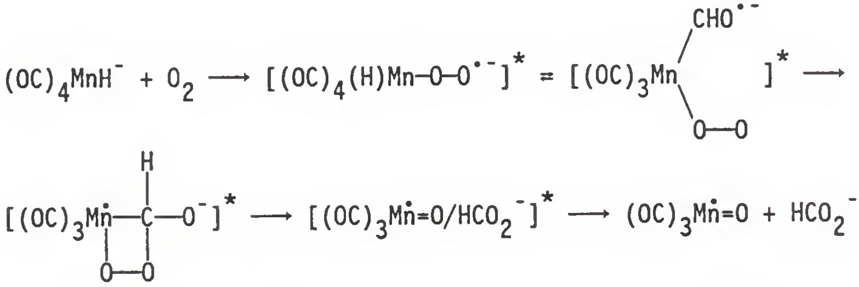
$(OC)_4MnH^- + O_2 \longrightarrow [(OC)_4(H)Mn{-}O{-}O^{\bullet -}]^* = [(OC)_3Mn(CHO^{\bullet -})(O{-}O)]^* \longrightarrow$
$[(OC)_3\dot{M}n{-}C(H){-}O^-]^* \longrightarrow [(OC)_3\dot{M}n{=}O/HCO_2^-]^* \longrightarrow (OC)_3\dot{M}n{=}O + HCO_2^-$

McDonald and co-workers have used the FA to study the ligand addition and substitution reactions of $Fe(CO)_3^{\bullet -}$ (eq 43).[6a] In eq 43a

$$Fe(CO)_3^{\bullet -} + L \xrightarrow{a} (CO)_3Fe(L)^{\bullet -} \quad (43a)$$
$$\xrightarrow{b} (CO)_2Fe(L)^{\bullet -} + CO \quad (43b)$$
$$\xrightarrow{c} (CO)Fe(L)^{\bullet -} + 2CO \quad (43c)$$

addition was observed when L = N_2, H_2, CO, $H_2C{=}CHCH_3$, and $H_2C{=}C{=}CH_2$. This addition was formally a termolecular reaction as the excess energy of the collision complex must be removed by the helium buffer gas. An oxidative insertion structure was proposed for product of reaction when

$L = H_2$, $(OC)_3Fe(H)_2^{\bullet -}$. Substitution of one CO ligand was observed (eq 43b) when L = HC≡CH. The addition product when L = allene, $(OC)_3Fe(C_3H_4)^{\bullet -}$, was observed to undergo a secondary ion/molecule substitution reaction with allene to give $(OC)_2Fe(C_3H_4)_2^{\bullet -}$ and CO. McDonald proposed that the structure of $(OC)_2Fe(C_3H_4)_2^{\bullet -}$ involved two η^2-π-bound allene molecules. A π-bound structure, similar to that of $(OC)_2Fe(C_3H_4)_2^{\bullet -}$, was also proposed for the acetylene adduct. Loss of two CO ligands was observed (eq 43c) when $L = CH_3Br$, with the proposed mechanism involving oxidative insertion into the C-Br bond.[6a] In addition, Br-atom transfer was also observed yielding $(OC)_3FeBr^-$. McDonald noted that none of the ligands L reacted with $Fe(CO)_4^{\bullet -}$ except for PF_3, emphasizing that this was expected since $Fe(CO)_4^{\bullet -}$ is formally a 17-electron complex and that any incoming two electron donor ligand would result in a 19-electron intermediate. The subtitution product observed in the reaction of $(OC)_4Fe^{\bullet -}$ with PF_3 was proposed to occur through a complex bound by ion-dipole attractive forces $(PF_3/(OC)_3Fe/CO)^{\bullet -}$, which would not formally be considered a 19-electron complex.

I.A.2.d. N-H Bond Activation.

Although uncommon, N-H bond activation was known in gas-phase transition metal ion chemistry. As previously mentioned, Freiser and co-workers reported oxidative insertion into an N-H bond in ammonia by atomic transition metal cations (eq 44).[138] Freiser proposed that the

$$M^+ + NH_3 \longrightarrow MNH^+ + H_2 \qquad (44)$$

M = Sc, Ti, V, Y, Zr, Nb, La, Ta

mechanism of dehydrogenation must occur via oxidative insertion into an N-H bond followed by α-hydrogen migration and reductive elimination of H_2.

Early work by Allison and Radecki indicated that reaction of Co^+ with simple amines gave exclusively the (adduct-H_2) positive ion.[144] Allison proposed a mechanism which involved initial insertion into the N-H bond of the amine followed by β-elimination of H_2 (eq 45).[144] The

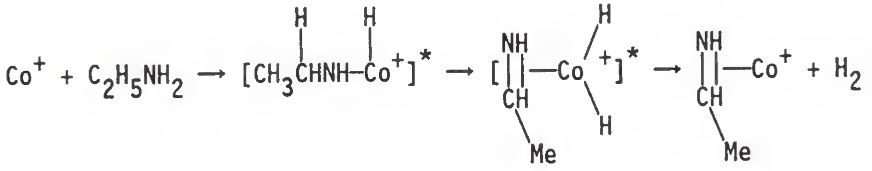

$$Co^+ + C_2H_5NH_2 \rightarrow [CH_3\overset{H}{\overset{|}{C}}HNH{-}\overset{H}{\overset{|}{Co^+}}]^* \rightarrow [\,\overset{NH}{\underset{\underset{\diagdown Me}{CH}}{\|}}{-}\overset{H}{\underset{H}{Co}}{}^+\,]^* \rightarrow \overset{NH}{\underset{\underset{\diagdown Me}{CH}}{\|}}{-}Co^+ + H_2 \quad (45)$$

mechanism was tested using $C_2H_5ND_2$ as the neutral substrate. The product of the reaction was the (adduct-HD) positive ion which is consistent with N-H insertion. However, neither the isotope effect nor rate constant for the reaction were reported.[144] In addition, there was no (adduct-H_2) product ion in the reaction of Co^+ with either _tert_-butylamine or triethylamine. In the former case, N-H insertion would yield an intermediate with no β-hydrogens to reductively eliminate H_2, while in the latter case, there are no N-H bonds for the oxidative addition reaction. All of the above observations are consistent with initial N-H insertion,[144] but it seems odd that C-H oxidative insertion was not observed, especially in the reaction with triethyl amine where primary C-H oxidative insertion would yield an intermediate with β-hydrogens acessible for elimination.

The only report of N-H activation in a transition metal negative ion complex involved the ICR study of $(OC)_3Cr^{\bullet -}$ with simple amines.[145] In this study, the major reaction pathways (among others) were formation of the (adduct-CO) and (adduct-H_2) negative ions. Deuterium labelling experiments provided information that suggested that the mechanism of product formation arises from initial N-H insertion rather than C-N insertion. However, the multitude of product forming channels in these reactions suggested that the metal ion complex was in an electronically or vibrationally excited state.

I.A.2.e. C-F Bond Activation.

C-F bond activation in a gas-phase transition metal complex was unknown until the recent report by McDonald and Jones of the reaction of $(OC)_3Mn^-$ with C_2F_6 and several fluorinated ethylenes (eq 46-49).[146]

$$(OC)_3Mn^- + C_2F_6 \longrightarrow Mn(C_2F_4) + F_2 + 3CO \text{ (or } COF_2 + 2CO) \quad (46)$$

$$(OC)_3Mn^- + C_2F_4 \longrightarrow Mn(C_2F_4)^- + 3CO \quad (47)$$

$$(OC)_3Mn^- + HFC{=}CF_2 \longrightarrow Mn(C_2HF_2)^- + 3CO \quad (48)$$

$$(OC)_3Mn^- + HFC{=}CHF \longrightarrow Mn(C_2H_2F_2)^- + 3CO \quad (49)$$

Reactions 47-49 were fast with rate constants on the order of $\approx 5 \times 10^{-10}$ cm^3 molecule^{-1} s^{-1}. The astonishing product ions corresponding to (adduct-3CO) were indicative of highly exothermic reactions which requires generation of strong new bonds, e.g. Mn-F. Characterization of the product ions structures was obtained from ligand substitution reactions with SO_2. In each case, the product negative ions was $F_2Mn(SO_2)^-$ formed by substitution of the corresponding acetylene (C_2F_2, C_2HF, and C_2H_2, respectively) for SO_2.[146] These results confirmed oxidative insertion of Mn into the C-F bonds of the alkenes. Further, the data suggested that the general structure of the (adduct-3CO) negative ion was **53.**[146]

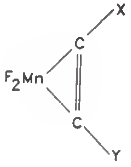

53

X,Y = H or F

I.B. Ojectives of this Investigation.

The objectives of this investigation were to (1) determine the kinetics and negative ion products from the reactions of $(OC)_2Fe^{\bullet -}$ and $(OC)_3Mn^-$ generated from dissociative electron attachment (DEA) of $Fe(OC)_5$ and $Mn_2(OC)_{10}$, respectively, with various neutral reagents including amines, fluorine containing molecules and ethers, and (2) to compare the reactivity of the 13-electron complex $(OC)_2Fe^{\bullet -}$ to the 14-electron complex $(OC)_3Mn^-$ based on the kinetic and product data.

I.C. Experimental.

I.C.1. General Procedure for the Study of Ion/Molecule Reactions in the Flowing Afterglow.

The gas-phase studies of negative ions were carried out in a flowing afterglow (FA) apparatus (Figure 1). The FA consists of three distinct regions, an ion production region, an ion/molecule reaction region, and an ion detection region. Helium is introduced into the the upstream end of the flow tube with 10% of the helium flow added below the electron gun and the remaining 90% added via the inlet through a glass frit at the left of the flow tube. A fast flow velocity ($\bar{\underline{v}} = 80$ m/s) and a modest pressure ($P_{He} = 0.5$ to 0.9 torr) are established and maintained during the experiment by a large, fast pumping system. The ions of interest are continuously generated by adding small concentrations of neutral precursors via inlet 1 located just downstream of the electron gun in the Pyrex glass side-arm.[147]

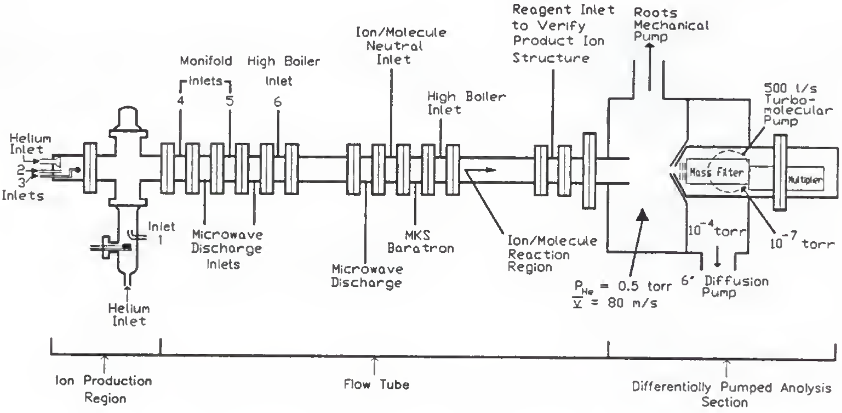

Figure 1. Schematic diagram of the flowing afterglow.

The added neutral precursor molecules undergo dissociative electron attachment (DEA) with the electrons present in the plasma in the vicinity of the electron gun to produce the ions of interest. The initially formed, vibrationally excited, negative ions are then cooled to their ground vibrational and electronic states in the next 70 cm of the flow tube through numerous collisions with the helium buffer gas. These ground state ions are then allowed to react with neutral reactant gases added via the neutral inlet port, and the ion/molecule reactions occurr in the final 65 cm of the flow tube. The helium flow is sampled through 1 mm orifices in two molybdenum nose cones into a differentially pumped compartment operating at $\approx 10^{-7}$ torr containing the quadrupole mass filter and electron multiplier which continuously monitor the ion composition of the flow. In this way, the signal intensity of starting and product ions are monitored as a function of the concentration of the added neutral reactant.

I.C.2. The Flow Tube.

The flow tube is a stainless steel pipe (Supplier: Hostettler Metals) with dimensions of 7.15 cm i.d. x 135 cm long of modular design consisting of various lengths of tube and inlet sections bolted together by mated flanges with O-ring seals. This design allows flow tube sections to be added or changed based on the experimental needs. The neutral inlet ports located along the length of the flow tube are glass tubing (2.5 mm i.d.) bent into doughnut-shaped ports with a diameter slightly smaller than the inside diameter of the flow tube. Small holes are punched along the inside of the glass ring so that the neutral gases are directed toward the center of the helium flow. The flow tube pressure is measured by a MKS Baratron manometer (model PDR-5b, MKS Instruments, Inc.), while the flow of helium is measured with a precalibrated tri-flat flowmeter (Fisher and Porter #449-306).[148] The helium flow velocity and flow tube pressure were adjusted by throttling a gate valve which connects the FA to a Stokes Roots blower/mechanical pump (model 1722-S) via an 8 in. diameter aluminum pipe.

I.C.3. The Ion Production Region.

The electron gun is located in the Pyrex glass side-arm (8 in. long x 45 mm diameter) in the upstream end of the flow tube. It consists of either a 0.0002 in. x 0.0027 in. x 1.25 in. long thorium oxide coated iridium filament (Electron Technology) or a 0.0001 in. x 0.0030 in. x 1.25 in. long uncoated rhenium filament (H. Cross Inc.) and an accelerating grid made of fine mesh tungsten screen. The power supply for the filament was a Hewlett Packard series MPB-S (model 6286A) DC power supply, capable of delivering 0 to 24 volts and 0 to 12 amps. The accelerating voltage power supply was a Keithley 245 high voltage power supply (model 49099 A), capable of supplying 0 to ±1000 V and 0 to 150 ma. The current between the filament and mesh grid was continuously monitored by a Micronta multimeter (Radio Shack) and varied between 10 uA and 10 mA. In order to reduce background noise, the Extrel C-50 mass spectrometer, filament DC power supply, high voltage power supply, and multimeter were connected to a common ground.

I.C.4. Differentially Pumped Analysis Section.

Since the Extrel C-50 mass spectrometer only gives good resolution at pressures < 10^{-6} torr, a differentially pumped analysis section was utilized. The fast helium flow was sampled through a 1.0 mm orifice in the first of two molybdenum nose cones (Amax Specialty Metals Corp.). The chamber directly behind the first nose cone was maintained at a pressure of ≈ 10^{-4} torr by a Varian 6" oil diffusion pump backed by a Welch model 1397 mechanical pump. The cylindrically shaped third differentially pumped chamber located behind the second molybdenum nose cone with a 1 mm orifice, houses the quadrupole mass filter and electron multiplier. This latter chamber is maintained at ≈ 10^{-7} torr by a Pfeiffer TPH-500 turbomolecular pump backed by a Welch model 1402 mechanical pump. With this pumping scheme, the ion/molecule reactions can be carried out at pressures between 0.4 to 1.2 torr, while the ion mass analysis with the quadrupole mass filter and electron multiplier is done at pressures of 2 to 7 x 10^{-7} torr. Pressures above 1 x 10^{-6} torr severly affect the unit mass resolution of the Extrel C-50 mass spectrometer.

I.C.4.A. Quadrupole Mass Filter and Electron Multiplier.

The nominal range of the Extrel C-50 mass filter is 10 to 1200 amu. A channeltron electron multiplier is used to count the ions and a conversion dynode (Figure 2) reduces mass discrimination. In Figure 2, the negatively charged ions exiting the mass filter pass through an aperture in the grounded shield and are attracted to the conversion dynode held at +4 KeV. When the negative ions strike the conversion

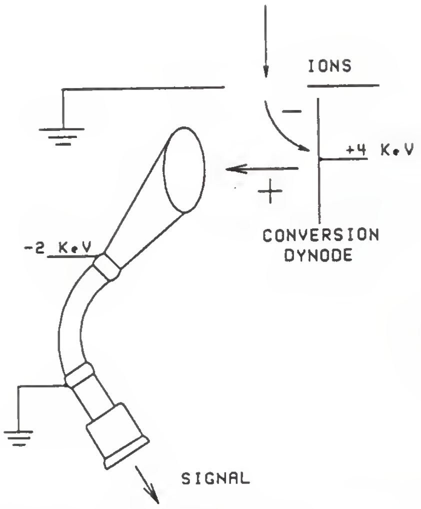

Figure 2. Conversion Dynode for Negative Ion Detection.

dynode they undergo charge stripping to produce positively charged ions and effect sputtering from either the metal of which the conversion dynode is made or from the gases adsorbed on its surface. These positive secondary ions are then attracted to the funnel of the channeltron held at -2 KeV.

The advantage of using a conversion dynode multiplier for negative ion detection is that the ions strike the conversion dynode at high potential energy. The secondary emission ratio for heavier ions is increased more than that of the lighter ions such that the mass discrimination of the multiplier is reduced.

The negative ions sampled from the flow tube are focused into the quadrupole mass filter by a series of ion lenses. The potential settings for these lenses are listed in Table V for each of the negative ions investigated.

Table V. Lens Settings and Potentials for Optimized Signals in the Extrel C-50 Mass Spectrometer.

Lens #	$Mn(CO)_3^-$	$Fe(CO)_2^{\bullet -}$
1	+ 84.5 mV	+ 69.4 mV
2	+ 80.9 mV	+114.1 mV
3	+ 23.7 mV	+ 31.8 mV
4	+ 29.7 mV	+ 31.2 mV
5	+ 7.9 mV	+ 13.6 mV
6	+ 2.3 mV	+ 4.6 mV
1st nose cone	- 5.1 V	- 1.2 V
1st NC holder	- 24.0 V	- 24.0 V
2nd nose cone	+ 24.0 V	+ 24.0 V

I.C.5. Kinetics

Kinetics of the bimolecular ion/molecule reactions in the FA were determined under psuedo-first-order conditions where the concentration of the added neutral reagent was in large excess of the starting ion. Experimental conditions dictate that the concentration of the starting ion is $< 10^8$ ions cm^{-3}, while the added neutral reagent was $> 10^{10}$ molecules cm^{-3} in a flow containing 10^{17} atoms cm^{-3} of helium at a $P_{He} = 0.5$ torr. The ion/molecule reaction distance, which is related to time in a flow system, was held constant while the concentration of added neutral reagent [N] was varied. At each new concentration of neutral reagent, the signal intensity of the starting ion I^- was measured. Principal destruction pathways of I^- were reaction with N, diffusion to the walls of the flow tube and reaction with impurities M. The integrated rate law for these processes is given in equation 50.

$$\ln([I_0^-]/[I^-]) = ((D_0/\Lambda^2P_{He}) + k_M[M] + k_N[N])(\underline{z}/\overline{\underline{v}})(1/\eta) \tag{50}$$

In equation 50, $[I_0^-]$ is the beginning concentration of the starting ion in the absence of the added neutral molecule. $[I^-]$ is the signal intensity of the starting ion, which is relative to the concentration of I^- when it reaches the first nose cone, D_0 is the pressure independent diffusion coefficient, η is the correction factor for parabolic flow (1.59),[149] Λ is the diffusion length of the flow tube, k_M represents the reaction rate of I^- with impurities in the flow, [M] is the concentration of impurities in the flow, and k_N represents the bimolecular rate constant for the reaction of I^- with the added neutral reactant N. The reaction time is given by the reaction distance $\underline{z}$ divided by the flow velocity $\overline{\underline{v}}$ (≈ 80 m/s).

Since the first two destruction terms in equation 50 are constant, the only change in the signal intensity of I^- will be due to reaction with N. A plot of the logarithm of the signal intensity of I^- vs d[N] will produce a straight line with a slope equal to $k_N(\underline{z}/\overline{\underline{v}})(1/\eta)$. It is assumed that the average buffer gas flow velocity $\overline{\underline{v}}$ multiplied by 1.59 is the average transport velocity of the ions $\overline{\underline{v}}_t$.[150] The slope of the $\log[I^-]$ vs [N] plots are used to calculate the rate constant at 298 K using equation 51, where $[I^-]$ is the signal intensity of the starting ion, F_{He} and P_{He} are the flow rate and the flow tube pressure of the helium buffer gas, respectively, r is the radius of the flow tube (3.56 cm), and D is the distance from the ion/molecule neutral inlet to the first nose cone (65.96 cm).

$$k(\text{cm}^3\ \text{molecule}^{-1}\ \text{s}^{-1}) = \frac{d(\log[I_0^-]/[I^-])}{d[N](\text{molecule cm}^{-3})} \times \qquad (51)$$

$$\frac{F_{He}(\text{atm cm}^3\ \text{s}^{-1}) \times 3.04 \times 10^3(\text{torr atm}^{-1})}{P_{He}(\text{torr}) \times r^2(\text{cm}^2) \times D(\text{cm})}$$

The constant in equation ?? (2.303 x 760 torr x 1.59 x (298 K / 273 K) = 3.04 x 10^3 torr atm^{-1}) contains the parabolic flow correction factor.[149] Most of the present research was done using the distance (D) given, but due to the move into a new Chemistry/Biochemistry building, (reconstruction of the FA apparatus), D for some of the rate constants was changed from 65.96 cm to 77.95 cm.

The concentration of the added neutral reagent [N] was determined by measuring the elapsed time (ΔT) for the pressure change (ΔP) of the neutral gas flowing into an evacuated vessel of known volume and using equation 52. By multiplying the number obtained from ΔP(torr)/ΔT(s) by

$$[N](\text{molecules cm}^{-3}) = P_{He}(\text{torr}) \times F_N(\text{atm cm}^{-3}\ \text{s}^{-1}) \times \qquad (52)$$

$$\frac{3.24 \times 10^{16}(\text{molecules cm}^{-3}\ \text{torr}^{-1})}{F_{He}(\text{atm cm}^{-3}\ \text{s}^{-1})}$$

equation 52, the concentration of [N] can be determined. In this equation F_N is the neutral reactant flow, F_{He} and P_{He} are the flow and the pressure of the helium buffer gas, respectively. The constant in equation 52 (3.24×10^{16} (molecules cm^{-3} $torr^{-1}$) = (6.023×10^{23}(molecules mol^{-1})) / (24.45 (cm^3 mol^{-1}) x 760 (torr atm^{-1}))) is a conversion factor.

Based on the above equations, it is assumed that I^- is formed only in the upstream end of the flow tube. To ensure this, Ar, N_2, or CH_4 can be added to the flow via inlet 2 or 5 in order to quench the $He^*(2^3S)$ atoms formed at the electron gun. These metastable atoms could ionize I to I^+ resulting in ejection of an electron. Due to its large cross section for electron attachment, SF_6 was added to the flow at the neutral inlet port to confirm that there were no electrons or helium metastable atoms present at this point. For the unsaturated organometallic species requiring energetic electrons in DEA, it was assumed that the high energy electrons are only present in the vicinity of the electron gun and are not present at the neutral inlet.

The negative ion mass spectrum of a particular reaction could be observed on the oscilloscope by scanning the quadrupole mass filter. The mass spectrum of the ions in the flow was recorded before and after addition of N to the flow, since the signal of the starting ion with no added neutral reagent did fluctuate throughout a kinetic experiment. The mass spectra were recorded by passing the analog signal through a fast A/D converter (AI13 from Interactive Structures, Bala Cynwyd, PA) and on to an Apple IIe computer through software developed by Interactive Microware (IMI, State College, PA). Eight spectra were recorded, stored on disk, and later averaged in order to maximize the signal to noise ratio. The averaged spectra were baseline corrected and integrated to obtain the peak area as a function of neutral reactant concentration. Rate constants were generally derived from the slope of at least six different neutral concentration additions.

Approximately one-half of the data was taken on the Apple computer. In order to increase peak resolution, data acquisition was changed to a Zenith model Z248 AT using Labtech Notebook software (Laboratory Technologies Corporation, 255 Ballardvale St., Wilmington, MA, 01887). The analog signal of the mass spectrometer was passed to a DAS-8 A/D converter (Metrabyte Corp., 440 Myles Standish Blvd., Taunton, MA 02780) and then to the Zenith computer through the Labtech Notebook software. Four spectra were taken for each data point and zero point. These spectra were then averaged, baseline corrected and integrated to obtain the peak area as a function of neutral reactant concentration. Plots of $\log([I_0^-]/[I^-])$ vs neutral concentration produced a straight line (<0.99) for the decay of the starting ion. The slope of this line was used to calculate the bimolecular rate constant for the ion/molecule reaction using equation 51.

The rate constants reported are usually the averages of three independent kinetic experiments in which at least one was performed with a different loading (concentration) of neutral reactant. The bulk of the reactions reported produced well-behaved pseudo-first-order decay constants for the starting ion to > 85% decay of the ion. The rate constants reported are thought to be accurate to ± 20% due to systematic errors in the flow and pressure measuring devices. However, rate constnats were usually reproducible to within ± 10%.[120]

The reported product ion branching fractions are estimated to be accurate to ± 5% absolute depending on the magnitude of difference between the mass of the starting and product ions. This error results from the faster diffusion rate of lighter ions vs heavier ions to the walls of the flow tube, and the mass discrimination of the nose cones, lens assembly, quadrupole mass filter, conversion dynode, and multiplier in the detection of the ions.[151]

The reported collision limited rate constants (k_{ADO}) for the ion/molecule reactions were calculated using the Average Dipole Orientation theory (eq 53).[152] In eq 53, q is the charge of the ion,

$$k_{ADO} = \frac{2\pi q}{\mu^{1/2}} [\alpha^{1/2} + C\mu_D(2/\pi\kappa T)^{1/2}] \qquad (53)$$

μ is the reduced mass of the ion and the neutral reactant, α is the polarizability of the neutral molecule which can be calculated using the method of Miller[153] when experimental values are not available, μ_D is the dipole moment of the neutral reactant, C is the dipole locking constant,[152a] κ is the Boltzmann constant, and T is the absolute temperature. If the dipole moment of the molecule is unknown, the Langevin collision limited rate constant can be calculated by equation 54.[152a] In equation 54, all the constants are the same as in the k_{ADO} equation except that μ_D is set to zero. The reaction efficiencies

$$k_{LAN} = 2\pi q(\alpha/\mu)^{1/2} \qquad (54)$$

listed in Tables VI-XI and XIV-XVII are calculated by equation 55. This is simply the experimental rate constant divided by either the k_{ADO} or k_{LAN}.

$$\text{Reaction Efficiency} = k_{total} / (k_{ADO} \text{ or } k_{LAN}) \qquad (55)$$

The ion/molecule reactions in which the major product was the total adduct negative ion are assumed to be termolecular since collisions of the excited adduct with the helium buffer gas are needed to remove excess energy and stabilize the adduct. These termolecular reactions can frequently be confirmed by changing the P_{He} which should change the rate constants or branching fractions. However, in the studies with $(CO)_2Fe^{\bullet -}$ and $(CO)_3Mn^-$ such P_{He} variations were not possible as changing the P_{He} significantly reduced the signal of the starting ion to a point where kinetic studies were not possible.

I.C.6. Materials

The helium buffer gas (99.99%, Welder products, Topeka, Kansas; 99.99%, Brown Welding, Salina, Kansas; 99.99%, Knoll Welding, Topeka, Kansas) was purified through two traps filled with Davison 4Å molecular sieves cooled with liquid nitrogen. The helium was then warmed to room temperature in a glass coil prior to introduction into the flow tube. Other gas purities and suppliers were argon (99.99%), nitrogen (99.99%), hydrogen (99.99%) and oxygen (Welder products); CH_3OCH_3 (99.87%), NH_3 (99.99%), CH_3NH_2 (98.0%), $(CH_3)_2NH$ (99.0%), $(CH_3)_3N$ (99.0%), SF_6 (99.99%), SO_2 (99.98%), CH_4 (99.0%), Xe (99.9%), Kr

(99.99%), (Matheson); D_2 (99.7%, Ideal Gas Products); $CF_2{=}CH_2$ (99.5%), (SCM Specialty Chemicals); $(CD_3)_2NH$ (99.6 atom % D), CD_3OCH_3 (99.27 atom % D) (MSD Isotopes). A liquid reagent Et_2NH (98.0%, Aldrich) was distilled prior to use and a center cut, constant boiling fraction (bp = 55° C) was loaded into 5-L glass storage bulbs immediately following three freeze-pump-thaw cycles using liquid nitrogen as coolant. Other reagents were purchased from commercial suppliers at the highest purity available and were used without further purification other than three freeze-pump-thaw cycles; 1,2-difluorobenzene (98.0%, Aldrich); $Fe(CO)_5$ (99.5%, Pfaltz & Bauer); $Mn_2(CO)_{10}$ (Strem Chemical Co.).

I.C.7. Generation of $(OC)_2Fe^{\bullet -}$ and $(OC)_3Mn^-$.

Generation of $(OC)_2Fe^{\bullet -}$ was accomplished by dissociative electron attachment (DEA) with high energy electrons with $Fe(CO)_5$. $Fe(CO)_5$ was placed in a glass finger and sealed with a Kontes O-ring valve under a nitrogen atmosphere. This finger was cooled in an acetone/ice bath and the $Fe(CO)_5$ was added to the FA at inlet 1 through a stainless steel needle valve at P_{He} = 0.900 torr in the flow tube. The rate of addition of $Fe(CO)_5$ was regulated by the stainless steel needle in order to optimize signal intensity. Typically, only very low concentrations of $Fe(CO)_5$ (needle valve barely open) were needed to generate sufficient signal intensities for kinetic and product measurements. At low emission currents of 500 μA, using the rhenium filament with the DC power supply at 4 A and the high voltage power supply at -100 V, DEA of $Fe(CO)_5$ gave $(OC)_4Fe^{\bullet -}$ (m/z 168) as the major

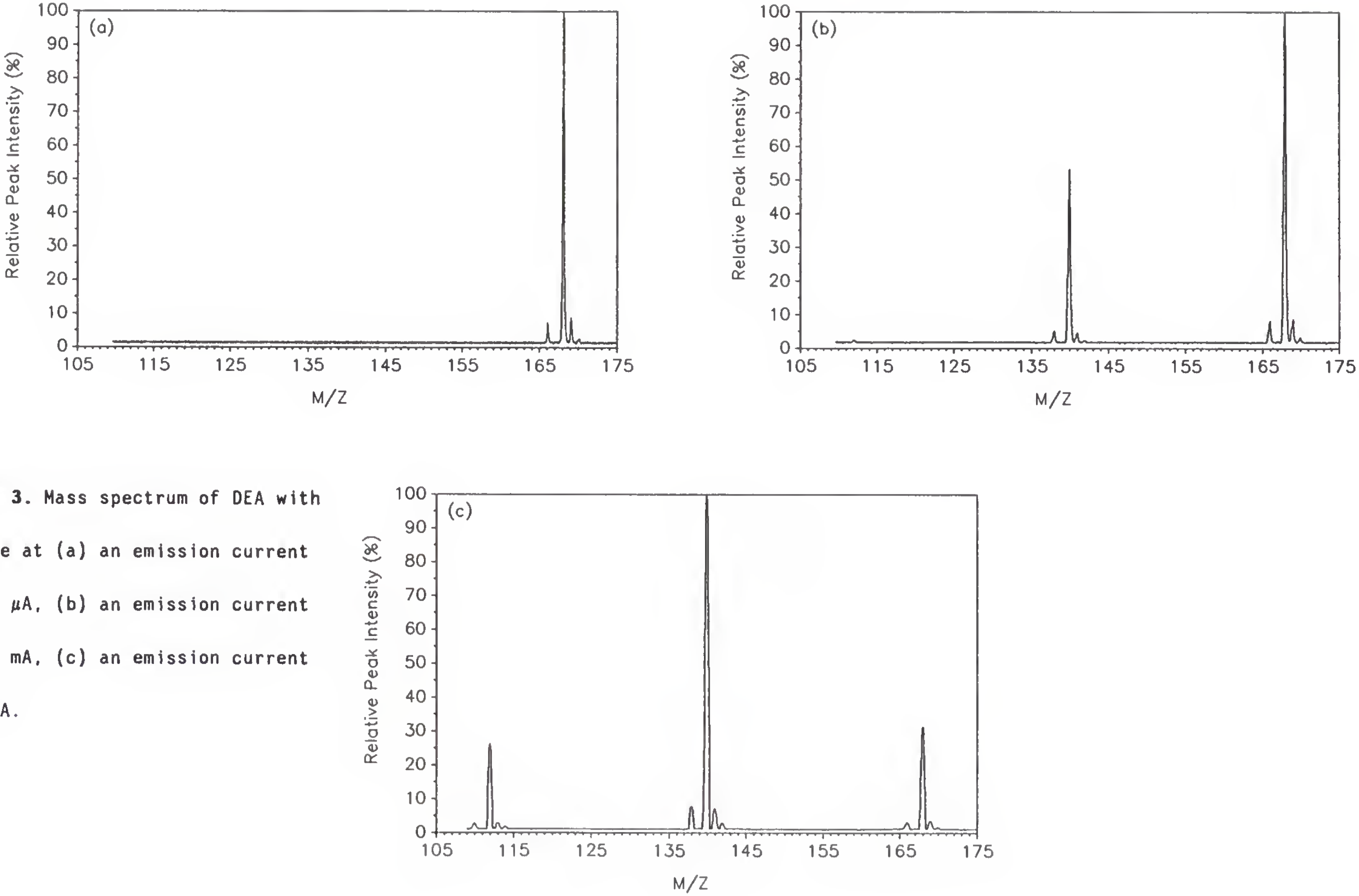

Figure 3. Mass spectrum of DEA with $(OC)_5Fe$ at (a) an emission current of 500 μA, (b) an emission current of 1.5 mA, (c) an emission current of 8 mA.

ion in the flow tube (Figure 3a), as well as smaller signals of $Fe_2(CO)_8^{\bullet -}$ (m/z 336) and $Fe_2(CO)_7^{\bullet -}$ (m/z 308). Increasing the emission current to 1.5 mA and operating the DC power supply at 5.5 A and the high voltage power supply at -150 V, DEA of $Fe(CO)_5$ gave a mixture of $(OC)_4Fe^{\bullet -}$ (m/z 168) and $(OC)_3Fe^{\bullet -}$ (m/z 140) (Figure 3b). Under these conditions, $(OC)_4Fe^{\bullet -}$ is still the dominant ion present, but appreciable amounts of $(OC)_3Fe^{\bullet -}$ are present and a trace amount of $(OC)_2Fe^{\bullet -}$ (m/z 112) is detectable with lesser amounts of the Fe_2 species present. Increasing the DC power supply to 6.5 A and the high voltage to -200 V produced an emission current of 8 mA to give $(OC)_3Fe^{\bullet -}$ (m/z 140) as the dominant ion in the FA and appreciable amounts of $(OC)_2Fe^{\bullet -}$ (m/z 112) and $(OC)_4Fe^{\bullet -}$ (m/z 168) (Figure 3c) with only trace amounts of the Fe_2 species present. Figure 3c is typical of the standard operating conditions used to determine the ion/molecule reactions of $(OC)_2Fe^{\bullet -}$. The isotope peaks at (M-2), (M+1), and (M+2) are due to the isotopes of iron (^{54}Fe = 5.8%, ^{57}Fe = 2.1%, ^{58}Fe = 0.3%), carbon (^{13}C = 1.1%), and oxygen (^{18}O = 0.2%).[154]

The ion/molecule reactions of the ions, $(OC)_{4,3,2}Fe^{\bullet -}$ can be determined on an individual basis. This determination is done by starting with the reaction of $(OC)_4Fe^{\bullet -}$ (m/z 168). As shown in Figure 3a, m/z 168 can be generated as the exclusive monometal ion present in the flow tube. The ion/molecule reaction of m/z 168 can, therefore, be determined exclusively. Once the chemistry of $(OC)_4Fe^{\bullet -}$ (m/z 168) has been determined, the separate chemistry of $(OC)_3Fe^{\bullet -}$ (m/z 140) can be observed from the mixture shown in Figure 3b. By the same principle, the chemistry of $(OC)_2Fe^{\bullet -}$ (m/z 112) can be determined from the mixture shown in Figure 3c. The only limitation to this procedure is that the new product ions of any of this series should not overlap with the signals of existing starting ions or their product ions.

Generation of $(OC)_3Mn^-$ was accomplished by DEA with $Mn_2(CO)_{10}$, which was added via inlet 1 from a glass finger sealed with a Kontes O-ring valve with the FA operating at P_{He} = 0.700 torr and $\bar{\underline{v}}$ = 70 m/s. The $Mn_2(CO)_{10}$ was inletted to the flow tube by fully opening the Kontes valve. At an emission current of 50 μA using the electron gun with a rhenium filament and the DC power supply at 4 A and the high voltage power supply at -100 V, $(OC)_5Mn^-$ (m/z 195) was produced (Figure 4a) with larger amounts of $Mn_2(CO)_9^{\bullet-}$ (not shown). In this study, the reactions of the dinuclear manganese compounds were not examined. Increasing the emission current to 500 μA with the DC power supply at 5 A and the high voltage power supply at -200 V, $(OC)_5Mn^-$ (m/z 195) and $(OC)_4Mn^-$ (m/z 167) were the dominant ions in the FA (Figure 4b) along with a trace amount of $(OC)_3Mn^-$ (m/z 139) and lesser amounts of the dinuclear mangnese ions $(OC)_9Mn_2^{\bullet-}$, $(OC)_8Mn_2^{\bullet-}$, $(OC)_7Mn_2^{\bullet-}$. Increasing the emission current to 3.5 mA with the DC power supply at 6 A and the high voltage power supply at -250 V yielded $(OC)_3Mn^-$ (m/z 139) as the dominant ion in the FA, with a lesser amount of $(OC)_4Mn^-$ (m/z 167) and trace amounts of $(OC)_5Mn^-$ (m/z 195) and the dinuclear manganese ions $(OC)_{7-9}Mn_2^{\bullet-}$ (Figure 4c). Since there are no naturally occurring isotopes of ^{55}Mn, the isotope peaks observed for the ions in Figure 4 are due only to the isotopes of carbon and oxygen.

The individual reactions of the ions $(OC)_{5,4,3}Mn^-$ can be determined by the same procedure described with $(OC)_{2,3,4}Fe^{\bullet-}$.

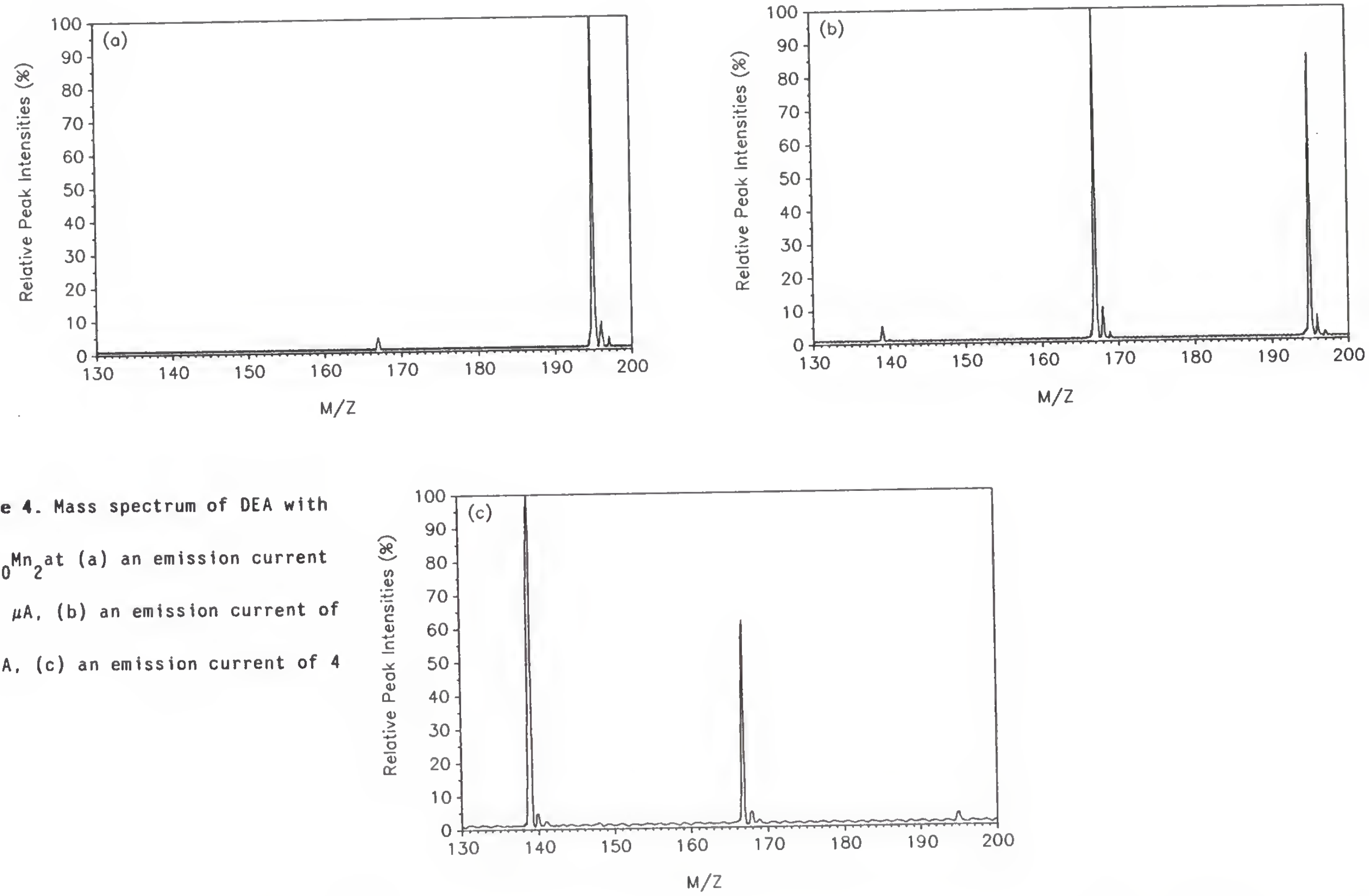

Figure 4. Mass spectrum of DEA with $(OC)_{10}Mn_2$ at (a) an emission current of 50 μA, (b) an emission current of 500 μA, (c) an emission current of 4 mA.

I.D. Results and Discussion.

I.D.1. Reactions of $(OC)_{2,3,4}Fe^{\bullet -}$ and $(OC)_{3,4,5}Mn^{-}$.

The reactions of the iron and manganese negative ions will be presented together since the related complexes in both sets exhibit similar reactivity. $(OC)_2Fe^{\bullet -}$ is a 13-electron multicoordinatively and multielectronically unsaturated (MCMEU) transition metal complex negative ion. Being deficient of five electrons and formally having two vacant coordination sites (one site is occupied by an electron), $(OC)_2Fe^{\bullet -}$ is a very reactive metal species. The other iron complex negative ions present in the helium flow from generation of $(OC)_2Fe^{\bullet -}$ include the 15-electron $(OC)_3Fe^{\bullet -}$ and the 17-electron $(OC)_4Fe^{\bullet -}$. $(OC)_3Mn^{-}$ is a 14-electron MCMEU transition metal complex negative ion that is deficient of four electrons and has two vacant coordination sites. Also present in the helium flow containing $(OC)_3Mn^{-}$ are the 16-electron $(OC)_4Mn^{-}$ and the 18-electron $(OC)_5Mn^{-}$ negative ions. Being deficient of one more electron than $(OC)_3Mn^{-}$, $(OC)_2Fe^{\bullet -}$ is expected and frequently found to be slightly more reactive than $(OC)_3Mn^{-}$. This was evidenced by the fact that $(OC)_2Fe^{\bullet -}$ forms adducts with CH_4 and $(CH_3)_4C$[137] while $(OC)_3Mn^{-}$ failed to react with these substrates and $(OC)_2Fe^{\bullet -}$ is experimentally more difficult to generate.

I.D.1.a. With Amines.

The reactions of $(OC)_2Fe^{\bullet -}$ and $(OC)_3Mn^{-}$ with various amines are listed in Tables VI and VII, respectively. The reactions of the less coordinatively unsaturated ions, $(OC)_{3,4}Fe^{\bullet -}$ and $(OC)_{4,5}Mn^{-}$ are listed in Tables VIII-XI. The reactions of $(OC)_2Fe^{\bullet -}$ and $(OC)_3Mn^{-}$ with NH_3

Table VI. Summary of Kinetic and Product Data for the Reactions of $(OC)_2Fe^{\bullet -}$ with Amines.

Rxn. No.	Amine	Product Ion [+ Assumed Neutral(s)]	Branching Fraction	k_{total},[a] cm^3 $molecule^{-1}$ s^{-1}	k_{ADO},[b] cm^3 $molecule^{-1}$ s^{-1}	Reaction Efficiency[c]
1	NH_3	$(OC)Fe(H)(NH_2)^{\bullet -}$ [+ CO]	1.00	$(1.9 \pm 0.1) \times 10^{-10}$ d	1.7×10^{-9}	0.11
2	ND_3	$(OC)Fe(D)(ND_2)^{\bullet -}$ [+ CO]	1.00	$(8.5 \pm 0.5) \times 10^{-11}$ d	1.6×10^{-9}	0.053
3	$MeNH_2$	$(OC)_2Fe(H_2C{=}NH)^{\bullet -}$ [+ H_2]	1.00	$(4.3 \pm 0.5) \times 10^{-10}$	1.4×10^{-9}	0.31
4	Me_2NH	$(OC)_2Fe(H_2C{=}N{-}CH_3)^{\bullet -}$ [+ H_2]	1.00	$(2.8 \pm 0.9) \times 10^{-10}$	1.7×10^{-9}	0.17
5	Me_3N	$(OC)_2Fe(NMe_3)^{\bullet -}$	1.00	$(2.3 \pm 1.3) \times 10^{-10}$ e	1.1×10^{-9}	0.21
6	Et_2NH	$(OC)_2Fe(CH_3HC{=}NEt)^{\bullet -}$ [+ H_2]	1.00	$(6.6 \pm 1.3) \times 10^{-10}$	1.2×10^{-9}	0.55
7a	$(CD_3)_2NH$	$(OC)_2Fe(D_2C{=}N{-}CD_3)^{\bullet -}$ [+ HD]	0.87	see text[f]		
7b		$(OC)_2Fe({=}CDNH{-}CD_3)^{\bullet -}$ [+ D_2]	0.13			

[a] k_{total}'s are estimated to be accurate to ± 20%. Errors are the maximum deviation in the average of at least three independent experiments at a P_{He} = 0.900 torr, $\bar{v}$ = 66 m/s. [b] The collision limit rate constants (k_{ADO}) were calculated by using the average dipole orientation theory (ref. 152) [c] The reaction efficiency is the fraction of collisions which result in reaction (k_{total}/k_{ADO}). [d] Rate constants reported by McDonald, R. N.; Chowdhury, A. K.; Jones, M. T. *J. Am. Chem. Soc.* **1986**, *108*, 3105. [e] This is the apparent bimolecular rate constant for the termolecular adduct forming reaction. [f] Experimental difficulties precluded determination of this rate constant. See pages 83-87.

Table VII. Summary Kinetic and Product Data for the Reactions of $(OC)_3Mn^-$ with Amines.

Rxn. No.	Amine	Product Ion [+ Assumed Neutral(s)]	Branching Fraction	k_{total},[a] cm^3 $molecule^{-1}$ s^{-1}	k_{ADO},[b] cm^3 $molecule^{-1}$ s^{-1}	Reaction Efficiency[c]
1	NH_3	$(OC)_3Mn(NH_3)^-$	1.00	$(2.0 \pm 0.1) \times 10^{-11}$ d,e	1.6×10^{-9}	0.013
2	ND_3	$(OC)_3Mn(ND_3)^-$	1.00	$(2.1 \pm 0.1) \times 10^{-11}$ d,e	1.5×10^{-9}	0.014
3	Me_2NH	$(OC)_3Mn(H_2C{=}N{-}CH_3)^-$ [+ H_2]	1.00	$(5.1 \pm 0.4) \times 10^{-10}$	3.1×10^{-9}	0.16
				$(4.5 \pm 0.4) \times 10^{-10}$ f		0.15
4	Me_3N	$(OC)_3Mn(NMe_3)^-$	1.00	$(2.4 \pm 0.3) \times 10^{-10}$ f,e	1.5×10^{-9}	0.16
5a	$(CO_3)_2NH$	$(OC)_3Mn(O_2C{=}N{-}CO_3)^-$ [+ HD]	0.96	$(5.4 \pm 0.2) \times 10^{-10}$	3.0×10^{-9}	0.18
5b		$(OC)_3Mn({=}CONH{-}CO_3)^-$ [+ O_2]	0.04			

---

[a] $k_{total's}$ are estimated to be accurate to ± 20%. Errors are the maximum deviation in the average of at least three independent experiments at a P_{He} = 0.700 torr, $\bar{\underline{v}}$ = 73 m/s. [b-e] See Table VI. [f] Rate constant corrected upward by 15%. Rate constant is the average of two independent experiments and was determined by McOonald, R. N.; Jones, M. T., unpublished results.

Table VIII. Summary of Kinetic and Product Data for the Reactions of $(OC)_3Fe^{\bullet -}$ with Various Neutral Substrates.

Rxn. No.	Neutral	Product Ion [+ Assumed Neutral(s)]	Branching Fraction	k_{total},[a] cm^3 $molecule^{-1}$ s^{-1}	k_{ADO},[b] cm^3 $molecule^{-1}$ s^{-1}	Reaction Efficiency[c]
1	NH_3	No Reaction		$< 1 \times 10^{-13}$ [d]		
2	$MeNH_2$	$(OC)_3Fe(MeNH_2)^{\bullet -}$	1.00	6.8×10^{-13} [e,f]	3.1×10^{-9}	0.00022
3	Me_2NH	$(OC)_3Fe(Me_2NH)^{\bullet -}$	1.00	[g]		
4	Me_3N	$(OC)_3Fe(Me_3N)^{\bullet -}$	1.00	[g]		
5	Et_2NH	$(OC)_3Fe(Et_2NH)^{\bullet -}$	1.00	[g]		
6	$(CO_3)_2NH$	$(OC)_3Fe((CO_3)_2NH)^{\bullet -}$	1.00	[g]		
7	H_3COCH_3	No Reaction		$< 1 \times 10^{-13}$		
8	H_3COCD_3	No Reaction		$< 1 \times 10^{-13}$		
9	$\underline{o}$-$C_6H_4F_2$	$(OC)_3Fe(C_6H_4F_2)^{\bullet -}$	1.00	$(5.2 \pm 0.4) \times 10^{-10}$ [e]	9.3×10^{-10} [h]	0.56
10	Xe	No Reaction		$< 1 \times 10^{-13}$		
11a	SO_2	$(OC)_3Fe(SO_2)^{\bullet -}$	0.5	[g]		
11b		$(OC)_2Fe(SO_2)^{\bullet -}$ [+ CO]	0.5			
12	D_2	$(OC)_3Fe(D_2)^{\bullet -}$	1.00	[g]		

[a-e] See Table VI. [f] This is the result of one kinetic experiment. [g] This rate constant was not determined. [h] The dipole moment of this molecule is not known. This is the Langevin rate constant calculated by ion-induced dipole theory. (ref. 152).

Table IX. Summary of Kinetic and Product Data for the Reactions of $(OC)_4Fe^{\bullet -}$ with Various Neutral Substrates.

Rxn. No.	Neutral	Product Ion [+ Assumed Neutral(s)]	Branching Fraction	k_{total},[a] cm^3 $molecule^{-1}$ s^{-1}	k_{ADO},[b] cm^3 $molecule^{-1}$ s^{-1}	Reaction Efficiency[c]
1	NH_3	No Reaction		$< 1 \times 10^{-13}$ d		
2	$MeNH_2$	No Reaction		$< 1 \times 10^{-13}$		
3	Me_2NH	No Reaction		$< 1 \times 10^{-13}$		
4	Me_3N	No Reaction		$< 1 \times 10^{-13}$		
5	Et_2NH	No Reaction		$< 1 \times 10^{-13}$		
6	$(CO_3)_2NH$	No Reaction		$< 1 \times 10^{-13}$		
7	$\underline{o}$-$C_6H_4F_2$	No Reaction		$< 1 \times 10^{-13}$		
8	H_3COCH_3	No Reaction		$< 1 \times 10^{-13}$		
9	H_3COCD_3	No Reaction		$< 1 \times 10^{-13}$		
10	O_2	No Reaction		$< 1 \times 10^{-13}$		
11	SO_2	$(OC)_3Fe(SO_2)^{\bullet -}$ [+ CO]	1.00	2.0×10^{-10} e	1.1×10^{-9}	0.18

[a-d] See Table VI. [e] Shell, P. L., Ph.D. Dissertation, Kansas State University, 1986.

Table X. Summary of Kinetic and Product Data for the Reactions of $(OC)_4Mn^-$ with Various Neutral Substrates.

Rxn. No.	Neutral	Product Ion [+ Assumed Neutral(s)]	Branching Fraction	k_{total},[a] cm^3 $molecule^{-1}$ s^{-1}	k_{A00},[b] cm^3 $molecule^{-1}$ s^{-1}	Reaction Efficiency[c]
1	NH_3	No Reaction		$<1 \times 10^{-13}$ [d]		
2	Me_2NH	$(OC)_4Mn(Me_2NH)^-$	1.00	e		
3	$(CO_3)_2NH$	$(OC)_4Mn((CO_3)_2NH)^-$	1.00	e		
4	$\underline{o}$-$C_6H_4F_2$	$(OC)_4Mn(C_6H_4F_2)^-$	1.00	$(1.9 \pm 0.6) \times 10^{-10}$ [f]	8.9×10^{-10} [g]	0.21[h]
5	$H_2C{=}CF_2$	$(OC)_4Mn(H_2C{=}CF_2)^-$	1.00	e		
6	H_3COCH_3	No Reaction		$< 1.0 \times 10^{-13}$		
7	H_3COCO_3	No Reaction		$< 1.0 \times 10^{-13}$		
8	O_2	$(OC)_4Mn(O_2)^-$	1.00	$(8.6 \pm 1.4) \times 10^{-13}$ [i]	1.0×10^{-9}	0.00086
9	Xe	No Reaction		$< 1.0 \times 10^{-13}$		
10	SO_2	$(OC)_3Mn(SO_2)^-$ [+ CO]	1.00	$(1.2 \pm 0.3) \times 10^{-9}$	1.1×10^{-9}	1.09

[a] See Table VII. [b-d] See Table VI. [e] This rate constant was not determined. [f] This is the apparent bimolecular rate constant for the termolecular adduct forming reaction. [g] The dipole moment of this molecule is unknown. This is the Langevin collision limit rate constant (k_{LAN}) calculated by ion-induced dipole theory (ref.152). [h] This reaction efficiency was calculated by (k_{total}/k_{LAN}).

[i] Jones, M. T. Ph.D. Thesis, Kansas State University, 1987.

Table XI. Summary of Kinetic and Product Data for the Reactions of $(OC)_5Mn^-$ with Various Neutral Substrates.

Rxn. No.	Neutral	Product Ion [+ Assumed Neutral(s)]	Branching Fraction	k_{total},[a] cm^3 $molecule^{-1}$ s^{-1}	k_{ADO},[b] cm^3 $molecule^{-1}$ s^{-1}	Reaction Efficiency[c]
1	NH_3	No Reaction[d]		$< 1 \times 10^{-13}$		
2	Me_2NH	No Reaction		$< 1 \times 10^{-13}$		
3	$(CD_3)_2NH$	No Reaction		$< 1 \times 10^{-13}$		
4	Me_3N	No Reaction		$< 1 \times 10^{-13}$		
5	CH_3OCH_3	No Reaction		$< 1 \times 10^{-13}$		
6	CH_3OCD_3	No Reaction		$< 1 \times 10^{-13}$		
7	$\underline{o}$-$C_6H_4F_2$	No Reaction		$< 1 \times 10^{-13}$		
8	SO_2	No Reaction		$< 1 \times 10^{-13}$		
9	Xe	No Reaction		$< 1 \times 10^{-13}$		
10	D_2	No Reaction		$< 1 \times 10^{-13}$		

[a-c] See Table VII.

and ND_3 were reported[155] (eq 56 and 57). It was found that $(OC)_2Fe^{\bullet -}$

$$(OC)_2Fe^{\bullet -} + NH_3 \longrightarrow (OC)Fe(H)(NH_2)^{\bullet -} + CO; \quad k_H/k_D = 2.1 \qquad (56)$$

$$(OC)_3Mn^- + NH_3 \xrightarrow{He} (OC)_3Mn(NH_3)^-; \quad k_H/k_D = 1.0 \qquad (57)$$

reacted with NH_3 by an oxidative insertion mechanism to yield the (adduct-CO) negative ion as evidenced by the isotope effect (k_H/k_D = 2.1) in the reaction of ND_3. The analogous reaction of $(OC)_3Mn^-$ with NH_3 formed the total adduct negative ion with no isotope effect observed with ND_3. The isotope effect observed in eq 56 indicated that an N-H bond was being broken in the rate limiting step of the reaction with $(OC)_2Fe^{\bullet -}$. The absence of an isotope effect in reaction 57 supported the contention that the Lewis acid-base complex was the product with $(OC)_3Mn^-$. Support for this mechanism was found in the comparison of rate constants, where $(OC)_3Mn^-$ reacted slower by a factor of 10, possibly due to the need for collisional stabilization of the total adduct negative ion with the helium buffer gas. The excess energy generated from forming Fe-NH_2 and Fe-H bonds in the reaction of NH_3 with $(OC)_2Fe^{\bullet -}$ caused expulsion of a CO ligand, while $(OC)_3Mn^-$ reacts with NH_3 to form only the total adduct negative ion. Neither $(OC)_{3,4}Fe^{\bullet -}$ (Table VIII and IX, respectively) or $(OC)_{4,5}Mn^-$ (Table X and XI, respectively) reacted with NH_3.

It was decided to investigate the reactions of these reactive metal species with the higher molecular weight amines which contain both N-H and C-H bonds. In the reactions of $(OC)_2Fe^{\bullet -}$ and $(OC)_3Mn^-$ with primary and secondary amines, the exclusive reaction channel was formation of the (adduct-H_2) negative ion with retention of the CO ligands (eq 58). The major source of the eliminated H_2 molecules in these reactions was a hydrogen from the N-H bond and a hydrogen from a C-H bond in the starting amine based on the results of the reactions with $(CD_3)_2NH$ which will be discussed in detail later. Both $(OC)_2Fe^{\bullet -}$ (Table VI) and $(OC)_3Mn^-$ (Table VII) reacted with the tertiary amine Me_3N to give the total adduct negative ion (eq 59). $(OC)_3Fe^{\bullet -}$ (Table VIII) and $(OC)_4Mn^-$ (Table X) reacted slowly with the investigated

$$(OC)_xM^- + HN(CH_2R^1)(R^2) \longrightarrow (OC)_xM(\pi\text{-}R^1HC{=}NR^2)^- + H_2 \qquad (58)$$

$R^1 = R^2 = H$; $R^1 = H$, $R^2 = Me$; $R^1 = Me$, $R^2 = Et$

$M = Fe$, $x = 2$; $M = Mn$, $x = 3$

$$(OC)_xM^- + NMe_3 \xrightarrow{He} (OC)_xM(NMe_3)^- \qquad (59)$$

$M = Fe^{\bullet -}$, $x = 2$; $M = Mn^-$, $x = 3$

amines (NH_3 failed to react) to yield only the total adduct negative ion, while neither $(OC)_4Fe^{\bullet -}$ (Table IX) nor $(OC)_5Mn^-$ (Table XI) gave any reaction products with the amines. The rate constants for the amine reactions with $(OC)_2Fe^{\bullet -}$ and $(OC)_3Mn^-$ are summarized in Table XII.

The rate constants for the reactions of $(OC)_2Fe^{\bullet -}$ and $(OC)_3Mn^-$ with NH_3 and the amines are generally large values with reaction efficiencies > 0.1; the exception is the smaller rate constant (by about a factor of 10) for the reaction of $(OC)_3Mn^-$ with NH_3 which yields the total adduct. In the larger data set for the reactions of $(OC)_2Fe^{\bullet -}$ (Table XII), the rate constants for the NH_3 and primary and secondary amine reactions showed a qualitative correlation with the

Table XII. Comparison of Rate Constants for the Reactions of $(OC)_2Fe^{\bullet -}$ and $(OC)_3Mn^-$ with Amines.

Amine	Amine PA[a]	Ion, k_{total}[b] $(OC)_2Fe^{\bullet -}$	Ion, k_{total}[b] $(OC)_3Mn^-$
NH_3	205.0	1.9×10^{-10}	2.0×10^{-11}
		(6.3×10^{-11})[c]	(6.7×10^{-12})[c]
$MeNH_2$	214.1	4.3×10^{-10}	---
		(2.2×10^{-10})[c]	---
Me_2NH	220.5	2.8×10^{-10}	5.1×10^{-10}
Et_2NH	225.1	6.6×10^{-10}	---
Me_3N	224.3	2.3×10^{-10}	2.4×10^{-10} [d]

[a] Units of kcal/mol, Ref. 156. [b] Units of cm^3 $molecule^{-1}$ s^{-1}. [c] Rate constant corrected (divided) downward by the number of N-H bonds in the amine. [d] The reported[157] rate constant is corrected upward by 15% due to an error in a constant used in calculating the rate constants.

proton affinities (PA),[156] a measure of the gas-phase base strength, of the amines. This same rough correlation was seen in the more limited data set for the reactions of $(OC)_3Mn^-$. This point suggested that equilibrium formation of the Lewis acid-base complexes between the $(OC)_xM^-$ and NH_3 and the amines may be occurring in these reactions.

If we assume that formation of the Lewis complexes is a fast preequilibrium step and that "insertion" of the metal center into the N-H bond contributes to k_{total} in the overall mechanism, the number of hydrogens on the nitrogen must be normalized in these comparisons.

These normalized rate constants for the reactions of NH_3 and the primary and secondary amines were obtained by dividing k_{total} by the number of N-H bonds in the neutral reactant molecule and are given in Table XII. A plot of these normalized rate constants for the bimolecular reactions of $(OC)_2Fe^{\bullet -}$ with NH_3, CH_3NH_2, $(CH_3)_2NH$, and $(C_2H_5)_2NH$ vs. the gas-phase PA of the neutral reactant is shown in Figure 5a. It is also seen in Figure 5b that these normalized rate constants increase as the N-H bond strength in NH_3 or the amine decreases.[24]

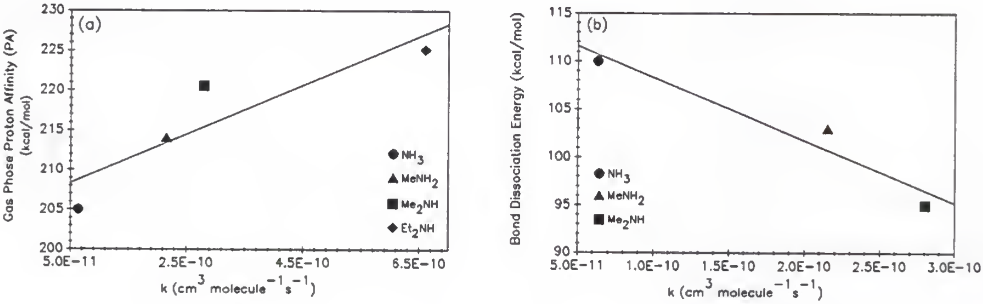

Figure 5. (a) Correlation of gas phase proton affinity (PA), with the normalized bimolecular rate constants for the reactions of $(OC)_2Fe^{\bullet -}$ with NH_3 and the amines (Table XII). (b) Correlation of the available NH_3 and amine N-H bond strengths with the normalized rate constants for the reactions of $(OC)_2Fe^{\bullet -}$ with NH_3 and the amines.

Obviously, the above considerations must be addressed in any general mechanism to describe these reactions. In addition, the mechanism must account for the ejection of a CO ligand from an intermediate in the reaction of $(OC)_2Fe^{\bullet -}$ with NH_3 while elimination of

H_2 is observed in the reactions of $(OC)_2Fe^{\bullet -}$ with the primary and secondary amines.

The proposed mechanism for these reactions is shown in Scheme VI.

Scheme VI.

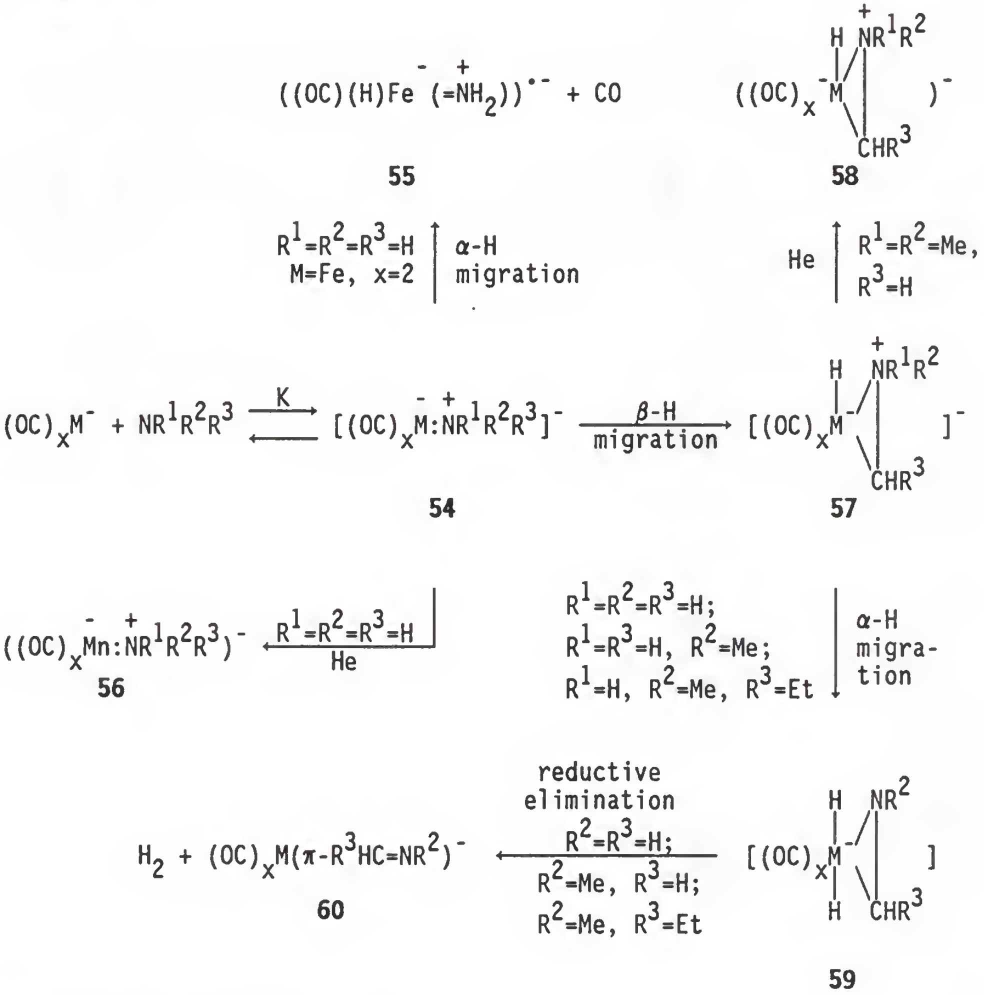

M = Fe, x = 2 : M = Mn, x = 3

It begins with either $(OC)_2Fe^{\bullet-}$ or $(OC)_3Mn^-$ reacting with NH_3 or an amine to form the Lewis complex **54** in which the amine has donated its nonbonded electron pair to the metal. The magnitude of the equilibrium constant K should depend on the relative binding energy in the Lewis complex which is related to the base strength of NH_3 and the amines (see Figure 5a). This initial coordination must be facile based on the large rate constants measured in the reactions with the amines and the fact that C-H oxidative insertion reactions of alkanes to yield the (adduct-H_2) product negative ions proceed with significantly smaller rate constants.[130]

It was shown that the reactions of $(OC)_2Fe^{\bullet-}$ and $(OC)_3Mn^-$ with NH_3 gave **55** and **56**, respectively, based on the products and the isotope effects.[155] It is important to note that a CO ligand was lost in the bimolecular reaction of $(OC)_2Fe^{\bullet-}$ with NH_3, while all CO ligands were retained when the neutral reactant was a primary or secondary amine. Also, the reactions of the metal complex negative ions with NH_3 had the smallest rate constants. This can be explained by the mechanism in Scheme VI, where **54** can only undergo a α-hydrogen migration when $NR^1R^2R^3$ = NH_3 and M = Fe, which in turn causes loss of a CO ligand to yield **55**, probably due to the multiple bonding of the amide group. The fact that the reaction of $(OC)_3Mn^-$ with NH_3 formed only the total adduct negative ion with NH_3 could be due to the weaker binding in the Mn-amide complex compared to the Fe-amide complex and/or to the increased number of vibrational states for collisional stabilization in the larger $(OC)_3Mn{:}NH_3^-$ complex compared to $(OC)_2Fe{:}NH_3^{\bullet-}$.

Complex **54** could then undergo a fast β-hydrogen migration from carbon when $NR^1R^2R^3$ = $MeNH_2$, Me_2NH, Me_3N, or Et_2NH to yield complex **57**. If the neutral amine was Me_3N, the product of the reaction would be the total adduct negative ion **58**; the alternate structure for this adduct is **56**. Since complex **57** already possesses a positive charge on nitrogen, a second β-hydrogen migration is not feasible when $NR^1R^2R^3$ = Me_3N. However, when R^1 = H, as with $MeNH_2$, Me_2NH, or Et_2NH, an α-hydrogen migration (as H^+) from nitrogen to the metal is possible to yield the complexes **59**. The migration of the proton from nitrogen in complex **57** removes the positive charge on the nitrogen and changes the amido group to a one-electron donor ligand. Reductive elimination of H_2 from **59** is proposed to proceed with formation of **60**, which could alternately exist as a cyclic three-membered ring structure.

To determine the sources of the H_2 molecule eliminated in the reactions of $(OC)_2Fe^{\bullet -}$ and $(OC)_3Mn^-$ with the primary and secondary amines and if an isotope effect could be measured, the reactions of $(OC)_2Fe^{\bullet -}$ and $(OC)_3Mn^-$ with $(CD_3)_2NH$ were examined. Both $(OC)_2Fe^{\bullet -}$ and $(OC)_3Mn^-$ reacted with Me_2NH to give exclusively the (adduct-H_2) negative ion (eq 60 and 61) with similar reaction efficiencies and rate

$$\underset{(m/z\ 112)}{(OC)_2Fe^{\bullet -}} + Me_2NH \longrightarrow \underset{(m/z\ 155)}{(OC)_2Fe(C_2H_5N)^{\bullet -}} + H_2 \qquad (60)$$

$$\underset{(m/z\ 139)}{(OC)_3Mn^-} + Me_2NH \longrightarrow \underset{(m/z\ 182)}{(OC)_3Mn(C_2H_5N)^-} + H_2 \qquad (61)$$

constants (Tables VI and VII, respectively). No experimental difficulties were encountered in the original determinations of the rate constants with the protio-amines as evidenced by the linear semi-log decay plots given in Figure 6.

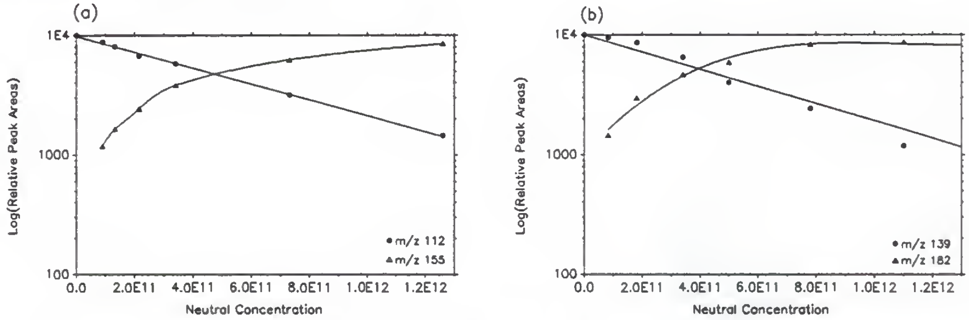

Figure 6. Semi-log plot for the decay of the starting ion and formation of the respective product ions. (a) $(OC)_2Fe^{\bullet -}$ (m/z 112) + $Me_2NH \longrightarrow (OC)_2Fe(C_2H_5N)^{\bullet -}$ (m/z 155) + H_2. (b) $(OC)_3Mn^-$ (m/z 139) + $Me_2NH \longrightarrow (OC)_3Mn(C_2H_5N)^-$ (m/z 182) + H_2.

There are three possibilities, **61**, **62**, or **63**, for the structure of the m/z 155 and 182 negative ions. Initial C-H or N-H bond oxidative insertion followed by β-hydrogen migration and reductive elimination of

$(OC)_xM(\pi\text{-}H_2C{=}NCH_3)^-$

61

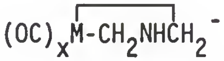

$(OC)_xM\text{-}CH_2NHCH_2^-$

62

$(OC)_xM{=}CHNHCH_3^-$

63

(M = Fe, x = 2 : M = Mn, x = 3)

H_2, would result in **61**. Alternately, C-H insertion followed by a C_γ-H or C_α-H migration and reductive elimination of H_2 would yield **62** and **63**, respectively. The results of the reaction of $(OC)_3Mn^-$ with $(CD_3)_2NH$ are presented in eq 62. The major primary product was the

$$\underset{(m/z\ 139)}{(OC)_3Mn^-} + (CD_3)_2NH \xrightarrow{0.96} \underset{(m/z\ 187)}{(OC)_3Mn(D_2C{=}NCD_3)^-} + HD \qquad (62a)$$

$$\xrightarrow{0.04} \underset{(m/z\ 186)}{(OC)_3Mn(C_2D_4NH)^-} + D_2 \qquad (62b)$$

(adduct-HD) at m/z 187, demonstrating that the source of H_2 in reaction 61 was vicinal dehydrogenation. The isotope effect measured for the reactions of the protio- and deutero-amines under the same experimental conditions on the same day was determined to be $k_H/k_D = 1.0$. The absence of an isotope effect in this reaction was consistent with the mechanism in Scheme VI with the α-hydrogen migration converting **57** to **59** as the likely slow, rate limiting step. This implies that the β-hydrogen migrations were fast in agreement with the previously determined vicinal dehydrogenations of alkanes with $(OC)_3Mn^-$.[130] The 4% reaction channel in eq 62b to yield the ion at m/z 186 could be rationalized by a minor amount of H/D scrambling via structure **59** in Scheme VI. This could occur by a reversal of a β-hydrogen migration as shown in eq 63 followed by reductive elimination of D_2 from **64** or **65**.

The results of the reaction of $(OC)_2Fe^{\bullet -}$ with $(CD_3)_2NH$ shown in eq 64 are similar to those in reaction 62 and yield the (adduct-HD) negative ion at m/z 160 as the major reaction product along with a small amount of the (adduct-D_2) product ion at m/z 159. Unfortunately, it was not possible to obtain linear psuedo-first order decay plots with $(CH_3)_2NH$ or $(CD_3)_2NH$ from this reaction that only two months previously yielded excellent psuedo-first order kinetics with $(CH_3)_2NH$

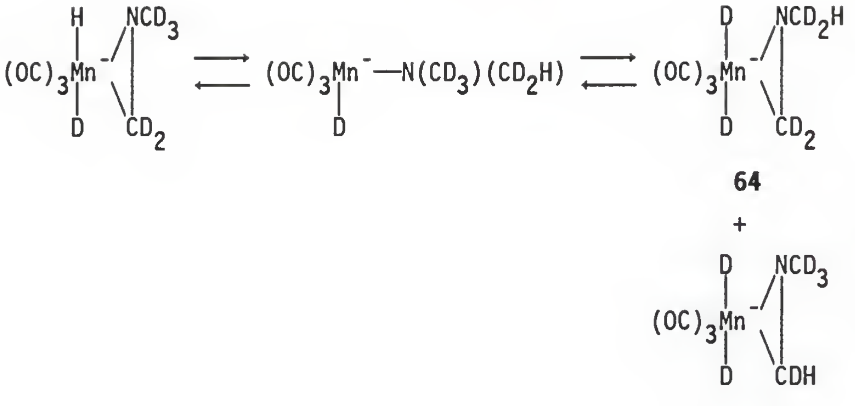

64

65

(63)

$$\underset{(m/z\ 112)}{(OC)_2Fe^{\bullet -}} + (CD_3)_2NH \xrightarrow{0.87} \underset{(m/z\ 160)}{(OC)_2Fe(D_2C{=}NCD_3)^{\bullet -}} + HD \qquad (64a)$$

$$\xrightarrow{0.13} \underset{(m/z\ 159)}{(OC)_2Fe(C_2D_4NH)^{\bullet -}} + D_2 \qquad (64b)$$

(Figure 6a). The nonlinear semi-logarithmic decay plots for these latter two reactions are presented in Figure 7. As can be seen from the semi-log plots, there is significant curvature in the decay of $(OC)_2Fe^{\bullet -}$ starting at ≈50 % reaction. It was originally thought that this was the result of Penning ionization of $(CH_3)_2NH$ by $He(2^3S)$ metastable atoms which could eject an energetic electron to effect DEA with $Fe(CO)_5$ to yield $(OC)_2Fe^{\bullet -}$ in the downstream part of the flow tube. However, all attempts to prevent this process failed, including adding from 1 to 5% argon, xenon, and CH_4 to the helium flow since these molecules are known to have better vibrational quenching efficiencies than helium. Other experimental variations included generation of $(OC)_2Fe^{\bullet -}$ at lower emission currents, varying the

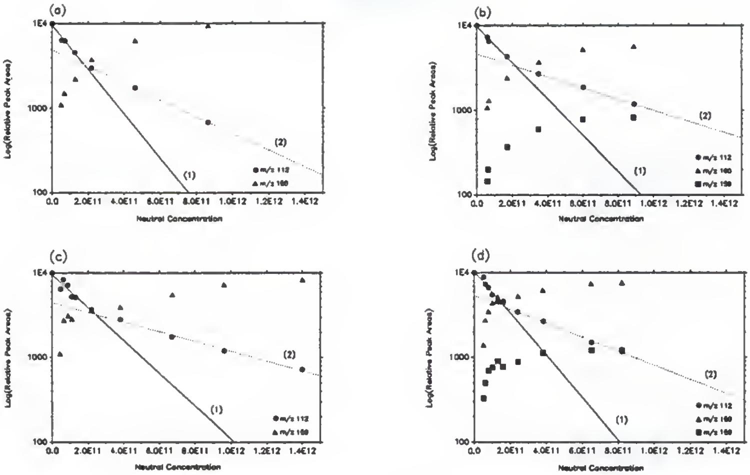

Figure 7. Semi-logarithmic plots for the reaction of $(OC)_2Fe^{\bullet -}$ with $(CH_3)_2NH$ (a,c) and $(CD_3)_2NH$ (b,d) showing curvature in the psuedo-first order decay of $(OC)_2Fe^{\bullet -}$ (m/z 112).

percentage of helium added through the electron gun side-arm, and using $(CH_3)_2NH$ from a new cylinder also failed to produce linear pseudo-first-order decay plots. The specific source of this problem is unknown.

The possibility of having two $(OC)_2Fe^{\bullet -}$ electronic states present in the flow in these latter experiments due to the poor electronic quenching efficiencies of the added buffer gases was considered. If the two electronic states reacted with the $(CH_3)_2NH$ and $(CD_3)_2NH$ with different rate constants, the result would be curvature in the pseudo-first-order decay plots as observed in Figure 7. Analysis of these curves on this basis yielded lines 1 and 2 in the separate plots (a-d) in Figure 7. Assuming that the lines 1 and 2 involved an excited and ground electronic states of $(OC)_2Fe^{\bullet -}$, respectively, the slopes of these lines were converted to the separate bimolecular rate constants for their reactions with $(CH_3)_2NH$ and $(CD_3)_2NH$. These rate constants are listed in Table XIII. From this analysis it was concluded that

Table XIII. Calculated Rate Constants from the Individual Slopes from the Reactions of $(OC)_2Fe^{\bullet -}$ with $(CH_3)_2NH$ and $(CD_3)_2NH$ in Figure 7.

$(CH_3)_2NH$

Plot	Line 1	Line 2
a	1.1×10^{-9}	4.0×10^{-10}
c	7.8×10^{-10}	2.3×10^{10}
Average	$(9.4 \pm 1.6) \times 10^{-10}$	$(3.1 \pm 0.9) \times 10^{-10}$

$(CD_3)_2NH$

Plot	Line 1	Line 2
b	8.8×10^{-10}	2.7×10^{-10}
d	9.9×10^{-10}	3.3×10^{-10}
Average	$(9.4 \pm 0.6) \times 10^{-10}$	$(3.0 \pm 0.3) \times 10^{-10}$

there was no kinetic isotope effect in these reactions and that the 13% formation of the (adduct-HD) product ion at m/z 159 in reaction 64b was the result of H/D scrambling analogous to that previously mentioned for the $(OC)_3Mn^-$ reaction with $(CD_3)_2NH$ (eq 63).

Are there two electronic states of $(OC)_2Fe^{\bullet -}$ present in these reactions with $(CH_3)_2NH$ and $(CD_3)_2NH$? This is a possibility. However, why is it that this is seen only with these two neutral reactants compared to the > 30 other reactants previously examined with this metal complex negative ion? And the previous reactions of $(OC)_2Fe^{\bullet -}$ with $(CH_3)_2NH$ had given linear pseudo-first-order decay plots.

It is believed that a more reasonable explanation of the curvatures of the decay plots in Figure 7 is due to the presence of some contaminating species introduced along with $(CH_3)_2NH$ and $(CD_3)_2NH$ gas flows, since they are the only variables in the experiment. Slower reactions with the two secondary amines were observed. However, the contaminant cannot be present in the gas-bulb containing the diluted (with He) amine, since as the concentration of the amine was increased, the concentration of the added contaminant would also increase leading to a continued decay of the $(OC)_2Fe^{\bullet -}$ ion signal along lines 1 of the decay plots. This contaminant must, therefore, be present on the walls of the glass manifold used for introducing the amine-helium mixture into the flow tube or absorbed in rubber O-rings of on-off valves in the manifold. In this way, the contaminant can be introduced in a constant concentration while the amine concentration is varied. Since no additional product was observed from $(OC)_2Fe^{\bullet -}$ reacting with the contaminant, this product ion must be unstable toward autodetachment of the electron or have the same mass as that of a product or starting ion in the flow.

I.D.1.b. With $F_2C{=}CH_2$.

The fast reactions of $(OC)_3Mn^-$ with several fluorinated ethylenes ($\approx 5 \times 10^{10}$ cm^3 molecule^{-1} s^{-1}) were determined by McDonald and Jones, with the results given in eq 47-49.[146] The remarkable product ions

$$(OC)_3Mn^- + C_2F_4 \longrightarrow Mn(C_2F_4)^- + 3CO \qquad (47)$$

$$(OC)_3Mn^- + HFC{=}CF_2 \longrightarrow Mn(C_2HF_3)^- + 3CO \tag{48}$$

$$(OC)_3Mn^- + HFC{=}CHF \longrightarrow Mn(C_2H_2F_2)^- + 3CO \tag{49}$$

corresponding to (adduct-3CO)$^-$ were indicative of highly exothermic reactions which required generation of strong new bonds. Structure characterization of these product ions was obtained from their ligand substitution reactions with SO_2. In each case, the product negative ion was $F_2Mn(SO_2)^-$ formed by substitution of SO_2 for the corresponding acetylene (C_2F_2, C_2H_F, and C_2H_2, respectively). These results led to the general structural assignment of **53** for the product ions in eqs 47-49. However, the nature of and the steps and intermediates involved effecting the ejection of the three CO ligands remained unknown.

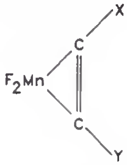

53 (X and Y = F or H)

The summary of product and kinetic data for the reactions of $(OC)_2Fe^{\bullet -}$ and $(OC)_3Mn^-$ with fluorine containing molecules are presented in Table XIV. Ion/molecule ligand substitution reactions of these product ions to elucidate their structures are presented in Table XV, for the products from $(OC)_2Fe^{\bullet -}$, and Table XVI, for the products from $(OC)_3Mn^-$. In an attempt to gain further information about the mechanism of the reactions in eq 47-49, the reaction of $(OC)_{3,4}Mn^-$ with $F_2C{=}CH_2$ was investigated (eq 65 and 66a-c). The reaction of $F_2C{=}CH_2$ with $(OC)_4Mn^-$ (Table X), which was also present in the flow, gave only the total adduct negative ion (eq 65). Formation of the (adduct-3CO)$^-$ at m/z 119 in the reaction of $(OC)_3Mn^-$ with $F_2C{=}CH_2$ (eq 66a) was

Table XIV. Summary Kinetic and Product Data for the Reactions of $(OC)_2Fe^{\bullet -}$ (1) and $(OC)_3Mn^-$ (2) with Fluorocarbons.

Rxn. No.	Ion	Neutral	Product Ion [+ Assumed Neutral(s)]	Branching Fraction	k_{total},[a] cm^3 $molecule^{-1}\ s^{-1}$	k_{LAN},[b] cm^3 $molecule^{-1}\ s^{-1}$	Reaction Efficiency[c]
1a	(1)	$\underline{o}$-$C_6H_4F_2$	$(OC)_2Fe(C_6H_4F_2)^{\bullet -}$	Trace	$(6.5 \pm 0.6) \times 10^{-10}$ [d]	9.8×10^{-10}	0.66
1b			$(OC)Fe(C_6H_4F_2)^{\bullet -}$ [+ CO]	0.25			
1c			$Fe(C_6H_4F_2)^{\bullet -}$ [+ 2CO]	0.75			
2a	(2)	$\underline{o}$-$C_6H_4F_2$	$(OC)_3Mn(C_6H_4F_2)^-$	0.17	$(6.6 \pm 0.6) \times 10^{-10}$ [d]	9.3×10^{-10}	0.71
2b			$(OC)_2Mn(C_6H_4F_2)^-$ [+ CO]	0.08			
2c			$(OC)Mn(C_6H_4F_2)^-$ [+ 2CO]	0.04			
2d			$Mn(C_6H_4F_2)^-$ [+ 3CO]	0.71			
3a	(2)	$F_2C{=}CH_2$	$Mn(F_2C{=}CH_2)^-$ [+ 3CO]	0.60	$(6.3 \pm 1.2) \times 10^{-10}$ [e]	1.1×10^{-9} [f]	0.57
3b			$(OC)Mn(F_2C{=}CH_2)^-$ [+ 2CO]	0.35			
3c			$(OC)_3Mn(FC{\equiv}CH)^-$ [+ HF]	0.05			

---

[a] $k_{total's}$ are estimated to be accurate to ± 20%. Errors are the maximum deviation in the average of at least three independent experiments at a P_{He} = 0.700 torr, $\underline{\bar{v}}$ = 73 m/s for $(CO)_3Mn^-$ and P_{He} = 0.900 torr, $\underline{\bar{v}}$ = 66 m/s for $(OC)_2Fe^{\bullet -}$. [b] The collision limit rate constants (k_{LAN}) were calculated by ion-induced dipole theory. (ref. 152). [c] The reaction efficiency is the fraction of collisions which result in reaction ($k_{total}/k_{LAN(ADO)}$. [d] This is the apparent bimolecular rate constant for the termolecular adduct forming reaction. [e] This is the average of two kinetic experiments. [f] This is the collision limited rate constant, k_{ADO}, calculated by average dipole orientation theory (ref. 152).

Table XV. Summary of Product Data for Secondary Ion Reactions of Various Iron Complex Negative Ions.[a]

Rxn. No.	Ion	Neutral	Product Ion [+ Assumed Neutral(s)]	Branching Fraction
1	$(OC)_2Fe(H_3COCH_3)^{\bullet -}$	D_2	No Reaction[b]	
2a	$(OC)_2Fe(=CHOCH_3)^{\bullet -}$	O_2	$(OC)_2Fe(=CHOCH_3)(D_2)^{\bullet -}$ [c]	0.77
2b			$(OC)_2Fe(=COOCH_3)^{\bullet -}$ [+ HD] [d]	0.23
3	$(OC)_2Fe(H_3COCH_3)^{\bullet -}$	SO_2	$(OC)_2Fe(SO_2)^{\bullet -}$ [+ H_3COCH_3]	1.00
4	$(OC)_2Fe(=CHOCH_3)^{\bullet -}$	SO_2	$(OC)Fe(=CHOCH_3)(SO_2)^{\bullet -}$ [+ CO]	1.00
5	$(OC)_2Fe(=CHOCH_3)^{\bullet -}$	CH_3OH	No Reaction[b]	
6	$(OC)_2Fe(H_3COCH_3)^{\bullet -}$	CH_3OH	No Reaction[b]	
7	$(OC)_3Fe(NMe_3)^{\bullet -}$	SO_2	$(OC)_3Fe(SO_2)^{\bullet -}$ [+ NMe_3]	1.00
8	$(OC)_3Fe(NMe_3)^{\bullet -}$	CH_3OH	No Reaction[b]	
9	$(OC)_2Fe(NMe_3)^{\bullet -}$	SO_2	$(OC)_2Fe(SO_2)^{\bullet -}$ [+ NMe_3]	1.00
10	$(OC)_2Fe(NMe_3)^{\bullet -}$	CH_3OH	No Reaction[b]	

---

[a] Experiments were performed at P_{He} = 0.900 torr, $\bar{\underline{v}}$ = 66 m/s. [b] k_{total} = < 1 x 10^{-13}. [c] k_{total} = (1.3 ± 0.1) x 10^{-11} cm^3 $molecule^{-1}$ s^{-1}. [d] A secondary ion/molecule reaction of this product ion was observed which corresponded to $(OC)_2Fe(=COOCH_3)(O_2)^{\bullet -}$.

Table XVI. Summary of Product Data for Secondary Ion Reactions of Various Manganese Complex Negative Ions.[a]

Rxn. No.	Ion	Neutral	Product Ion [+ Assumed Neutral(s)]	Branching Fraction
1	$(OC)_4Mn(H_2C{=}CF_2)^-$	SO_2	$(OC)_3Mn(SO_2)^-$ [+ CO + $H_2C{=}CF_2$]	1.00
2	$Mn(H_2C{=}CF_2)^-$	SO_2	$Mn(F_2)(SO_2)^-$ [+ HC≡CH]	1.00
3	$(OC)Mn(H_2C{=}CF_2)^-$	SO_2	$Mn(HC{\equiv}CF)(SO_2)^-$ [+ CO + HF]	1.00
4	$(OC)_4Mn(C_6H_4F_2)^-$	SO_2	$(OC)_4Mn(SO_2)^-$ [+ $C_6H_4F_2$]	1.00
5	$Mn(C_6H_4F_2)^-$	SO_2	$Mn(F_2)(SO_2)^-$ [+ C_6H_4]	1.00
6	$(OC)_3Mn(H_3COCH_3)^-$	O_2	No Reaction[b]	
7	$(OC)_3Mn({=}CHCOCH_3)^-$	O_2	No Reaction[b]	
8	$(OC)_3Mn(H_3COCH_3)^-$	CH_3OH	No Reaction[b]	
9	$(OC)_3Mn({=}CHCOCH_3)^-$	CH_3OH	No Reaction[b]	
10	$(OC)_3Mn(H_3COCH_3)^-$	NH_3	No Reaction[b]	
11	$(OC)_3Mn({=}CHCOCH_3)^-$	NH_3	No Reaction[b]	

[a] Experiments were performed at P_{He} = 0.700 torr, $\underline{\bar{v}}$ = 73 m/s. [b] k_{total} = < 1×10^{-13}.

$$(OC)_4Mn^- + F_2C{=}CH_2 \xrightarrow{He} (OC)_4Mn(C_2H_2F_2)^- \qquad (65)$$

(m/z 167) (m/z 231)

$$(OC)_3Mn^- + F_2C{=}CH_2 \xrightarrow{0.60} Mn(C_2H_2F_2)^- + 3CO \qquad (66a)$$

(m/z 139) (m/z 119)

$$\xrightarrow{0.35} (OC)Mn(C_2H_2F_2)^- + 2CO \qquad (66b)$$

(m/z 147)

$$\xrightarrow{0.05} (OC)_3Mn(C_2HF)^- + HF \qquad (66c)$$

(m/z 183)

analogous to the results of McDonald and Jones (eqs 47-49).[146] Observation the minor product forming channels 66b and 66c yielding the (adduct-2CO)$^-$ and (adduct-HF)$^-$ negative ions, respectively, were obviously the result of the structural change (from vicinal (eq 47-49) to geminal (65 and 66) in the difluoroolefin used.

To determine the structures of the adduct formed from reaction with $(OC)_4Mn^-$ and at least the two major product ions formed from reaction with $(OC)_3Mn^-$, their mixture was allowed to react with SO_2 (eqs, 67-69). The adduct at m/z 231 gave the (adduct-CO-$C_2H_2F_2$)$^-$ ion at m/z 203 (eq 67), which is consistent with a π-bound olefin structure in the m/z 231 negative ion. The reaction of the ion at m/z 119 with

$$(OC)_4Mn(C_2H_2F_2)^- + SO_2 \longrightarrow (OC)_3Mn(SO_2)^- + CO + C_2H_2F_2 \qquad (67)$$

(m/z 231) (m/z 203)

$$Mn(C_2H_2F_2)^- + SO_2 \longrightarrow F_2Mn(SO_2)^- + C_2H_2 \qquad (68)$$

(m/z 119) (m/z 157)

$$\underset{(m/z\ 147)}{(OC)Mn(C_2H_2F_2)^-} + SO_2 \longrightarrow \underset{(m/z\ 163)}{Mn(C_2HF)(SO_2)^-} + CO + HF \qquad (69)$$

SO_2 gave the (adduct-C_2H_2)$^-$ negative ion at m/z 157 (eq 68). This was the same type of substitution product found by McDonald and Jones, and indicated very strong Mn-F bonds effecting the loss of three CO ligands in the initial reaction (eq 66a). However, the reaction of the m/z 147 ion with SO_2 gave the (adduct-HF-CO)$^-$ negative ion at m/z 163 (eq 69), a substitution product which had not been observed by McDonald and Jones in the reaction of $(OC)_3Mn^-$ with HFC=CHF.[146]

The two minor product negative ions in eqs 66b and 66c, $(OC)_3Mn(\pi\text{-}HC{\equiv}CF)^-$ at m/z 183 and $(OC)Mn(\pi\text{-}HC{\equiv}CF)(H)(F)^-$ at m/z 147, must have been formed by stepwise insertions into vicinal C-H and C-F bonds since the former ion eliminated HF in its formation while the latter ion ejects (HF+CO) in its reaction with SO_2. However, the sequence of these oxidative insertion and migration steps must be reversed in these two product forming channels to form such structurally different ions. The formation of the major product ion at m/z 119 (eq 66a), $F_2Mn^-{=}C{=}CH_2$ or its isomer $F_2Mn^-(\pi\text{-}HC{\equiv}CH)$, must occur by two oxidative insertions into the geminal C-F bonds of $F_2C{=}CH_2$ and be exothermic enough to extrude all three CO ligands from the intermediate complex.

Based on these considerations, the mechanism shown in Scheme VII is proposed. The common π-complex intermediate **66** is suggested as the initial step in the mechanism based on the results in the reactions of CF_3CF_3, $F_2C{=}CF_2$, $F_2C{=}CHF$, and FHC=CHF with $(OC)_3Mn^-$.[146] Rate data from these reactions showed that the reaction of $(OC)_3Mn^-$ with CF_3CF_3 to

Scheme VII.

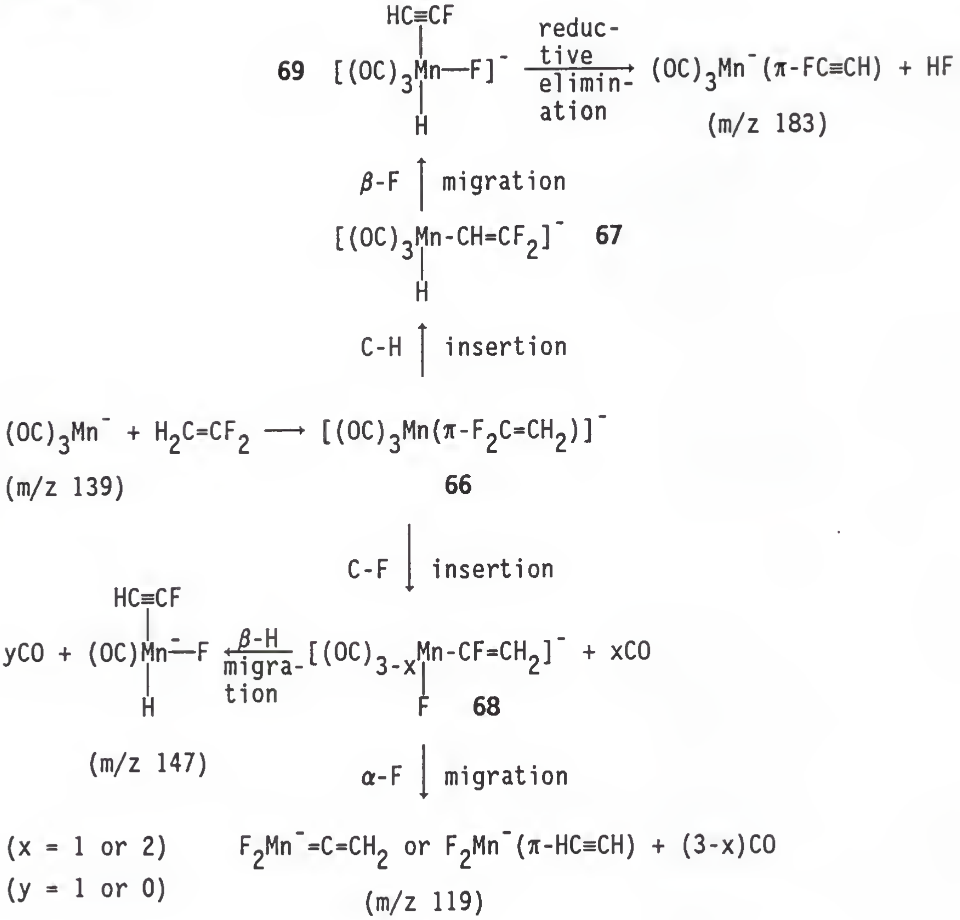

yield the (adduct-2CO-COF_2)$^-$ (eq 46) ions at m/z 157 was slower than the reactions with fluorinated olefins to yield the (adduct-3CO)$^-$ negative ions by more than two-orders of magnitude. Since the ions at m/z 183 in the present study retain all three CO ligands while the ions at m/z 147 and 119 have lost two and three CO ligands, respectively, a partition between C-H insertion to yield **67** and C-F insertion to yield **68** is suggested as the next steps in the mechanism.

Reactions of alkanes with $(OC)_3Mn^-$ yield the $(adduct-H_2)^-$ negative ion with retention of all CO ligands by a mechanism involving C-H oxidative insertion, β-H migration and reductive elimination of H_2.[130] The reactions of $(OC)_3Mn^-$ with alkenes ($H_2C=CH_2$, $H_2C=CH_2CH_3$) yield the total adduct negative ion where the alkene is π-bound ($k_H/k_D = 1.0$).[130] To account for formation of the m/z 183 ions in Scheme VII, it is suggested that C-H insertion of the fluoroalkene occurs from **66**. This could be due to the increased stabilization of the negative charge by the two electronegative β-fluorine substituents to yield a more stable complex **67** than would result from C-H insertion into $H_2C=CH_2$. The vinyl intermediate **67** can undergo a β-F migration to yield the 18-electron intermediate **69**, which reductively eliminates HF to yield the small amount of ions at m/z 183. The large dissociation energy of HF ($D° = 135.9 \pm 0.3$ kcal mol^{-1})[158] must exceed the Mn-F and Mn-H bond energies which accounts for fragmentation of **69** to expel HF rather than CO or HC≡CF.

Conversely, C-F insertion from **66** to yield **68** is believed to occur with loss of at least one, and possibly two, CO ligands due to the strong Mn-F and $Mn-CF=CH_2$ bonds that are formed which must exceed 118.7 kcals mol^{-1} ($D°$ $H_2C=CF—F$).[159] The only information on the Mn-X bond strengths is for Mn-Cl ($D° \approx 85$ kcals/mol) and Mn-Br ($D° \approx 74$ kcals/mol) in $(OC)_5MnX$.[88] This trend suggests that the single Mn-F bond exceeds 95 kcals mol^{-1}. In intermediate **68**, the electron count about Mn is 14 if $x = 1$ or 12 if $x = 2$ counting fluorine as a one electron donor. Either of these electron counts for structure **68** can easily accomodate fluorine as a 3-electron donor ligand. This Mn=F multiple bond leads to a stronger bond supplying additional energy to cause fragmentation of one or two CO ligands.

The $(p\rightarrow d)\pi$ donation of a halogen to a metal complex is not without precedent. Halide backbonding was established in silicon complexes by photoelectron spectroscopy[160] and was suggested to explain the relatively short V-Cl bond lengths in $Cl_3V(PMePh_2)_2$.[161] In addition, $(OC)_2NiX^{\bullet -}$ (X = Cl, Br) was a product of the halogen-atom transfer between $(OC)_3Ni^{\bullet -}$ and haloalkanes.[130,162] However, these formally 16-electron product complexes fail to react with excess haloalkane even though the truly 16-electron complex negative ions $(OC)_3Co^-$ and $(OC)_4Mn^-$ react with the haloalkanes at nearly the collision limit. Also, very similar reactivity was found for halogen-atom transfers to $(OC)_3MnBr^-$ and $(OC)_4MnBr^-$. These results suggested that the halogen ligands in $(OC)_2NiX^{\bullet -}$ and $(OC)_3MnBr^-$ were functioning as a three-electron donors.[162]

Intermediate **68** is next believed to partition between β-H migration to yield the product at m/z 147 and α-F migration to yield the product at m/z 119. If **68** possess two CO ligands (16-electron complex), β-H migration must be exothermic enough to expel a CO ligand to give m/z 147. Alternately, if **68** posesses one CO ligand (14-electron complex), the β-H migration is not exothermic enough to expel the last CO. Available data to address this question is found in the stepwise reaction of $(OC)_3Mn^-$ (14-electron complex) with acetylene to sequentially produce $(OC)_2Mn(C_2H_2)^-$, $(OC)Mn(C_2H_2)_2^-$, and $Mn(C_2H_2)_3^-$, where each coordinated acetylene causes expulsion of one CO.[130] However, $(OC)_4Mn^-$ (16-electron complex) reacts with acetylene to give only the total adduct negative ion.[130] The interpretation is that either the bound acetylene in the reaction with $(OC)_3Mn^-$ is functioning as a 4-electron donor (not possible in $(OC)_4Mn^-$) to cause loss of CO or the Mn-CO bond strength in $(OC)_3Mn^-$ is less than in $(OC)_4Mn^-$. McDonald and Jones found that reaction of SO_2 with the product ions $F_2Mn(FC{\equiv}CF)^-$, $F_2Mn(HC{\equiv}CF)^-$ and $F_2Mn(HC{\equiv}CH)$ give 6% loss of FC≡CF, 73% loss of HC≡CF, and 100% loss of HC≡CH, respectively.[146] This suggested that the relative bond strength of the acetylene ligand increased with increasing fluorine substitution and that formation of the FC≡CH bond to manganese could help to eject a CO ligand. Whether **68** possess one or two CO ligands is subject to debate and at this time is unknown. However, it is clear that the initial C-F insertion to form intermediate **68** does not cause expulsion of all three CO ligands due to the observation of the ions at m/z 147.

The branching fractions from partitioning of **68** between α-F and β-H migration indicate that α-F migration is favored by a factor of 1.7. Formation of the second Mn-F bond and converting a σ-vinyl ligand to a vinylidene or a π-bound acetylene ligand in m/z 119 could facilitate loss of the remaining CO ligands (1 or 2) bound to manganese in **68**. Since m/z 119 reacts with SO_2 to give the $(\text{adduct-}C_2H_2)^-$ negative ion at m/z 157 (eq 68), it seems reasonable to assume that the ligand expelled is HC≡CH and not $C{=}CH_2$. Whether the rearrangement of the vinylidene to acetylene occurs in the α-F migration step or is promoted in the reaction with SO_2 is unknown.

Considering the overall mechanism, the question arises as to why the β-F migration of **67** to form **69** causes loss of HF rather than a CO ligand when C-F insertion to form **68** and β-H elimination of **68** to form the ions at m/z 147 are proposed to cause loss of two CO ligands. The explanation involves the different hapticities of the Mn-F bonds in these intermediates. In **68**, the electron count about manganese is either 12- or 14-electrons depending on the number of CO ligands present. However, the electron count about manganese in **69** is 18-electrons; thus, fluorine can only be a 1-electron donor in **69**. Therefore, the formation of the stronger Mn-F bond in **68**, where fluorine is multiply bound to manganese causes loss of CO, while formation of the Mn-F bond in **69**, where fluorine is singly bound results in retention of CO and fragmentation of the strongly bound HF molecule.

I.D.1.c. With o-Difluorobenzene.

The results of the reactions of $(OC)_2Fe^{\bullet -}$ and $(OC)_3Mn^-$ with $\underline{o}$-$C_6H_4F_2$ are presented in equation 70 and 71, respectively, and are listed in Table XIV. $(OC)_3Fe^{\bullet -}$ (Table VIII) and $(OC)_4Mn^-$ (Table X) reacted with $\underline{o}$-$C_6H_4F_2$ to yield the total adduct negative ion while $(OC)_4Fe^{\bullet -}$ and $(OC)_5Mn^-$ did not react with $\underline{o}$-$C_6H_4F_2$ (Table IX and XI,

$$\underset{(m/z\ 112)}{(OC)_2Fe^{\bullet -}} + \underline{o}\text{-}C_6H_4F_2 \xrightarrow{\text{trace}} \underset{(m/z\ 226)}{(OC)_2Fe(C_6H_4F_2)^{\bullet -}} \tag{70a}$$

$$\xrightarrow{0.25} \underset{(m/z\ 198)}{(OC)Fe(C_6H_4F_2)^{\bullet -}} + CO \tag{70b}$$

$$\xrightarrow{0.75} \underset{(m/z\ 170)}{Fe(C_6H_4F_2)^{\bullet -}} + 2CO \tag{70c}$$

$$(OC)_3Mn^- + \underline{o}\text{-}C_6H_4F_2 \xrightarrow{0.17} (OC)_3Mn(C_6H_4F_2)^- \quad (m/z\ 253) \qquad (71a)$$

$$\xrightarrow{0.08} (OC)_2Mn(C_6H_4F_2)^- + CO \quad (m/z\ 225) \qquad (71b)$$

$$\xrightarrow{0.04} (OC)Mn(C_6H_4F_2)^- + 2CO \quad (m/z\ 197) \qquad (71c)$$

$$\xrightarrow{0.71} Mn(C_6H_4F_2)^- + 3CO \quad (m/z\ 169) \qquad (71d)$$

respectively). Similar to the reactions of $(OC)_3Mn^-$ with fluorinated ethylenes, both $(OC)_2Fe^{\bullet-}$ and $(OC)_3Mn^-$ yielded the (adduct-3CO) negative ion as the major reaction channel with large rate constants ($\approx 6 \times 10^{-10}$ cm^3 molecule^{-1} s^{-1}).

With both $(OC)_2Fe^{\bullet-}$ and $(OC)_3Mn^-$, the reactions with $\underline{o}$-$C_6H_4F_2$ produced the (adduct-2CO) and (adduct-3CO) negative ions, respectively, as the major products. Minor reaction channels were also present in which the CO ligands are lost in a stepwise manner from the total adduct negative ion. These reaction products are contrasted with the reaction of $(OC)_2Fe^{\bullet-}$ and $(OC)_3Mn^-$ with benzene in which the only products were the total adduct negative ions.[130] However, the rate constants determined in the reactions of $(OC)_2Fe^{\bullet-}$ and $(OC)_3Mn^-$ with benzene (5.6×10^{-10} cm^3 molecule^{-1} s^{-1} and 5.4×10^{-10} cm^3 molecule^{-1} s^{-1}, respectively) were similar to those with $\underline{o}$-$C_6H_4F_2$. In addition, the total adduct negative ion, $(OC)_3Mn(C_6H_6)^-$, failed to react with either H_2S or $HSi(CH_3)_3$. This suggested that benzene was functioning as a 4-electron donor, similar to a 1,3-butadiene ligand, which would result in an 18-electron complex.[130] $(OC)_3Mn(C_6H_6)^-$ did, however, react with SO_2 to yield $(OC)_3MnSO_2^-$ and C_6H_6.

To characterize the major products fromed in the reaction of $(OC)_3Mn^-$ with o-$C_6H_4F_2$, their reactions with SO_2 were investigated (eq 72-73) (Table XVI). The products of the reaction of $(OC)_2Fe^{\bullet -}$ with o-$C_6H_4F_2$ were not reacted with SO_2 due to the multitude of impurity ions

$$\underset{(m/z\ 253)}{(OC)_3Mn(C_6H_4F_2)^-} + SO_2 \longrightarrow \underset{(m/z\ 203)}{(OC)_3Mn(SO_2)^-} + C_6H_4F_2 \tag{72}$$

$$\underset{(m/z\ 169)}{Mn(C_6H_4F_2)^-} + SO_2 \longrightarrow \underset{(m/z\ 157)}{(F_2)Mn(SO_2)} + C_6H_4 \tag{73}$$

that were present in that reaction. Similar to the reaction of $(OC)_3Mn(C_6H_6)^-$ with SO_2, the ions at m/z 253 reacted with SO_2 to yield the (adduct-$C_6H_4F_2$) negative ions at m/z 203 (eq 72). This result is consistent with a π-bound adduct structure for m/z 253. $Mn(C_6H_4F_2)^-$ at m/z 169 reacted with SO_2 to yield the ions at m/z 157 with loss of C_6H_4 (eq 73) and suggests that both fluorine atoms are strongly σ-bound to the metal in the m/z 169 ions. The formation of the ions at m/z 157 in eq 73 coupled with the reaction products in eq 71 showing multiple loss of CO ligands led to the conclusion that C-F oxidative insertion must be part of the mechanism to form the respective reaction products. The similarity of rate constants for the reactions of benzene and o-difluorobenzene with the coordinatively unsaturated metal complexes suggest that both reactions proceed via π-complex intermediates.

For these reasons, a general mechanism is proposed for the reaction of $(OC)_2Fe^{\bullet -}$ and $(OC)_3Mn^-$ with $\underline{o}$-$C_6H_4F_2$ in Scheme VIII, which begins with initial π-complexation of $\underline{o}$-$C_6H_4F_2$ with the metal

Scheme VIII.

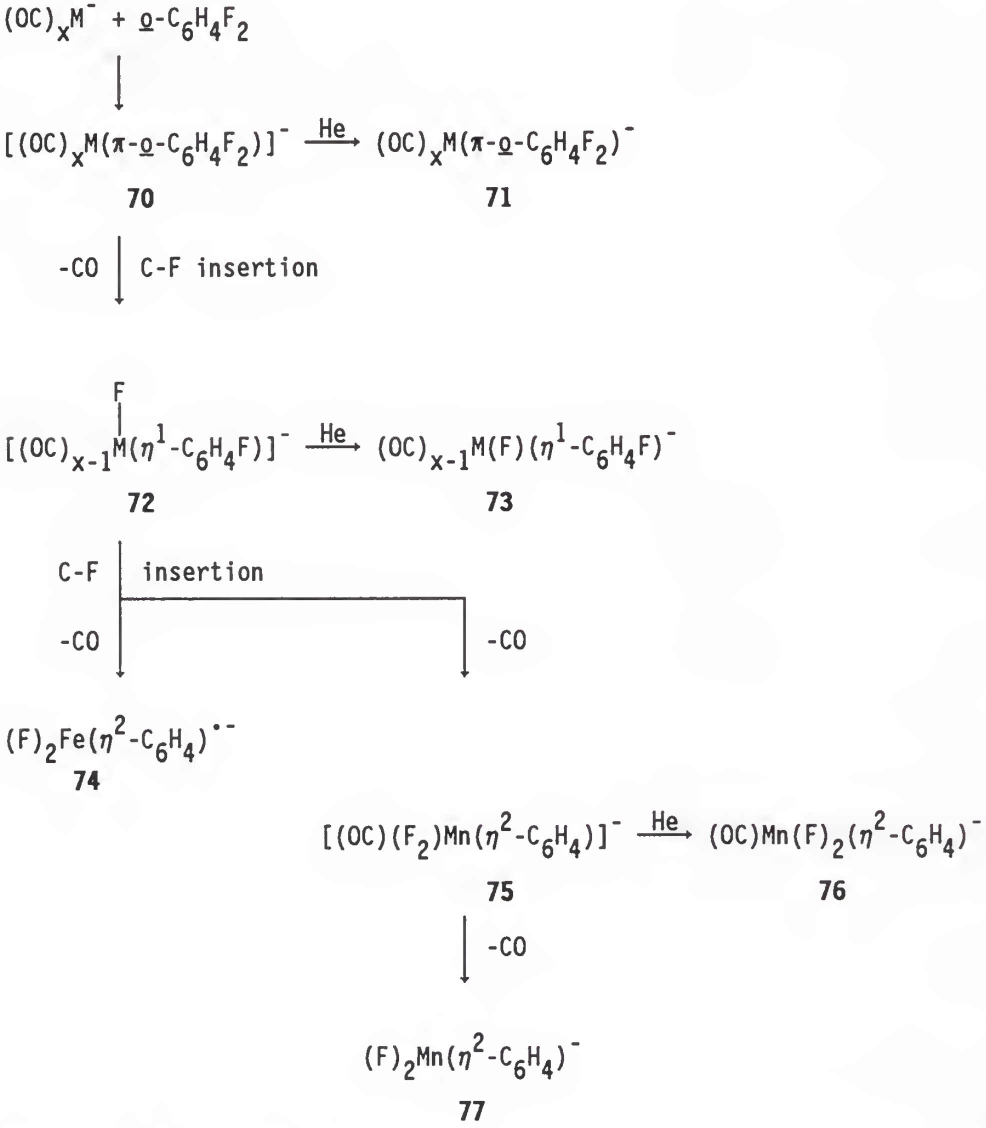
$(OC)_xM^- + \underline{o}$-$C_6H_4F_2$
$[(OC)_xM(\pi$-$\underline{o}$-$C_6H_4F_2)]^-$
He
$(OC)_xM(\pi$-$\underline{o}$-$C_6H_4F_2)^-$
70
71
-CO
C-F insertion
F
$[(OC)_{x-1}M(\eta^1$-$C_6H_4F)]^-$
He
$(OC)_{x-1}M(F)(\eta^1$-$C_6H_4F)^-$
72
73
C-F
insertion
-CO
-CO
$(F)_2Fe(\eta^2$-$C_6H_4)^{\bullet -}$
74
$[(OC)(F_2)Mn(\eta^2$-$C_6H_4)]^-$
He
$(OC)Mn(F)_2(\eta^2$-$C_6H_4)^-$
75
76
-CO
$(F)_2Mn(\eta^2$-$C_6H_4)^-$
77

M = Fe, x = 2 : M = Mn, x = 3

complex ($(OC)_2Fe^{\bullet -}$ or $(OC)_3Mn^-$) to form the vibrationally excited **70**. Intermediate **70** can either be cooled to its ground state by collisions with the helium buffer gas to yield **71**, the total adduct negative ion, or undergo a fast intramolecular C-F oxidative insertion to yield **72**, which is exothermic enough to expel at least one CO ligand. Intermediate **72**, like **70**, can then either be cooled to its vibrational ground state through collisions with the helium buffer gas to yield **73**, or can undergo a second C-F oxidative insertion to yield **74**, when M = Fe, or **75**, when M = Mn. This second C-F insertion is believed to cause loss of a CO ligand from **cc** to form either **74** or **75**. Intermediate **75**, is now partitioned between collisional stabilization to yield **76**, or loss of a CO ligand to yield **77**. The fact that sequential loss of CO ligands are observed as reaction products, suggests that loss of the CO ligands is stepwise and is due to competitive collisional stabilization with the helium buffer gas.

I.D.1.d. With CH_3OCH_3.

The results of the reactions of $(OC)_2Fe^{\bullet -}$ and $(OC)_3Mn^-$ with CH_3OCH_3 are given in equations 74 and 75, respectively, and are listed in Table XVII. In equation 74, $(OC)_2Fe^{\bullet -}$ reacted with CH_3OCH_3 to yield

$$\underset{m/z\ 112}{(OC)_2Fe^{\bullet -}} + CH_3OCH_3 \xrightarrow{0.62} \underset{m/z\ 156}{(OC)_2Fe(C_2H_4O)^{\bullet -}} + H_2 \qquad (74a)$$

$$\xrightarrow{0.38} \underset{m/z\ 158}{(OC)_2Fe(CH_3OCH_3)^{\bullet -}} \qquad (74b)$$

Table XVII. Summary Kinetic and Product Data for the Reactions of $(OC)_2Fe^{\bullet -}$ (1) and $(OC)_3Mn^-$ (2) with H_3COCH_3 and H_3COCD_3.

Rxn. No.	Ion	Neutral	Product Ion [+ Assumed Neutral(s)]	Branching Fraction	k_{total},[a] cm^3 $molecule^{-1}$ s^{-1}	k_{ADO},[b] cm^3 $molecule^{-1}$ s^{-1}	Reaction Efficiency[c]
1a	(1)	H_3COCH_3	$(OC)_2Fe(=CHOCH_3)^{\bullet -}$ [+ H_2]	0.62	$(7.3 \pm 0.7) \times 10^{-11}$ [d]	1.9×10^{-9}	0.038
1b			$(OC)_2Fe(H_3COCH_3)^{\bullet -}$	0.38			
2a	(1)	H_3COCD_3	$(OC)_2Fe(=CDOCH_3)^{\bullet -}$ [+ D_2]	0.67	see text[e]		
2b			$(OC)_2Fe(=CHOCD_3)^{\bullet -}$ [+ H_2]	0.33			
3a	(2)	H_3COCH_3	$(OC)_3Mn(H_3COCH_3)^-$	0.64	$(1.6 \pm 0.3) \times 10^{-11}$ [d]	1.2×10^{-9}	0.013
3b			$(OC)_3Mn(=CHOCH_3)^-$ [+ H_2]	0.36			
4a	(2)	H_3COCD_3	$(OC)_3Mn(H_3COCD_3)^-$	0.76	see text[d,e]		
4b			$(OC)_3Mn(=CHOCD_3)^-$ [+ H_2]	0.24			
4c			$(OC)_3Mn(=CDOCH_3)^-$ [+ D_2]	trace			

---

[a] k_{total}'s are estimated to be accurate to ± 20%. Errors are the maximum deviation in the average of at least three independent experiments at a P_{He} = 0.700 torr, $\bar{\underline{v}}$ = 73 m/s for $(CO)_3Mn^-$ and P_{He} = 0.900 torr, $\bar{\underline{v}}$ = 66 m/s for $(OC)_2Fe^{\bullet -}$. [b] The collision limit rate constants (k_{ADO}) were calculated by using the average dipole orientation theory (ref. 152). [c] The reaction efficiency is the fraction of collisions which result in reaction (k_{total}/k_{ADO}). [d] This is the apparent bimolecular rate constant for the termolecular adduct forming reaction. [e] Impure H_3COCD_3 (CH_3I) precluded determination of this rate constant. See text pages 111-114.

$$(OC)_3Mn^- + CH_3OCH_3 \xrightarrow{0.64} (OC)_3Mn(CH_3OCH_3)^- \qquad (75a)$$

m/z 139 m/z 185

$$\xrightarrow{0.36} (OC)_3Mn(C_2H_4O)^- + H_2 \qquad (75b)$$

m/z 183

the (adduct-H_2) negative ion at m/z 156 as the major reaction channel (62%) (eq 74a) along with formation of the total adduct negative ion (38%) (eq 74b) at m/z 158. The experimentally determined rate constant (k_{total} = (7.3 ± 0.7) x 10^{-11} cm^3 $molecule^{-1}$ s^{-1}) for this reaction was somewhat faster (by a factor of 5) than that previously reported for the reaction of $(OC)_2Fe^{\bullet -}$ with CH_3CH_3 to yield the (adduct-H_2) negative ion.[130] This suggested that either the oxygen atom in CH_3OCH_3 helped to stablize the negative charge in the complex, thus increasing the reaction rate or that the adduct may be due to the formation of a Lewis acid-base complex.

$(OC)_3Mn^-$ reacted with CH_3OCH_3 (eq 75) to yield a mixture of the total adduct negative ion at m/z 185 (64%) (eq 75a) and the (adduct-H_2) negative ion at m/z 183 (36%) (eq 75b) with k_{total} = (1.6 ± 0.3) x 10^{-11} cm^3 $molecule^{-1}$ s^{-1}. This rate constant is in good agreement with the previously measured rate constant ((8.0 ± 0.1) x 10^{-12} cm^3 $molecule^{-1}$ s^{-1})[130] in the reaction of $(OC)_3Mn^-$ with CH_3CH_3 to yield the (adduct-H_2) negative ion. The fact that $(OC)_3Mn^-$ reacted with CH_3OCH_3 to yield more adduct than did $(OC)_2Fe^{\bullet -}$ suggested that the additional CO ligand in $(OC)_3Mn^-$ resulted in more efficient collisional stabilization by the helium buffer gas. The less coordinatively unsaturated ions $(OC)_{3,4}Fe^{\bullet -}$ (Table VIII and IX) and $(OC)_{4,5}Mn^-$ (Table X and XI) did not react with CH_3OCH_3.

Since both reactions 74 and 75 yielded the (adduct-H_2) negative ion, the question arose as to the source of the expelled H_2 molecule. Was the source H_2 reductive elimination of originally geminal hydrogen atoms (eq 76) or from a reductive elimination of H_2 involving one hydrogen atom from each of the terminal carbons (eq 77)? Both eq 76

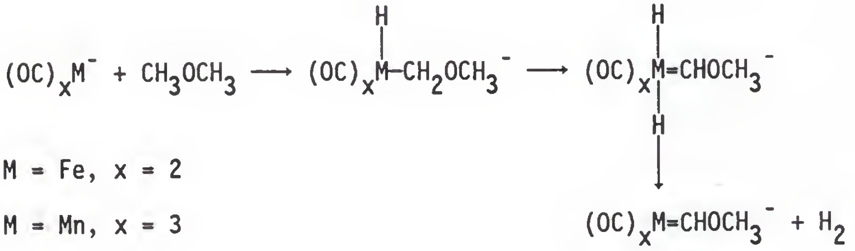

$$(OC)_xM^- + CH_3OCH_3 \longrightarrow (OC)_x\overset{H}{M}\text{-}CH_2OCH_3^- \longrightarrow (OC)_x\overset{H}{\underset{H}{M}}{=}CHOCH_3^- \longrightarrow (OC)_xM{=}CHOCH_3^- + H_2 \quad (76)$$

M = Fe, x = 2

M = Mn, x = 3

78

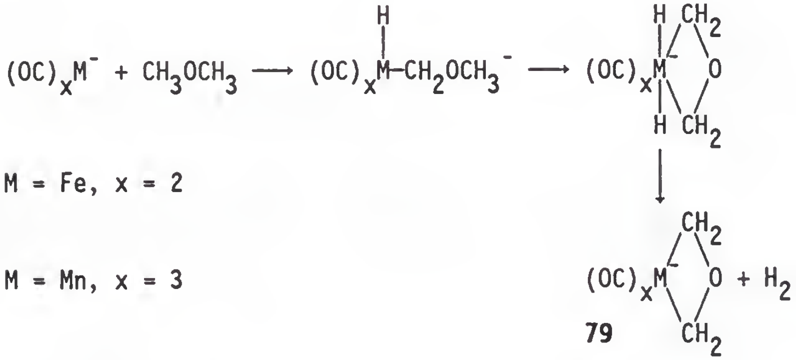

M = Fe, x = 2

M = Mn, x = 3

79

(77)

and 77 proceed by initial C-H oxidative insertion. The difference between the two equations is in which hydrogen atom migrates to the metal center in the second step. In eq 76, migration of the hydrogen on the α-carbon results in an intermediate which can then reductively eliminate H_2 to form the carbene complex **78**. In eq 77, migration of the hydrogen on the γ-carbon results in an intermediate that reductively eliminates H_2 to form the 1-metallo-3-oxocyclobutane **79**.

In an attempt to answer the question of α- or γ-H migration, the (adduct-H_2) negative ions (eq 74a and 75b) were allowed to react with D_2 (eq 78a-c and 79) (Table XV and XVI, respectively). The reaction

$$(OC)_2Fe(C_2H_4O)^{\bullet -} + D_2 \xrightarrow{0.77} (OC)_2Fe(C_2H_4O)(D)_2^{\bullet -} \qquad (78a)$$

m/z 156 m/z 160

$$\xrightarrow{0.23} (OC)_2Fe(C_2H_3DO)^{\bullet -} + HD \qquad (78b)$$

m/z 157

$$(OC)_2Fe(C_2H_3DO)^{\bullet -} + D_2 \longrightarrow (OC)_2Fe(C_2H_3DO)(D)_2^{\bullet -} \qquad (78c)$$

m/z 157 m/z 161

$$(OC)_3Mn(C_2H_4O)^{-} + D_2 \longrightarrow \text{no reaction} \qquad (79)$$

m/z 183

products for the reaction of D_2 with ($(OC)_2Fe(C_2H_4O)^{\bullet -}$) (m/z 156) and ($(OC)_3Mn(C_2H_4O)^{-}$) (m/z 183) would depend on the structure of the ion. If the sturcture were **78**, it would be expected that one H/D exchange is possible. However, if the sturture of the (adduct-H_2) negative ion were **79**, up to four H/D exchanges would be possible. As equation 78 indicates, the products of reaction were 77% D_2 addition (eq 78a) and 23% H/D exchange (eq 78b). The exchange product was also observed to undergo a secondary ion/molecule reaction with D_2 to yield m/z 161 (eq 78c). The branching fraction of eq 78b, 23%, is the sum of the product distributions from eqs 78b and 78c. The total rate constant measured for eq 78 was $k_{total} = (1.3 \pm 0.1) \times 10^{-11}$ cm^3 molecule^{-1} s^{-1}. Kinetic simulation of eq 78 was performed in order to compare the individual rate constants for eqs 78a and 78b. The simulation yielded $k_{78a} = 1.2 \times 10^{-11}$ cm^3 molecule^{-1} s^{-1} and $k_{78b} = 3.2 \times 10^{-12}$ cm^3 molecule^{-1} s^{-1}. These values are in good agreement with the experimetally determined k_{total} and correlate with the observed branching fractions. Based on these results, the structure of the product (adduct-H_2) negative ions (eqs 74a and 75b, respectively) is suggested to be 78.

In contrast to the above results, $(OC)_3Mn(C_2H_4O)^-$ (m/z 183) did not react ($k_{total} < 1 \times 10^{-13}$ cm^3 molecule^{-1} s^{-1}) with D_2 (eq 79) nor did the adducts $(OC)_2Fe(CH_3OCH_3)^{\bullet-}$ (Table XV) or $(OC)_3Mn(CH_3OCH_3)^-$ (Table XVI). A possible reason for the absence of an observed reaction between the 16-electron complex $(OC)_3Mn(C_2H_4O)^-$ and D_2 can be seen by the previously measured rate constant in the reaction of the 16-electron complex $(OC)_4Mn^-$ with D_2.[130] This rate constant was found to be $(8.6 \pm 1.4) \times 10^{-13}$ cm^3 molecule^{-1} s^{-1} which is indicative of a very slow reaction. Thus, the reaction in eq 79 as well as the reaction of $(OC)_3Mn(CH_3OCH_3)^-$ with D_2 must be at least as slow. The fact that $(OC)_2Fe(C_2H_4O)^{\bullet-}$ did react with D_2 and $(OC)_3Mn(C_2H_4O)^-$ did not can be explained by comparison of rate constants in the reaction of $(OC)_3Fe^{\bullet-}$ and $(OC)_4Mn^-$ with H_2. The rate constants previously measured for these reactions were 5.9×10^{-12} cm^3 molecule^{-1} s^{-1} [163] and 1.2×10^{-12} cm^3 molecule^{-1} s^{-1},[130] respectively, where the iron complex reated faster by a factor of ≈ 5. Apparently, it is the increased reactivity of the iron complex that allows it to react with D_2 while the manganese complex does not.

Further structure probing reactions were performed with the adduct and (aduct-H_2) negative ions in eqs 74 and 75. The reactions of these ions with CH_3OH were carried out to probe the possible existence of a Lewis acid-base sturcture in the adduct reaction products of eqs 74b and 75a. However, neither the adduct nor the (adduct-H_2) ions of iron (Table XV) or manganese (Table XVI) reacted with CH_3OH. This does not rule out the existence of the Lewis complex since the 16-electron complex $(OC)_4Mn^-$ did not react with CH_3OH or CH_3CH_2OH.[130] However, the product from the reaction of $(OC)_3Mn^-$ with NH_3 was considered to be the Lewis structure $((OC)_3\overset{-}{Mn}-\overset{+}{N}H_3)^-$. This ion reacted with CH_3OH to yield the same products, $(OC)_2Mn(H)(OCH_3)^-$ and $(OC)_3\overset{-}{Mn}-(\pi\text{-}CH_2O)$, as those formed in the reaction of $(OC)_3Mn^-$ with CH_3OH, but with a rate constant 200 times smaller.[157]

The reactions of the iron reaction products in eq 74 with SO_2 (Table XV) were investigated and the results are given in eq 80 and 81.

$$\underset{m/z\ 158}{(OC)_2Fe(CH_3OCH_3)^{\bullet -}} + SO_2 \longrightarrow \underset{m/z\ 176}{(OC)_2Fe(SO_2)^{\bullet -}} + CH_3OCH_3 \tag{80}$$

$$\underset{m/z\ 156}{(OC)_2Fe(=CHOCH_3)^{\bullet -}} + SO_2 \longrightarrow \underset{m/z\ 192}{(OC)Fe(=CHOCH_3)(SO_2)^{\bullet -}} + CO \tag{81}$$

Reaction of the products from the reaction of $(OC)_3Mn^-$ with CH_3OCH_3 (eqs 75a-b) were not performed since those product ions did not react with D_2 and thus complete characterization of those ions was not possible. The reaction of the iron complex adduct ions at m/z 158 with SO_2 (eq 80) yielded the (adduct-CH_3OCH_3) negative ions at m/z 176. This is consistent with the adduct structure of a Lewis acid-base complex or a product of C-H oxidative insertion. The fact that the (adduct-H_2) ions at m/z 156 reacted with SO_2 and gave the (adduct-CO) negative ions at m/z 192 was consistent with the carbene structure **78**.

The proposed mechanism (Scheme IX) for formation of the (adduct-H_2) and the total adduct negative ions is based on the results of the D_2 (eqs 78 and 79) and SO_2 (eqs 80 and 81) reactions with the metal complexes. The mechanism proceeds by formation of the Lewis acid-base

Scheme IX.

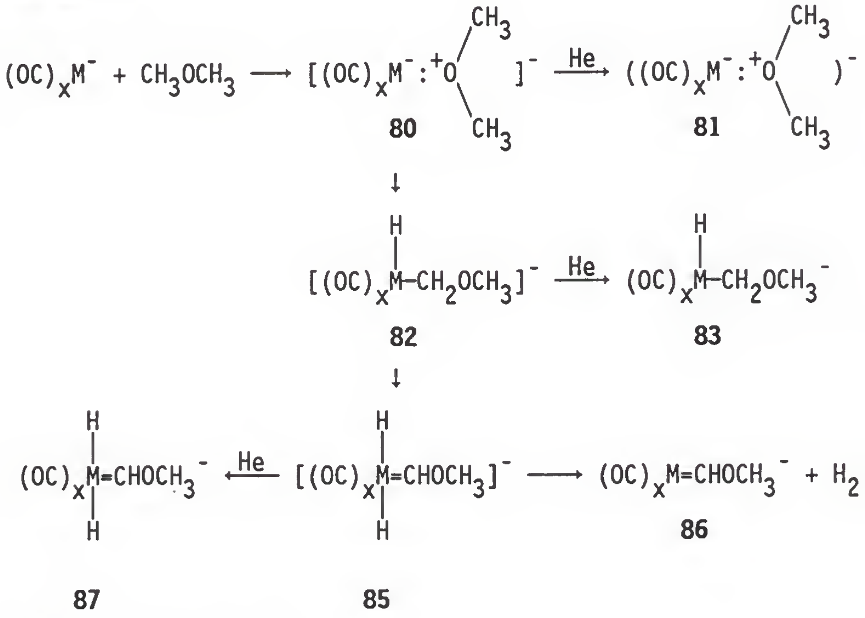

M = Fe, x = 2; M = Mn, x = 3

complex **80**. This initial coordination was suggested from previously studied C-H oxidative insertion reactions to yield the (adduct-H_2) negative ions which gave rate constants at 8.0×10^{-12} cm^3 $molecule^{-1}$ s^{-1} for $(OC)_3Mn^-$ with ethane and 1.6×10^{-11} cm^3 $molecule^{-1}$ s^{-1} for $(OC)_2Fe^{\bullet -}$ with ethane.[130] The rate constants measured in the reaction of the metal complexes with CH_3OCH_3 were faster by a factor of 2 for reaction with $(OC)_3Mn^-$ and a factor of 5 for reaction with $(OC)_2Fe^{\bullet -}$. Complex **80** was partitioned between collisional stabilization of the helium buffer gas to yield **81** and C-H oxidative insertion to yield **82**. Since the adduct of neither metal complex reacted with methanol, the existence of **80** was not conclusive. Intermediate **82** likely partitions between collisional stabilization with the helium buffer gas to yield **83** and α-hyrogen migration to yield **85**. Intermediate **85** could then reductively eliminate H_2 to yield the observed (adduct-H_2) product **86** or be collisionally stabilized by the helium buffer gas to yield the adduct **87**.

The structure of the adducts are proposed to be either **81**, **83**, or **87**. If the adduct structure were **81**, reaction with CH_3OH could have yielded an observable product since the proposed 16-electron Lewis complex $((OC)_3\overset{-}{Mn}–\overset{+}{N}H_3)^-$ did react with methanol. However, **81** would be a 15-electron complex when M = Fe and a 16-electron complex when M = Mn and neither the 15-electron $(OC)_3Fe^{\bullet -}$[136] nor the 16-electron complex $(OC)_4Mn^-$ reacted with CH_3OH.[130]

If the adduct structure were **83**, reaction of the 15-electron iron adduct **83** with D_2 should give some exchange since the 15-electron

$(OC)_3Fe^{\bullet -}$ reacted with H_2 with a rate constant of 5.9×10^{-12}.[163] The 16-electron $(OC)_4Mn^-$, however, reacted more slowly with H_2 with a rate constant of 1.2×10^{-12} cm^3 molecule^{-1} s^{-1},[130] so that if the manganese adduct were **83**, reaction with D_2 might have been too slow to observe. For the reasons stated above, adduct structure **87** is proposed as it is a 17-electron complex when M = Fe and an 18-electron complex when M = Mn, which would not react with either D_2 or CH_3OH.

α-Hydrogen migration is proposed from the reaction of **86** when M = Fe with D_2 (eqs 78a-c), in which the products were addition, a single H/D exchange, and addition of D_2 to the H/D exchange product. This single H/D exchange suggests the carbene **86**. Alternately, the structure of **86** could be the hydrido-carbyne, $(OC)_xM(H)(\equiv COCH_3)^-$ (**88**) when M = Fe or Mn. However, this structure is considered less probable than **86** since **88** is a 17-electron complex when M = Fe and an 18-electron complex when M = Mn. Both the 17-electron iron complex and the 18-electron manganese complex is unrective toward oxidative addition and thus would not react with D_2. Therefore, the (adduct-H_2) negative ion for both the iron and manganese complexes is proposed to be **87**.

In an attempt to confirm the proposed structure **86** of the (adduct-H_2) negative ions, the reactions of $(OC)_2Fe^{\bullet -}$ and $(OC)_3Mn^-$ with CD_3OCH_3 were examined. The 1,1,1-d$_3$-dimethylether was purchased from MSD Isotopes. During the initial investigation of the reaction of CD_3OCH_3 with $(OC)_3Mn^-$, it was observed that an impurity was present in the neutral reactant that decayed the signal of the starting ion and resulted in a very large signal of I^- at m/z 127 (approximately three times the signal of the starting ion) with no other product signals observable.

Further investigation suggested that the impurity in the CD_3OCH_3 might be CH_3I. Communication with MSD Isotopes revealed that CH_3I could be the impurity because the synthesis of CD_3OCH_3 involved the substitution reaction of CD_3O^- and CH_3I.

It was determined that CH_3I reacted with $(OC)_3Mn^-$ to yield I^- (m/z 127) and a trace amount of $(OC)_3Mn(I)^-$ (m/z 266) inletting CH_3I vapor at the high boiling inlet of the flow tube. However, the electron affinity of CH_3I is 4.6 kcal/mole[164] while the electron affinity of I_2 is 59.5 kcal/mol.[165] Since much more I^- was observed than could be explained from reaction with $(OC)_3Mn^-$, it was suggested that the impurity could be a mixture of CH_3I and I_2. In this mixture, CH_3I could react with $(OC)_3Mn^-$ (due to the low electron affinity of CH_3I) while I_2 is reacting to form I^- from electron transfer from $(OC)_3Mn^-$ and also is reacting with free electrons to form I^-. The reaction of $(OC)_3Mn^-$ with I_2 (inletted at the high boiling inlet) gave predominant formation of I^- (m/z 127) and a trace amount of I_2^- (m/z 254). Since the concentration of the impurity in the deuterated ether was thought to be small, the absence of m/z 254 and 266 in the reaction with $(OC)_3Mn^-$ is reasonable for either an I_2 or CH_3I impurity.

Since the purchased sample of CD_3OCH_3 was of no use in its received form, MSD Isotopes agreed to further purify a second sample of CD_3OCH_3 for our studies. This second sample also contained a small amount of the same impurity. The rates of the impurity reactions with $(OC)_2Fe^{\bullet-}$ and $(OC)_3Mn^-$ were so fast compared to the reaction of

CD_3OCH_3, that kinetic analysis of the reactions of CD_3OCH_3 with the metal complexes was impossible. Therefore, the only information obtainable were the low levels of the products and their relative distributions (eqs 82 and 83).

$$(OC)_3Mn^- + CD_3OCH_3 \xrightarrow{0.76} (OC)_3Mn(CD_3OCH_3)^- \tag{82a}$$

m/z 139 m/z 188

$$\xrightarrow{0.24} (OC)_3Mn(=CHOCD_3)^- + H_2 \tag{82b}$$

m/z 186

$$\xrightarrow{trace} (OC)_3Mn(=CDOCH_3)^- + D_2 \tag{82c}$$

m/z 184

$$(OC)_2Fe^{\bullet -} + CD_3OCH_3 \xrightarrow{0.67} (OC)_2Fe(=CDOCH_3)^{\bullet -} + D_2 \tag{83a}$$

m/z 112 m/z 157

$$\xrightarrow{0.32} (OC)_2Fe(=CHOCD_3)^{\bullet -} + H_2 \tag{83b}$$

m/z 159

As can be seen from the above equations, the absence of formation of (adduct-HD) negative ions suggested that the mechanism in eq 76 was operating. The reaction of $(OC)_3Mn^-$ with CD_3OCH_3 formed the total adduct at m/z 188 (76%) (eq 82a), compared to a 64% yield of the adduct formed with CH_3OCH_3 (eq 75a). An increased amount of adduct formation with the deuterated ether was expected relative to the protio ether due to a larger density of states because of the C-D bonds in the deuterated ether adduct to improve the efficiency of collisional stabilization. However, the isotope effect derived from the product channels 82b and 82c is ridiculously large, > 50.

In contrast, the reaction of $(OC)_2Fe^{\bullet -}$ with CH_3OCH_3 gave a significant amount of adduct (eq 74) while no adduct was observed with CD_3OCH_3. The absence of adduct formation in the reaction of CD_3OCH_3 with $(OC)_2Fe^{\bullet -}$ is unexplainable. There should have been an increased proportion of adduct formation due to the larger density of states with the deuterated ether, as was observed in the reaction with $(OC)_3Mn^-$. In addition, the isotope effect calculated from the branching fractions gave an inverse isotope effect of 0.5 for the reaction of $(OC)_2Fe^{\bullet -}$ with CD_3OCH_3 compared to the very large, normal isotope effect for the reaction of $(OC)_3Mn^-$ with CD_3OCH_3. Neither of these isotope effect results can be explained. For these reasons, as well as the possibility of unknown impurities that might have been present in the neutral sample, it is believed that the data obtained from the reaction of the reactive metal complexes with CD_3OCH_3 should be discounted.

I.E. Summary.

Dissociative electron attachment (DEA) of $Mn_2(CO)_{10}$ was controlled to produce $(OC)_5Mn^-$ (m/z 195), $(OC)_4Mn^-$ (m/z 167), and $(OC)_3Mn^-$ (m/z 139), while DEA of $Fe(CO)_5$ produced $(OC)_4Fe^{\bullet -}$ (m/z 168), $(OC)_3Fe^{\bullet -}$ (m/z 140), and $(OC)_2Fe^{\bullet -}$ (m/z 112). Regulation of the electron guns emission current allowed for optimization of the signal of the complex negative ion of interest.

The 18-electron complex negative ion $(OC)_5Mn^-$ failed to react with any of the neutral reagents studied. The 17-electron complex negative ion $(OC)_4Fe^{\bullet -}$ also failed to react with any of the neutral reagents studied except for SO_2 which produced $(OC)_3Fe(SO)_2^{\bullet -}$, the ligand substitution product.

The 16-electron complex $(OC)_4Mn^-$ reacted with Me_2NH, $(CD_3)_2NH$, o-$C_6H_4F_2$, $F_2C{=}CH_2$, and D_2 to form the total adduct negative ions. The only ligand substitution reaction of $(OC)_4Mn^-$ observed was that with SO_2, in which $(OC)_3Mn(SO_2)^-$ was the only product. The 15-electron complex $(OC)_3Fe^{\bullet -}$ also reacted with $MeNH_2$, Me_2NH, NMe_3, Et_2NH, $(CD_3)_2NH$, o-$C_6H_4F_2$, and D_2 to form the total adduct negative ions. As in the case with $(OC)_4Mn^-$, the only ligand substitution reaction of $(OC)_3Fe^{\bullet -}$ was with SO_2 to yield a 1:1 mixture of $(OC)_3Fe(SO_2)^{\bullet -}$ and $(OC)_2Fe(SO)_2^{\bullet -}$.

The 14-electron complex $(OC)_3Mn^-$ reacted with the amines Me_2NH and NMe_3 to yield the (adduct-H_2) and (adduct) negative ions, respectively. A deuterium labeling study involving $(CD_3)_2NH$ revealed that the mechanism involved both β-H migration from the methyl groups and N-H oxidative insertion. Initial coordination of the lone electron pair on nitrogen was proposed based on the correlation of the experimentally determined rate constants of $(OC)_2Fe^{\bullet -}$ with the amines and the proton affinity.

$(OC)_3Mn^-$ reacted with $H_2C{=}CF_2$ and o-$C_6H_4F_2$ to yield the (adduct-3CO) negative ions as the major reaction channel. The reaction of $(OC)_3Mn^-$ with $H_2C{=}CF_2$ also gave the (adduct-2CO) and (adduct-HF) negative ions as reaction products, while the reaction with o-$C_6H_4F_2$ also yielded the (adduct), (adduct-CO), and (adduct-2CO) negative ions. The mechanism for formation of these products was proposed to involve C-F oxidative insertion which caused sequential loss of CO ligands.

$(OC)_3Mn^-$ reacted with dimethyl ether to form the (adduct-H_2) and (adduct) negative ions. The mechanism for formation of the (adduct-H_2) negative ion was proposed to involve C-H oxidative insertion followed by α-H migration and reductive elimination of H_2 to yield a carbene. The suggested structure of the (adduct) was either to be the Lewis complex or the C-H oxidative insertion complex.

$(OC)_2Fe^{\bullet -}$ reacted with the amines $MeNH_2$, Me_2NH, and Et_2NH to yield the (adduct-H_2) negative ions. The mechanism for formation of the (adduct-H_2) negative ions was proposed to involve initial coordination of the nitrogen lone electron pair to form a Lewis complex, which then underwent β-hydrogen migration followed by N-H activation and reductive elimination of H_2. The Lewis complex formation was proposed by the correlation of the experimetal rate constants with the gas-phase proton affinity of the amines. N-H bond activation was proposed from the results of $(OC)_2Fe^{\bullet -}$ reacting with $(CD_3)_2NH$ to yield mainly the (adduct-HD) negative ion. $(OC)_2Fe^{\bullet -}$ reacted with NMe_3 to form the total adduct negative ion. The structure of this latter ion was proposed to be the Lewis complex derived from collisional stabilization with the helium buffer gas.

$(OC)_2Fe^{\bullet -}$ reacted with $\underline{o}$-$C_6H_4F_2$ to yield $(F)_2Fe(C_6H_4)^{\bullet -}$ as the major product; formation of the (adduct) and (adduct-CO) negative ions was also observed. The proposed mechanism involved sequential C-F oxidative insertion to yield an intermediate that was fractionated between collisional stabilization with the helium buffer gas and loss of a CO ligand.

$(OC)_2Fe^{\bullet -}$ reacted with dimethyl ether to yield the (adduct-H_2) and (adduct) negative ions. Reaction of the (adduct-H_2) negative ion with D_2 resulted in a single H/D exchange which suggested that the structure of the (adduct-H_2) negative ion possessed one unique hydrogen. Based on this information, the structure of the (adduct-H_2) negative ion was proposed to be the carbene derived from C-H oxidative insertion followed by α-hydrogen migration and reductive elimination of H_2. The structure of the adduct formed from the above mentioned reactions was suggested to be a C-H oxidative insertion product or a Lewis complex.

I.F. References.

(1) (a) Foster, M. S.; Beauchamp, J. L. J. Am. Chem. Soc. **1971**, 93, 4924. (b) Foster, M. S.; Beauchamp, J. L. J. Am. Chem. Soc. **1975**, 97, 4808.

(2) (a) Winters, R. E.; Kiser, R. W. J. Chem. Phys. **1966**, 44, 1964. (b) Dunbar, R. C.; Hutchinson, B. B. J. Am. Chem. Soc. **1974**, 96, 3816. (c) Compton, R. N.; Stockdale, J. A. D. Int. J. Mass. Spectrom. Ion. Phys. **1976**, 22, 47.

(3) For representative papers see: (a) MacMahon, T. C.; Freiser, B. S. J. Am. Chem. Soc. **1989**, 111, 421. (b) Pan, Y. H.; Ridge, D. P. J. Am. Chem. Soc. **1989**, 111, 1150. (c) Shin, S. K.; Beauchamp, J. L. J. Am. Chem. Soc. **1989**, 111, 900. (d) Graul, S. T.; Squires, R. R. J. Am. Chem. Soc. 111, 892. (e) Stepnowski, R.; Allison, J. J. Am. Chem. Soc. **1989**, 111, 449. (f) DePuy, C. H.; Gronert, S.; Barlow, S. E.; Bierbaum, V. M.; Dramrauer, R. J. Am. Chem. Soc. **1989**, 111, 1968.

(4) Sallens, L.; Lane, K. R.; Squires, R. R.; Freiser, B. S. J. Am. Chem. Soc. **1985**, 107, 4379.

(5) Squires, R. R. Chem. Rev. **1987**, 87, 623.

(6) (a) McDonald, R. N.; Chowdhury, A. K.; Schell, P. L. J. Am. Chem. Soc. **1984**, 106, 6095. (b) Lane, K. R.; Sallens, L.; Squires, R. R. J. Am. Chem. Soc. **1984**, 106, 2719.

(7) (a) Fehsenfeld, F. C.; Ferguson, E. E.; Schmeltkoff, A. L. Adv. At. Mol. Phys. **1969**, 5, 1. (b) Fehsenfeld, F. C.; Ferguson, E. E.; Schmeltkoff, A. L. Planet. Space Sci. **1964**, 12, 1169.

(8) Vaska, L Acc. Chem. Res. **1968**, 1, 335.

(9) Bruce, M. I. Angew. Chem. Int. Ed. Engl. **1977**, 16, 73.

(10) (a) Halpern, J. Inorg. Chim. Acta **1985**, 57, 1897. (b) Crabtree, R. H. Chem. Rev. **1985**, 85, 245. (c) Green, M. L. H.; O'Hare, D. Pure & Appl. Chem. **1985**, 57, 1897. (d) Rothwell, I. P. Polyhedron **1985**, 4, 177. (e) Shilov, A. E. "The Activation of Saturated Hydrocarbons by Transition Metal complexes"; Reidel: Dordrech, 1984. (f) Parshall, G. W. Chem. Tech. **1984**, 14, 628. (g) Muetterties, E. L. Chem. Soc. Rev. **1983**, 12, 283. (h) Brookhart, M.; Green, M. L. H. J. Organomet. Chem. **1983**, 250, 395. (i) Somorjai, G. "Chemistry in Two dimensions"; Cornell University Press, Ithaca, NY, 1981. (j) Parshall, G. W. "Homogeneous Catalysis"; Wiley: NY, 1980. (k) James, B. R. "Homogeneous Hydrogenation"; Wiley: NY, 1980; Chapter 7. (l) Muetterties, E. L.; Rhodin, T. N.; Band, E.; Brucker, C. F.; Pretzer, W. R. Chem. Rev. **1979**, 79, 91. (m) Webster, D. E. Adv. Organomet. Chem. **1977**, 15, 147. (n) Parshall, G. W. In Catalysis; Specialist Periodical Report; The Chemical Society: London, 1977; Vol 1, 335. (o) Parshall, G. W. Acct. Chem. Res. **1975**, 8, 113. (p) Parshall, G. W. Acct. Chem. Res. **1970**, 3, 139. (q) Halpern, J. Acct. Chem. Res. **1970**. 3, 386. (r) Collman, J. P. Acc. Chem. Res. **1968**, 1, 136. (s) Parshall, G. W. "Homogeneous Hydrogenation"; Wiley: NY, 1973. (t) Parshall, G. W. Catalysis, **1972**, 1, 335.

(11) Tolman, C. A. Chem. Soc. Rev. **1972**, 1, 337.

(12) Constable, E. C. Polyhedron **1984**, 3, 1037.

(13) Kleiman, J. P.; Dubeck, M. J. J. Am. Chem. Soc. **1963**, 85, 1544.

(14) Chatt, J.; Davidson, J. M. J. Chem. Soc. **1965**, 843.

(15) Hawthorne, M. F.; Chetcuti, P. A. J. Am. Chem. Soc. **1987**, 109, 942.

(16) Chency, A. J.; Shaw, B. L. J. Chem. Soc., Dalton Trans. **1972**, 754, 860-865.

(17) (a) Collman, M.P.; Hegedus, L. S. "Principles and Applications of Organotransition Metal Chemistry"; University Science Books: California, 1980; Chapter 5. (b) Werner, H.; Gotzig, J. Organometallics **1983**, 2, 547. (c) Cloke, F. G. N.; Cox, K. P.; Green, M. L. H.; Bashkin, J.; Prout, K. J. Chem. Soc., Chem. Commun. **1982**, 393. (d) Gibson, V. C.; Grebnik, P. D.; Green, M. L. H. J. Chem. Soc., Chem. Commun. **1983**, 1101. (e) Chiu, K. W.; Wong, W. K.; Wilkinson, G. J. Chem. Soc., Chem. Commun. **1981**, 451. (f) Karsch, J. J.; Klein, H. F.; Schmidbauer, H. Agnew. Chem. Int. Ed. Engl. **1975**, 14, 637. (g) Karsch, H. H.; Klein, H. F. Schmidbauer, H. Chem. Ber. **1977**, 110, 2200. (h) Rathke, J. W.; Muetterties, E. L. J. Am. Chem. Soc. **1975**, 97, 3272. (i) Werner, H.; Werner, R. J. Organomet. Chem. **1981**, 201, C60. (j) Goel, R. G.; Montemayor, R. G. Inorg. Chem. **1977**, 16, 2183. (k) Cheney, A. J.; Mann, B. E.; Shaw, B. L.; Slade, R. M. J. Chem. Soc., A **1971**, 3833.

(18) (a) Keeley, D. F.; Johnson, R. E. Inorg. Nucl. Chem. **1959**, 4, 33. (b) Graham, J. R.; Angelici, R. J. Inorg. Chem. **1967**, 6, 2082.

(19) Tipper, C. F. H. J. Chem. Soc. **1955**, 2045.

(20) Stoutland, P. O.; Bergman, R. G. J. Am. Chem. Soc. **1985**, 107, 4581.

(21) Stoutland, P. O.; Bergman, R. G. J. Am. Chem. Soc. **1988**, 110, 5732.

(22) Janowicz, A. H.; Bergman, R. G. J. Am. Chem. Soc. **1982**, 104, 352.

(23) Hoyano, J. K.; Graham, W. A. G. J. Am. Chem. Soc. **1982**, 104, 3723.

(24) Weast, R. C.; Astle, M. J. "CRC Handbook of Chemistry and Physics"; CRC Press: Boca Raton, Florida, 1982, F196.

(25) Sallens, L.; Lane, K. R.; Squires, R. R.; Freiser, B. S. J. Am. Chem. Soc. **1985**, 107, 4379.

(26) Armentrout, P. B.; Halle, L. F.; Beauchamp, J. L. J. Am. Chem. Soc. **1981**, 103, 6502.

(27) (a) Crabtree, R. H.; Mihelcic, J. M.; Quirk, J. M. J. Am. Chem. Soc. **1979**, 101, 7738. (b) Crabtree, R. H.; Mellea, M. F.; Mihelcic, J. M.; Quirk, J. M. J. Am. Chem. Soc. **1982**, 104, 107. (c) Crabtree, R. H.; Demou, P. C.; Eden, D.; Mihelcic, J. M.; Parnell, C. A.; Quirk, J. M.; Morris, G. E. J. Am. Chem. Soc. **1982**, 104, 6694. (d) Baudry, D.; Ephritikhine, M.; Felkin, H. J. Chem. Soc., Chem. Commun. **1980**, 1243. (e) Baudry, D.; Ephritikhine, M.; Felkin, H.; Zakrzewski, J. J. Chem. Soc., Chem. Commun. **1982**, 1235.

(28) Janowicz, A. H.; Bergman, R. G. J. Am. Chem. Soc. **1983**, 105, 3929.

(29) McMillen, D. F.; Golden, D. M. Ann. Rev. Phys. Chem. **1982**, 33, 493.

(30) Nolan, S. P.; Hoff, C. D.; Stoutland, P. O.; Newman, L. J.; buchanan, J. M.; Bergman, R. G.; Yang, G. K.; Peters, K. S. J. Am. Chem. Soc. **1987**, 109, 3143.

(31) Baghal-Vayjooee, M. H.; Benson, S. W. J. Am. Chem. Soc. **1979**, 101, 2838.

(32) Perianna, R. A.; Bergman, R. G. J. Am. Chem. Soc. **1986** 108, 7346.

(33) (a) Janowicz, A. H.; Periana, R. A.; Buchanan, J. M.; Kovac, C. A.; Stryker, J. M.; Wax, M. J.; Bergman, R. G. Pure & Appl. Chem. **1984**, 56, 13. (b) Bergman, R. G.; Seidler, P. F.; Wenzel, T. T. J. Am. Chem. Soc. **1985**, 107, 4358. (c) Periana, R. A.; Bergman, R. G. J. Am. Chem. Soc. **1986**, 108, 7332.

(34) Jones, W. D.; Feher, F. J. J. Am. Chem. Soc., **1985**, 107, 620.

(35) (a) Davidson, P. J.; Lappert, M. F.; Pearce, R. Chem. Rev. **1976**, 76, 219. (b) Schrock, R. R.; Parshall, G. W. Chem. Rev. **1976**, 76, 243. (c) Cross, R. J. "The Chemistry of the Metal-Carbon Bond"; Wiley: New York, 1985; Vol. 2, Chapter 8.

(36) (a) Whitesides, g. M.; Gaasch, J. F.; Stedronsky, E. R. J. Am. Chem. Soc. **1972**, 94, 5258. (b) McDermont, J. X.; White, J. F.; Whitesides, G. M. J. Am. Chem. Soc. **1976**, 98, 6521. (c) McDermont, J. X.; White, J. F.; Whitesides, G. M. J. Am. Chem. Soc. **1973**, 95, 4451.

(37) Bönnemann, H.; Grard, C.; Kopp, W.; Wilke, G. Proc. Int. Congr. Pure Appl. Chem., 23rd **1971**, 6, 265.

(38) (a) Watson, P. L.; Roe, D. C. J. Am. Chem. Soc. **1982**, 104, 6471. (b) Watson, P. L.; Parshall, G. W. Acct. Chem. Res. **1985**, 18, 51.

(39) Bunel, E.; Burger, B. J.; Bercaw, J. E. J. Am. Chem. Soc. **1988**, 110, 976.

(40) Mole, T.; Jeffrey, E. A. "Organoaluminum Compounds"; Elsevier: Amsterdam, 1974.

(41) Jarvie, A. W. F. Organometal. Chem. Rev. **1970**, 6, 153.

(42) (a) Sasson, Y.; Blum, J. J. Chem. Soc., Chem. Commun. **1974**, 309. (b) Whitesides, G. M.; Sadowski, J. S.; Lilburn, J. J. Am. Chem. Soc. **1974**, 96, 2829.

(43) Benfield, F. W. S.; Green, M. L. H. J. Chem. Soc., Dalton Trans. **1974**, 1244.

(44) Sneeden, R. P. A.; Zeiss, H. H. J. Organomet. Chem. **1971**, 26, 101.

(45) Schwartz, J.; Hart, D. W.; McGiffert, B. J. Am. Chem. Soc. **1974**, 96, 5613.

(46) Whitesides, G. M.; Stedronsky, E. R.; Casey, C. P.; Filippo, J. S. Jr. J. Am. Chem. Soc. **1970**, 92, 1426.

(47) Evans, J.; Schwartz, J.; Urquhart, P. W. J. Organomet. Chem. **1974**, 81, C37.

(48) (a) Calderazzo, F. Pure Appl. Chem. **1973**, 33, 453. (b) Braterman, P. S.; Cross, R. J. Chem. Soc. Rev. **1973**, 2, 271. (c) Baird, M. C. J. Organomet. Chem. **1974**, 64, 289.

(49) (a) Dvorak, J.; O'Brien, R. J.; Santo, W. Chem. Commun. **1970**, 411. (b) Shur, V. B.; Berkovitch, E. G.; Vasiljeva, L. B.; Kudryavtsev, R. V.; Vol'pin, M. E. J. Organomet. Chem. **1974**, 78, 127.

(50) (a) Boekel, C. P.; Teuben, J. H.; de Liefde Meijer, H. J. J. Organomet. Chem. **1974**, 81, 371. (b) Boekel, C. P.; Teuben, J. H.; de Leifde Meijer, H. J. J. Organomet. Chem. **1975**, 102, 161.

(51) Erker, G. J. Organomet. Chem. **1977**, 134, 189.

(52) (a) Cooper, N. J.; Green M. L. H. J. Chem. Soc., Chem. Commun. **1974**, 208. (b) Cooper, N. J.; Green M. L. H. J. Chem. Soc., Chem. Commun. **1974**, 761. (c) Cooper, N. J.; Green M. L. H. J. Chem. Soc., Dalton Trans. **1979**, 1121.

(53) (a) Schrock, R. R. Acct. Chem. Res. **1979**, 12, 98. (b) Schrock, R. R. J. Am. Chem. Soc. **1974**, 96, 6796.

(54) Goddard, R. J.; Hoffmann, R.; Jemmis, E. D. J. Am. Chem. Soc. **1980**, 102, 7667.

(55) Shilov, A. E.; Shteinman, A. A. Coord. Chem. Rev. **1977**, 24, 97.

(56) Turner, H. W.; Schrock, R. R.; Fellmann, J. D.; Holmes, S. J. J. Am. Chem Soc. **1983**, 105, 4942.

(57) (a) Forsen, S.; Hoffman, R. A. J. Chem. Phys. **1964**, 40, 1189. (b) Forsen, S.; Hoffman, R. A. J. Chem. Phys. **1963**, 39, 2892. (c) Morris, G. A.; Freeman, R. J. Magn. Reson. **1978**, 29, 443.

(58) Churchill, M. R.; Wasserman, H. J.; Turner, H. W.; Schrock, R. R J. Am. Chem. Soc. **1982**, 104, 1710.

(59) Fellman, J. D.; Schrock, R. R.; Traficante, D. D. Organometallics, **1982**, 1, 481.

(60) Cree-Uchiyama, M.; Shapley, J. R.; St. George, G. M. J. Am. Chem. Soc. **1986**, 108, 1316.

(61) Brookhart, M.; Green, M. L. H. J. Organomet. Chem. **1983**, 250, 395.

(62) Burk, M. J.; McGrath, M. P.; Crabtree, R. H. J. Am. Chem. Soc. **1988**, 110, 620.

(63) Parkin, G.; Bunel, E.; Burger, B. J.; Trimmer, M. S.; Van Asselt, A.; Bercaw, J. E. J. Mol. Catal. **1987**, 41, 21.

(64) Chisholm, M. H.; Eichhorn, B. W.; Huffman, J. C. Organometallics **1989**, 8, 80. (b) Chisholm, M. H.; Eichhorn, B. W.; Huffman, J. C. Organometallics **1989**, 8, 67.

(65) (a) Al-Essa, R. J.; Ling, S. M.; Puddephatt, R. J. Organometallics, **1987**, 6, 951. (b) Al-Essa, R. J.; Puddephatt, R. J. J. Chem. Soc., Chem. Commun. **1980**, 45.

(66) Johnson, T. H.; Cheng, S.-S. J. Am. Chem. Soc. **1979**, 101, 5277.

(67) (a) Bevan, W. I.; Haszeldine, R. N.; Young, J. C. Chem. Ind. (London) **1961**, 789. (b) Bevan, W. I.; Haszeldine, R. N. J. Chem. Soc., Dalton Trans. **1974**, 2509. (c) Bevan, W. I.; Haszeldine, R. N.; Middleton, J.; Tipping, A. E. J. Chem. Soc., Dalton Trans. **1975**, 252, 260.

(68) Osborn, V. A.; Parker, C. A.; Winter, M. J. J. Chem. Soc., Chem. Commun. **1986**, 1185.

(69) (a) Brookhart, M.; Buck, R. C. J. Am. Chem. Soc. **1989**, 111, 559. (b) Le Bozec, H.; Fillaut, J. L.; Dixneuf, P. H. J. Chem. Soc., Chem. Commun. **1986**, 1182.

(70) (a) Brook, A. G.; Dillon, P. J. Can. J. Chem. **1969**, 47, 4347. (b) Seyferth, D. Acc. Chem. Res. **1972**, 5, 65.

(71) (a) Werner, H. Angew. Chem. Internat. Ed. **1968**, 7, 930. (b) Angelici, R. J. Organomet. Chem. Rev. **1968**, 3, 173. (c) Howell, J. A. S.; Burkinshaw, P. M. Chem. Rev. **1983**, 83, 557. (d) Cross,

R. J. Chem. Soc. Rev. **1985**, 14, 197. (e) Peloso, A. Coor. Chem. Rev. **1973**, 10, 123. (f) Basolo, F. Inorg. Chim. Acta **1981**, 50, 65. (g) Ibid. **1985**, 100, 33. (h) Atwood, J. D.; Wovkulich, M. J.; Sonnenberger, D. C. Acc. Chem. Res. **1983**, 16, 350.

(72) Basolo, F.; Pearson, R. G. "Mechanisms of Inorganic Reactions", 2nd ed.; Wiley: New York, 1967.

(73) (a) Keeley, D. F.; Johnson, R. E. Inorg. Nucl. Chem. **1959**, 4, 33. (b) Graham, J. R.; Angelici, R. J. Inorg. Chem. **1967**, 6, 2082.

(74) Pardue, J. E.; Dobson, G. R. Inorg. Chim. Acta **1976**, 20, 207.

(75) Angelici, R. J.; Graham, J. R. J. Am. Chem. Soc. **1966**, 88, 3658.

(76) Davison, A.; Ellis, J. E. J. Organomet. Chem. **1971**, 31, 239.

(77) (a) Hieber, W.; Wollmann, K. Chem. Ber. **1962**, 95, 1552. (b) Bellus, P. A.; Brown, T. L. J. Am. Chem. Soc. **1980**, 102, 6020.

(78) (a) Basolo, F.; Wojcicki, A. W. J. Am. Chem. Soc. **1961**, 83, 520. (b) Siefert, E. E.; Angelici, R. J. J. Organomet. Chem. **1967**, 8, 374.

(79) (a) Rest, A. J.; Turner, J. J. J. Organomet. Chem. **1970**, 25, C30. (b) Rest, A. J.; Turner, J. J. J. Chem. Soc., Chem. Commun. **1969**, 375. (c) McHugh, T. M.; Rest, A. J.; Taylor, D. J. J. Chem. Soc., Dalton Trans. **1980**, 1803. (d) Purcell, K. F.; Kotz, J. C. "Inorganic Chemistry"; W. B. Saunders: Philadelphia, 1977. (e) Zingales, F.; Faraone, R.; Graziani, M.; Belluco, U. Inorg. Chim. Acta **1967**, 1, 172. (f) Atwood, J. D.; Brown, T. L. J. Am. Chem. Soc. **1975**, 97, 3380. (g) Berry, A.; Brown, T. L. Inorg. Chem. **1972**, 11, 1165. (h) Wojcicki, A.; Basolo, F. J. Am. Chem. Soc. **1961**, 83, 525. (i) Johnson, B. F. G.; Lewis, J.; Miller, J. R.;

Robinson, B. H.; Wojcicki, A. J. Chem. Soc. A **1968**, 522. (j) Brown, D. A.; Lyons, H. J.; Sane, R. T. Inorg. Chem. **1967**, 6, 1246.

(80) (a) Schenk, W.; Muller, H. Inorg. Chem. **1981**, 20, 6. (b) Lichtenberger, D. L.; Brown, T. L. J. Am. Chem. Soc. **1978**, 100, 366.

(81) (a) Cardaci, G. J. Chem. Soc., Dalton Trans. **1974**, 1808, 2452. (b) Cardaci, G.; Murgia, S. M. J. Organomet. Chem. **1970**, 25, 483. (c) Basolo, F.; Palmer, G. T. J. Am. Chem. Soc. **1985**, 107, 3122. (d) Muetterties, E. L.; Hirsekorn, F. J. J. Am. Chem. Soc. **1973**, 95, 5419. (e) Muetterties, E. L.; Hirsekorn, F. J. J. Am. Chem. Soc. **1974**, 96, 4063. (f) Stuhl, L. S.; Muetterties, E. L. Inorg. Chem. **1978**, 17, 2148. (g) Muetterties, E. L.; Bleeke, J. R. Acc. Chem. Res. **1979**, 12, 324. (h) Muetterties, E. L.; Bleeke, J. R. J. Am. Chem. Soc. **1981**, 103, 556.

(82) Casey, C. P.; O'Connor, J. M. Organometallics **1985**, 4, 384.

(83) Ji, L. -N.; Rerek, M. E.; Basolo, F. Organometaliics **1984**, 3, 740.

(84) (a) Rerek, M. E.; Basolo, F. J. Am. Chem. Soc. **1984**, 106, 5908. (b) Schuster-Woldan, H. G.; Basolo, F. J. Am. Chem. Soc. **1966**, 88, 1657.

(85) Muetterties, E. L.; Bleeke, J. R.; Wucherer, E. J.; Albright, T. A. Chem. Rev. **1982**, 82, 499.

(86) Chan, D. M. -T.; Fultz, W. C.; Nugent, W. A.; Roe, D. C.; Tulip, T. H. J. Am. Chem. Soc. **1985**, 107, 251.

(87) (a) Keulks, G. W.; Krenzke, L. D.; Notermann, T. M. Adv. Catal. **1978**, 27, 183. (b) Haber, J.; Bielanski, A. Catal. Rev. **1979**, 19, 1. (c) Gates, B. C.; Katzer, J. R.; Schuitt, G. C. A. "Chemistry of Catalytic Processes"; McGraw-Hill: New York, 1979; 325. (d) Burrington, J. D.; Kartisek, C. T.; Grasselli, R. K. J. Catal. **1983**, 81, 489. (e) Burrington, J. D.; Kartisek, C. T.; Grasselli, R. K. J. Catal. **1984**, 87, 363.

(88) Connor, J. Top. Curr. Chem. **1977**, 71, 71.

(89) Lewis, E. K.; Golden, D. M.; Smith, G. P. J. Am. Chem. Soc. **1984**, 106, 3906.

(90) Halle, L. F.; Houriet, R.; Kappes, M. M.; Staley, R. H.; Beauchamp, J. L. J. Am. Chem. Soc. **1982**, 104, 6293.

(91) Jacobsen, D. B.; Freiser, B. S. J. Am. Chem. Soc. **1984**, 106, 3891.

(92) Cassady, C. J.; Freiser, B. S. J. Am. Chem. Soc. **1985**, 107, 1566.

(93) Armentrout, P. B.; Halle, L. F.; Beauchamp, J. L. J. Phys. Chem. **1982**, 76, 2449.

(94) Hettich, R. L.; Jackson, T. C.; Stanko, E. M.; Freiser, B. S. J. Am. Chem. Soc. **1986**, 108, 5086.

(95) Bernstein, J. D.; Simon, J. D.; Peters, K. S. Chem. Phys. Lett. **1983**, 100, 241.

(96) Sappa, E.; Milone, L J. Organomet. Chem. **1973**, 61, 383.

(97) Lin, Y. C.; Mayr, A.; Knobler, C. B.; Kaesz, H. D. J. Organomet. Chem. **1984**, 272, 207.

(98) (a) Suss-Fink, G. Z. Naturforsch., B: Anorg. chem., Org. Chem. **1980**, 35B, 454. (b) Johnson, B. F. G.; Lewis, J.; Odiaka, T.;

Raithby, P. R. J. Organomet. Chem. **1981**, 216, C56. (c) Johnson, B. F. G.; Lewis, J. J. Chem. Soc., Dalton Trans. **1977**, 1328.

(99) (a) Armor, J. N. Inorg. Chem. **1978**, 17, 203. (b) Armor, J. N. Inorg. Chem. **1978**, 17, 213.

(100) Hillhouse, G. L.; Bercaw, J. E. J. Am. Chem. Soc. **1984**, 106, 5472.

(101) Hedden, D.; Roundhill, D. M.; Fultz, W. C.; Rheingold, A. L J. Am. Chem. Soc. **1984**, 106, 5014.

(102) Casalnuovo, A. L.; Calabrese, J. C.; Milstein, D. Inorg. Chem. **1987**, 26, 971.

(103) Walsh, P. J.; Hollander, F. J.; Bergman, R. G. J. Am. Chem. Soc. **1988**, 110, 8729.

(104) Benson, S. W. "Thermochemical Kinetics"; John Wiley & Sons: NY, 1976; 309.

(105) Huheey, J. E. "Inorganic Chemistry"; Third Ed., Harper and Row: NY, 1983, A35.

(106) (a) Massa, W.; Babel, D. Chem. Rev. **1988**, 88, 275. (b) Carl. R. T.; Doig, S. J.; Geiger, W. E.; Hemond, R. C.; Hughes, R. P.; Kelly, R. S.; Samkoff, D. E. Organometallics **1987**, 6, 611. (c) Burch, R. R.; Calabrese, J. C.; Ittel, S. D. Organometallics **1988**, 7, 1642. (d) Huang, Y.; Zhou, J. J. Organomet. Chem. **1988**, 348, 235. (e) Burch, R. R.; Harlow, R. L.; Ittel, S. D. Organometallics **1987**, 6, 982. (f) Burch, R. R.; Calabrese, J. C. J. Am. Chem. Soc. **1986**, 108, 5359. (g) Doig, S. J.; Hughes, R. P.; Davis, R. E.; Gadol, S. M.; Holland, K. D. Organometallics **1984**, 3, 1921.

(107) Fahey, D. R.; Mahan, J. E. J. Am. Chem. Soc. **1977**, 99, 2501.

(108) Bruce, M.I.; Goodall, B. L.; Sheppard, G. L.; Stone, F. G. A. J. Chem. Soc., Dalton Trans. **1975**, 591.

(109) Bruce, M. I.; Gardner, R. C. F.; Goodall, B. L.; Stone, F. G. A. J. Chem. Soc., Chem. Commun. **1974**, 185.

(110) Gross, M. E.; Johnson, C. E.; Maroney, M. J.; Trogler, W. C. Inorg. Chem. **1984**, 23, 2968.

(111) Richmond, T. G.; Osterberg, C. E.; Arif, A. M. J. Am. Chem. Soc. **1987**, 109, 8091.

(112) Kubas, G. J. Inorg. Chem. **1983**, 22, 692.

(113) Richmond, T. G.; Kelson, M. A.; Arif, E. P. Organometallics **1987**, 6, 1995.

(114) For a discussion on low valent metal fluorides, see: Branan, D. M.; Hoffman, N. W.; McElroy, E. A.; Miller, N. C.; Ramage, D. L.; Young, S. H. Inorg. Chem. **1987**, 26, 2915.

(115) Depuy, C. H.; Bierbaum, V. M. Acct. Chem Res. **1981**, 14, 146.

(116) Allison, J. Prog. Inorg. Chem. **1986**, 34.

(117) (a) Armentrout, P. B.; Hodges, R. V.; Beauchamp, J. L. J. Chem. Phys. **1977**, 66, 4683. (b) Hodges, R. V.; Armentrout, P. B.; Beauchamp, J. L. Int. J. Mass Spectrom. Ion Phys. **1979**, 29, 375.

(118) (a) Lehman, T. A.; Bursey, M. M. "Ion Cyclotron Resonance Spectrometry"; Wiley-Interscience: New York, 1976. (b) Burnier, R. C.; Byrd, G. D.; Freiser, B. S. J. Am. Chem. Soc. **1980**, 103, 4360. (c) Burnier, R. C.; Byrd, G. D.; Freiser, B. S. Anal. Chem. **1980**, 52, 1641. (c) Allison, R. B.; Freas, R. B.; Ridge, D. P. J. Am. Chem. Soc. **1979**, 101, 4998. (d) Allison, R. B.; Freas, R. B.;

Ridge, D. P. J. Am. Chem. Soc. **1979**, 101, 1332. (e) Jones, R. W.; Staley, R. H. J. Am. Chem. Soc. **1980**, 102, 3794.

(119) Cody, R. B.; Burnier, R. C.; Greiser, B. S. Anal. Chem. **1982**, 54, 96.

(120) McDonald, R. N.; Chowdhury, A. K.; Setser, D. W. J. Am. Chem. Soc. **1980**, 102, 6491.

(121) Kebarle, P.; Chowdhury, S. Chem. Rev. **1987**, 87, 513 and references therein.

(122) Foster, M. S.; Beauchamp, J. L. J. Am. Chem. Soc. **1971**, 93, 4924. (b) Foster, M. S.; Beauchamp, J. L. J. Am. Chem. Soc. **1975**, 97, 4808.

(123) Comasirow, M. B.; Marshall, A. G. J. Chem. Phys. **1976**, 64, 110. (b) Comasirow, M. B.; Burnier, R. G.; Parisod, G. Chem. Phys. Lett. **1978**, 57, 413.

(124) Pilcher, G.; Skinner, H. A. "The Chemistry of the Metal-Carbon Bond"; Hartley, F. R.; Patal, S. Eds., Wiley: New York, 1982; Chapter 2.

(125) Tolbert, M. A.; Beauchamp, J. L. J. Am. Chem. Soc. **1984**, 101, 8117.

(126) (a) Corderman, R. R.; Beauchamp, J. L. Inorg. Chem. **1976**, 15, 665. (b) Stevens, A. E.; Beauchamp, J. L. J. Am. Chem. Soc. **1981**, 103, 190.

(127) (a) Cunningham, A. J.; Payzant, J. D.; Kebarle, P. J. Am. Chem. Soc. **1972**, 94, 7627. (b) McIver, R. T., Jr. Rev. Sci. Instrum. **1978**, 49, 111. (c) Wolf, J. F., Staley, R. H.; Taagepera, M.; McIver, R. T., Jr.; Beauchamp, J. L.; Taft, R. W. J. Am. Chem.

Soc. **1977**, 99, 5417. (d) Farneth, W. E.; Brauman, J. I. J. Am. Chem. Soc. **1976**, 98, 7891.

(128) (a) Feigerle, C. S.; Corderman, R. R.; Bobashev, S. V.; Lineberger, W. C. J. Chem. Phys. **1981**, 74, 1580. (b) Engelking, P. C.; Lineberger, W. C. J. Am. Chem. Soc. **1979**, 101, 5569. (c) Mead, R. D.; Stevens, A. E.; Lineberger, W. C. "Gas Phase Ion Chemistry"; Bower, M. T. ed., Academic Press: New York, 1984; Vol 3.

(129) (a) Armentrout, P. B.; Beauchamp, J. L. J. Am. Chem. Soc. **1981**, 103, 784. (b) Michaels, G. D.; Flesch, G. D.; Svec, H. J. Inorg. Chem. **1980**, 19, 479. (c) Hildenbrand, D. L.; Kleinschmidt, P. D.; Lau, K. H. Gov. Rep. Announce. Index (US) **1978**, 71, 110.

(130) Jones, M. T. Ph.D. Thesis, Kansas State University, **1987**.

(131) (a) Byrd, G. D.; Burnier, R. C.; Freiser, B. S. J. Am. Chem. Soc. **1982**, 104, 3565. (b) Byrd, G. D.; Freiser, B. S. J. Am. Chem. Soc. **1982**, 104, 5944. (c) Jacobson, D. B.; Freiser, B. S. J. Am. Chem. Soc. **1983**, 105, 736, 5197, 7484, 7492. (d) Jacobsen, D. B.; Byrd, G. D.; Freiser, B. S. Inorg. Chem. **1984**, 23, 553. (e) Jackson, T. C.; Carlin, T. J.; Freiser, B. S. J. Am. Chem. Soc. **1986**, 108, 1120.

(132) (a) Armentrout, P. B.; Halle, L. F.; Beauchamp, J. L. J. Am. Chem. Soc. **1981**, 103, 6624. (b) Armentrout, P. B.; Halle, L. F.; Beauchamp, J. L. J. Am. Chem. Soc. **1981**, 103, 6501. (c) Armentrout, P. B.; Halle, L. F.; Beauchamp, J. L. Organometallics **1982**, 1, 963. (d) Armentrout, P. B.; Beauchamp, J. L. J. Am.

Chem. Soc. **1981**, 103, 6628. (e) Tolbert, M. A.; Beauchamp, J. L. J. Am. Chem. Soc. **1984**, 101, 8117.

(133) (a) Larsen, B. S.; Ridge, D. P. J. Am. Chem. Soc. **1984**, 106, 1912. (b) Radecki, B. D.; Allison, J. Organometallics **1986**, 5, 411.

(134) Tipper, C. F. H. J. Chem. Soc. **1955**, 2045.

(135) McDonald, R. N.; Jones, M. T. J. Am. Chem. Soc. **1986**, 108, 8097.

(136) McDonald, R. N.; Chowdhury, A. K., unpublished results.

(137) McDonald, R. N.; Reed, D. J.; Chowdhury, A. K. Organometallics, **1989**, 8, 1122.

(138) Buckner, S. W.; Gord, J. R.; Freiser, B. S.; J. Am. Chem. Soc. **1988**, 110, 6606

(139) Sieck, L. W.; Mautner, M. J. Phys. Chem. **1982**, 86, 3646.

(140) Corderman, R. R.; Beauchamp, J. L. Inorg. Chem. **1977**, 12, 3135.

(141) (a) Corderman, R. R.; Beauchamp, J. L. J. Am. Chem. Soc. **1976**, 98, 3998. (b) Jones, R. W.; Staley, R. H. J. Am. Chem. Soc. **1982**, 104, 2296. (c) Weddle, G. H.; Allison, J.; Ridge, D. P. J. Am. Chem. Soc. **1977**, 99, 105.

(142) McDonald, R. N.; Schell, P. L. Organometallics **1988**, 7, 1820.

(143) McDonald, R. N.; Shell, P. L. Organometallics **1988**, 7, 1806.

(144) Radecki, B. D.; Allison, J. J. Am. Chem. Soc. **1984**, 106, 946.

(145) Gregor, I. K. Inorg. Chim. Acta **1987**, 132, 3.

(146) Jones, M. T.; McDonald, R. N. Organometallics **1988**, 7, 1221.

(147) McDonald, R. N.; Chowdhury, A. K. J. Am. Chem. Soc. **1985**, 107, 4123.

(148) Reed, D. J. "Research Notebook I", **1987**, 45-58.

(149) Strohmeir, W.; Muller, R. Z. Physik. Chem. N.F. **1964**, 85, 40.

(150) DePuy, C. H.; Bierbaum, V. M. Acct. Chem. Res. **1981**, 14, 146.

(151) Stafford, G. G. "Instrumental Aspects of Positive and Negative Ion Chemical Ionization Mass Spectrometry"; presented to the American Society for Mass Spectrometry, Seattle, WA, June 1979.

(152) (a) Su, T.; Bowers, M. T. J. Chem. Phys. **1973**, 58, 3027. (b) Su, T.; Bowers, M. T. "Gas Phase Ion Chemistry"; Vol 1, Bowers, M. T., Ed.: Academic Press, NY, Chapter 3.

(153) Miller, K. J.; Savchik, J. A. J. Am. Chem. Soc. **1979**, 101, 7206.

(154) Heath, R. L. "CRC Handbook of Chemistry and Physics"; Weast, R. C.; Astle, M. J. Eds., CRC Press, Inc., Boca Raton, Florida, 1982; B255-264.

(155) McDonald, R. N.; Jones, M. T.; Chowdhury, A. K. J. Am. Chem. Soc. **1986**, 108, 3105.

(156) Aue, D. H.; Bowers, M. T. "Gas Phase Ion Chemistry"; Bowers, M. T., Ed., Academic Press: New York, 1979; Vol II, Chapter 9, 46.

(157) McDonald, R. N.; Jones, M. T., unpublished results.

(158) Gaydon, A. G. "Dissociation Energies and Spectra of Diatomic Molecules"; Chapman and Hall: London, 1968.

(159) Egger, K. W.; Cocks, A. T. Helv. Chem. Acta. **1973**, 56, 1516.

(160) Cradock, S.; Ebsworth, E. A. V. Chem. Commun. **1971**, 57.

(161) Bansmeir, R. L.; Huffman, J. C.; Caulton, K. G. Inorg. Chem. **1985**, 24, 3003.

(162) Jones, M. T.; McDonald, R. N.; Schell, P. L.; Ali, M. H. J. Am. Chem. Soc. **1989**, 111, in press.

(163) Schell, P. L. Ph.D. Thesis, Kansas State University, **1986**.

(164) Moutinho, A. M. C.; Aten, J. A.; Los, J. *Chem. Phys.* **1974**, *5*, 84.

(165) Baede, A. P. M.; Auerbach, D. J.; Los, J. *Physica (Utrecht)* **1973**, *64*, 134.

Acknowledgements

I wish to express my appreciation and gratitude to my research advisor Dr. Richard N. McDonald, for his encouragement, guidance and support. Thanks also to Dr. Mike Jones who patiently taught me the operation of the flowing afterglow apparatus and to Ed Bianchina, Gerry Greb, Dr. E. A. Maatta, Dr. D. W. Macomber, and Dr. D. W. Setser whose discussions were of great help. Special thanks to Ed Bianchina, Mark Madison, Rob Everist and John Linzi for their help in setting up the computer data acquisition system and also to Mr. Morris of MSD Isotopes for his attempts to purify the sample of CD_3OCH_3.

I also want to thank my wife, Vicki, and my family for their support, patience, confidence, and encouragement throughout the course of my graduate studies.

Appreciation is expressed to the National Science Foundation, and the Petroleum Research Fund, administered by the American Chemical Society, for financial support of this research, and to the Department of Chemistry, Kansas State University, for financial support in the form of a teaching assistantship during part of my studies.

A Flowing Afterglow Study of $(OC)_2Fe^{\bullet -}$ and $(OC)_3Mn^-$ with Amines, Fluorocarbons and CH_3OCH_3

by

Daniel J. Reed

B.S., Arkansas College, 1986

AN ABSTRACT OF A MASTER'S THESIS

submitted in partial fulfillment of the
requirements for the degree

MASTER OF SCIENCE

Department of Chemistry
KANSAS STATE UNIVERSITY
Manhattan, Kansas

1989

Abstract

Dissociative electron attachmet (DEA) of $Mn_2(CO)_{10}$ yields $(OC)_5Mn^-$, $(OC)_4Mn^-$, and $(OC)_3Mn^-$, while DEA of $Fe(CO)_5$ yields $(OC)_4Fe^{\bullet -}$, $(OC)_3Fe^{\bullet -}$, and $(OC)_2Fe^{\bullet -}$. Neither $(OC)_5Mn^-$ nor $(OC)_4Fe^{\bullet -}$ reacted with the neutral reagents studied, except for $(OC)_4Fe^{\bullet -}$ which reacted with SO_2 to yield $(OC)_3Fe(SO)_2^{\bullet -}$.

$(OC)_4Mn^-$ reacted with several of the neutral reagents studied; Me_2NH, $(CD_3)_2NH$, o-$C_6H_4F_2$, $F_2C{=}CH_2$, and D_2 to form the total adduct negative ions as well as with SO_2 to yield $(OC)_3Mn(SO_2)^-$. $(OC)_3Fe^{\bullet -}$ also reacted with the neutral reagents; $MeNH_2$, Me_2NH, NMe_3, Et_2NH, $(CD_3)_2NH$, D_2, and o-$C_6H_4F_2$ to form the total adduct negative ions as well as with SO_2 to form a 1:1 mixture of $(OC)_3Fe(SO_2)^{\bullet -}$ and $(OC)_2Fe(SO)_2^{\bullet -}$.

$(OC)_3Mn^-$ reacted with the amines Me_2NH and NMe_3 to yield the (adduct-H_2) and (adduct) negative ions, respectively. A deuterium labeling study involving $(CD_3)_2NH$ revealed that the mechanism involved both β-H migration from the amine methyl groups and N-H oxidative insertion.

$(OC)_3Mn^-$ was observed to react with $H_2C{=}CF_2$ and o-$C_6H_4F_2$ to yield the (adduct-3CO) negative ions. The reaction of $(OC)_3Mn^-$ with $H_2C{=}CF_2$ also gave the (adduct-2CO) and (adduct-HF) negative ions as minor reaction products, while the reaction with o-$C_6H_4F_2$ also yielded the (adduct), (adduct-CO), and (adduct-2CO) negative ions. The mechanism for formation of these products was believed to involve C-F oxidative insertion which causes stepwise loss of CO ligands.

$(OC)_2Fe^{\bullet -}$ reacted with the amines $MeNH_2$, Me_2NH, and Et_2NH to yield the (adduct-H_2) negative ions and with NMe_3 to yield the total adduct negative ion. N-H activation was proposed from the results of $(OC)_2Fe^{\bullet -}$ reacting with $(CD_3)_2NH$ to yield primarily the (adduct-HD) negative ion.

$(OC)_2Fe^{\bullet -}$ reacted with $\underline{o}$-$C_6H_4F_2$ to yield primarily $(F)_2Fe(C_6H_4)^{\bullet -}$, as well as the (adduct) and (adduct-CO) negative ions. The proposed mechanism involved stepwise C-F oxidative insertion which causes stepwise loss of CO ligands.

Both $(OC)_3Mn^-$ and $(OC)_2Fe^{\bullet -}$ reacted with dimethyl ether to yield the (adduct-H_2) and (adduct) negative ions. Reaction of the iron (adduct-H_2) negative ion with D_2 resulted in a single H/D exchange which suggested that the structure of the (adduct-H_2) negative ion was the Fischer carbene.